How does exposure to valproic acid and lamotrigine during pregnancy affect foetal neuronal development?

A pharmacology study exploring effects in vivo and in vitro in chicken embryos and PC12-cells

Josephine Sena Lumor

Thesis submitted for the degree of
Master in Pharmacy
45 credits

Department of Pharmaceutical Biosciences
School of Pharmacy
The Faculty of Mathematics and Natural Sciences

UNIVERSITY OF OSLO

May 2019

Hvordan vil eksponering av valproat og lamotrigin under graviditet påvirke fosterets nevronal utvikling?

En farmakologisk studie som undersøker mulige effekter in vivo *og* in vitro *i kyllingembryo og PC12-celler*

Josephine Sena Lumor

Seksjon for farmasøytisk biovitenskap
Farmasøytisk institutt
Det matematisk-naturvitenskaplige fakultet

UNIVERSITETET I OSLO

Mai 2019

Veiledere:
Professor Ragnhild Elisabeth Paulsen
Postdoktor Mussie Ghezu Hadera

May 2019

How does exposure to valproic acid and lamotrigine during pregnancy affect foetal neuronal development?
A pharmacology study exploring effects in vivo and in vitro in chicken embryos and PC12-cells

Josephine Sena Lumor

http://www.duo.uio.no/

Print: Reprosentralen, Universitetet i Oslo

Acknowledgments

The work presented in this master thesis was carried out at the Department of Pharmaceutical Biosciences, School of Pharmacy at the University of Oslo from August 2018 to May 2019. This thesis is a project in the Pharmatox Strategic Research Initiative. Their aim is to generate novel insight on effects of pharmaceuticals on human and neurodevelopment.

First and foremost, I would like to thank my supervisors Ragnhild Elisabeth Paulsen and Mussie Ghezu Hadera. Ragnhild, thank you for your constructive comments, your knowledge and your help through the challenging parts during the writing phase. Our conversations made me feel calm and like I was on the right track. Your passion for this field is inspirational. Mussie, thank you for your help during the lab phase. Even though things did not always go well, you still had words of encouragement and always saw the positive side. I would like to thank you both for always being available when needed.

Additionally, I would also like to thank the whole group at ZEB, for all the help I have received. I would like to give a special thanks to Mona Gaarder for the practical training in the lab and the willingness to help with everything. And Beata Urbanczyk Mohebi for the help in the lab, and for the wonderfully distracting conversations. It has truly been appreciated.

I would like to thank Fred Haugen from STAMI, Fernando Boix Escolan, Jannike Mørch Andersen, and Gerd-Wenche from Oslo University Hospital for willing to analyse my samples and generate data.

Last but not least, I would like to thank my family. Evelyn and Dad for your support throughout this whole period, Francesca for proofreading my thesis even though you were busy yourself, and especially you Mom. You have been my biggest supporter throughout this period. I really could not have done this without you!

Abstract

Many women have medical conditions that require pharmaceutical use during pregnancy. This can be detrimental for foetal development, especially during treatment for epilepsy. Valproic acid (VPA) and lamotrigine (LTG) are widely used antiepileptic drugs (AED) to treat epilepsy, and VPA is known to be teratogenic. Discontinuing them during pregnancy can be harmful for both the mother and the foetus. For this reason, it would be beneficial to understand the mechanisms in neuronal development that are affected by these AEDs. Safety pharmacological studies explore the potentially adverse effects a substance may have on physiological function. The chick embryo model is a proposed model for *in vivo* developmental studies where the cerebellum is a well-suited structure of the brain to study, since it undergoes all the stages of neuronal development in a limited time period. PC12 cells are an extensively studied *in vitro* cell model that can be used to study neurotoxicity.

Chicken embryos were exposed to VPA, LTG or LTG isethionate through an *in ovo* injection. *In vivo* experiments were conducted, where the entire brain was isolated to assess the distribution of the AEDs to the brain, or where only the cerebellum was isolated for western blot or RT-qPCR. The genes, *PCNA, PAX6, MMP9, GRIN2B, BDNF, SLC6A13,* and *GABBR1*, were studied with RT-qPCR. Western blotting was employed to compare the gene expression of PCNA, PAX6, MMP9 and GluN2B with their subsequent protein expression. The cerebella from untreated chicken embryos were utilised for cerebellar granule neurons (CGNs) culture to carry out *in vitro* studies. In conjunction with CGNs, PC12 cells were used to study the promoter activation of PAX6 and MMP9 after exposure through a luciferase assay.

VPA, LTG and LTG isethionate were rapidly distributed to the chicken embryo brain after injection. Yet the AEDs did not significantly affect protein levels of markers important during development. Neurite outgrowth was unaffected by VPA and LTG in CGNs. LTG in therapeutic concentrations did not affect PAX6 and MMP9 promoter activity. The chick embryo model is a good supplement for safety pharmacology, and combining RT-qPCR and western blot with luciferase assay gives a clearer picture of drug-induced alterations in gene expression. Few of the genes studied were affected by VPA more than LTG. *PAX6* was down-regulated by VPA, and could contribute to the morphological aspects of its teratogenicity. LTG up-regulated *BDNF,* which could affect cognitive functions.

Sammendrag

Mange kvinner har medisinske lidelser som krever behandling med medikamenter under graviditet. Dette kan være skadelig for fosterutviklingen, spesielt ved behandling av epilepsi. Valproat (VPA) og lamotrigin (LTG) er blant de mest brukte antiepileptika (AE) for behandlingen av epilepsi, hvor VPA er assosiert med teratogene effekter. Seponering under graviditet kan være uheldig for både mor og foster. Av den grunn, er det viktig å forstå mekanismene bak teratogene effekter av antiepileptika. Sikkerhetsfarmakologiske studier utforsker potensielt skadelige effekter stoffer kan ha på fysiologiske funksjoner. Kyllingembryomodellen er en foreslått modell for *in vivo* utviklingsstudier, hvor lillehjernen er en egnet del av hjernen til å studere nevronale utviklingsprosesser fordi den gjennomgår alle stegene ved nevronal utvikling i et begrenset tidsrom. PC12-celler er en mye studert *in* vitro cellemodell som kan benyttes til å studere nevrotoksisitet.

Kyllingembryo ble eksponert for VPA, LTG eller LTG isetionat ved *in ovo* injeksjon. *In vivo* forsøk ble gjennomført hvor hele hjernen ble isolert for å undersøke distribusjonen av AE til hjernen, eller hvor bare lillehjernen ble isolert for westernblotting eller RT-qPCR. Endringer i genuttrykk ble studert med RT-qPCR for *PCNA, PAX6, MMP9, GRIN2B, BDNF, SLC6A13,* og *GABBR1*. Westernblotting ble brukt for å sammenligne genekspresjonen til PCNA, PAX6, MMP9 og GluN2B med deres proteinuttrykk. Lillehjerner fra ubehandlede kyllingembryo ble anvendt til korncellekulturer for å gjennomføre *in vitro* forsøk. Sammen med kyllingkornceller, ble PC12-celler benyttet til å studere promotoraktiviteten til PAX6 og MMP9 med luciferaseassay etter eksponering.

VPA, LTG og LTG isetionat ble raskt distribuert til kyllingembryohjerne etter injeksjon. Allikevel ble det ingen signifikant endring i proteinuttrykket til markørene viktig for nevronal utvikling. LTG og VPA oppregulerte henholdsvis bare *BDNF*, og *SLC6A13* og *GABBR1*. Nevrittutvekst var upåvirket av VPA og LTG i kyllingkornceller. LTG i terapeutiske konsentrasjoner påvirket ikke PAX6 eller MMP9 promotoraktivitet. Kyllingembryomodellen er et godt supplement i sikkerhetsfarmakologi, og kombinering av RT-qPCR, westernblotting med luciferaseassay, gir et klarere bilde av eventuell legemiddelindusert endring i genuttrykk.

Et fåtall av genene studert ble påvirket av VPA enn LTG. *PAX6* ble nedregulert av VPA, som kan bidra til de morfologiske aspektene ved dens teratogenese. LTG oppregulerte *BDNF*, som kan påvirke kognisjon.

Abbreviations

ACN	Acetonitrile
ACTB	β-actin
ADHD	Attention deficit hyperactivity disorder
ANOVA	Analysis of Variance
AraC	Cytosine-beta-D-arabinofuranoside
ASD	Autism spectrum disorder
AUC	Area under the curve
BDNF	Brain-derived neurotrophic factor
BME	Basal Medium Eagle
BSA	Bovine serum albumin
cDNA	Complementary deoxyribonucleic acid
CGN	Cerebellar granule neuron
C_{max}	Maximum concentration
CMV	Cytomegalovirus
CNS	Central nervous system
C_t	Cycle threshold
DMEM	Dulbecco's Modified Eagle Medium
DMSO	Dimethyl sulfoxide
DNA	Deoxyribonucleic acid
dsDNA	Double stranded deoxyribonucleic acid
DTT	Dithiothreitol
E	Embryonic day
EDTA	Ethylenediaminetetraacetic acid
EEG	Electroencephalography
EGL	External germinal layer
EMA	European Medicine Agency
EURAP	The International Registry of Antiepileptic Drugs and Pregnancy
GABA	Gamma-aminobutyric acid

GABA-T	Gamma-aminobutyric acid transaminase
GABRR1	Gamma-aminobutyric acid receptor subunit rho-1
GAD	Glutamic acid decarboxylase
GAPDH	Glyceraldehyde-3-phosphate dehydrogenase
GC/MS	Gas chromatography mass spectrometry
GL	Granular layer
HAT	Histone acetyl transferase
HCl	Hydrochloric acid
HDAC	Histone deacetylase
HRP	Horseradish peroxidase
ILAE	International League Against Epilepsy
K_a	Absorption rate constant
K_{el}	Elimination rate constant
LAF	Laminar air flow
LC-MS/MS	Liquid chromatography tandem mass spectrometry
LTG	Lamotrigine
m/z	Mass-to-charge
MeOH	Methanol
MES	2-(N-morpholino)ethanesulfonic acid
ML	Molecular layer
MMP	Matrix metalloproteinase
MQ	Milli-Q
MRI	Magnetic resonance imaging
MSTFA	N-Methyl-N-(trimethylsilyl)trifluoroacetamide
MTT	MTT 3-(4,5-dimethylthiazol-2-yl)-2,5-diphenyltetrazolium bromide
NGF	Nerve growth factor
NMDA	N-methyl D-aspartate
NR2B/GluN2B	N-methyl D-aspartate receptor subtype 2B
PAX	Paired box protein
PBS	Phosphate-buffered saline

PCL	Purkinje cell layer
PCNA	Proliferating cell nuclear antigen
PLL	Poly-L-lysine
PRAC	Pharmacovigilance Risk Assessment Committee
RNA	Ribonucleic acid
rpm	Rounds per minute
RT	Reverse transcription
RT-qPCR	Quantitative reverse transcription polymerase chain reaction
S&G	Stop&Glo
SDS	Sodium dodecyl sulfate
SLC6A13/GAT-2	Solute Carrier Family 6 Member 13
$t_{1/2}$	Half-life
TBS	Tris-buffered saline
TBS-T	Tris-buffered saline polysorbate 20
TE	Ethylenediaminetetraacetic acid-Tris
TK	Thymidine kinase
T_{max}	Time to reach maximum concentration
TSA	Trichostatin A
Tween	Polysorbate 20
U	Untreated
VPA	Valproic acid/valproate

Table of contents

1 Introduction

1.1 Safety pharmacology

Countless women have medical conditions that require a continuation of drug use through gestation. Exposures to an agent that interferes with a developmental process could lead to neurotoxicity [1, 2]. With that being said, numerous factors have prevented the ability to study drugs in these patients for safe and effective use. These include concerns for maternal and foetal safety, ethical considerations, and lastly, the difficulty of designing appropriate trials to assess the study objectives [1]. Therefore, it is vital to conduct pharmacology studies in test systems (*in vivo* and *in vitro* models) to help elucidate mechanisms that can affect foetal development.

Pharmacology studies are largely divided into three categories: primary pharmacodynamics (studies on the effects related to the therapeutic target of a pharmaceutical), secondary pharmacodynamics (studies on the effects not related to the therapeutic target of a pharmaceutical), and safety pharmacology [3]. Safety pharmacology is a rapidly developing discipline that uses the basic principles of pharmacology to generate data to inform risk/benefit assessment of pharmaceuticals [4].

European Medicines Agency (EMA) developed a guideline (ICH S7A Safety Pharmacology Studies for Human Pharmaceuticals) to help protect clinical trial participants and patients receiving marketed pharmaceuticals [3, 4]. The aim of safety pharmacology is to characterise the pharmacodynamic and pharmacokinetic relationship of the undesirable effects of a drug in the therapeutic range and above on physiological functions using continuously evolving methodology [3, 4].

The core battery in safety pharmacology studies are the assessment of effects in the cardiovascular system, respiratory system, and the central nervous system (CNS). The guideline from EMA specify that safety pharmacology studies should examine motor activity, behavioural changes, coordination and sensory/motor reflexes in CNS, a matter that can be affected with the use of antiepileptic drugs (AED) during pregnancy [3]. Supplementary mechanistic studies may be included as well [5].

1.2 Epilepsy

An epileptic seizure is characterised by sudden recurrent episodes of sensory disturbance, loss of consciousness, or convulsion. This is associated with an abnormal electrical activity in the central nervous system, where AEDs are employed to try to rectify the balance between neuronal excitation and inhibition. There is no cure for this disease, as AEDs are neither preventive nor curative, and their use is solely to suppress seizures through different mechanisms [6].

In 2017, the definitions describing epileptics, the classification of seizure types, and epilepsy types, were revised by the International League Against Epilepsy (ILAE). The current operational definition states three conditions for an individual to be diagnosed as epileptic:

1. Has experienced either two unprovoked (or reflex) seizure occurring more than 24 hours apart.

2. Has experienced one unprovoked (or reflex) seizure, with more than a 60% likelihood of experiencing another after two unprovoked seizures occurring over the next 10 years.

3. A diagnosis of an epilepsy syndrome [7]. An epilepsy syndrome refers to a condition were a collection of symptoms and signs occur simultaneously, including epileptic seizure types, EEG-, and MRI findings [8, 9].

In view of the revised seizure types and the new classification (as seen in figure 1.1), ILAE maintains the primary distinction of focal- versus generalised-onset-seizures, as well as including unknown onset. Focal seizures are seizures originating from a relatively delimited area in the cerebral cortex. It may demonstrate retention or impairment of awareness, resulting in focal-aware or focal-impaired awareness seizures. Generalised seizures are seizures occurring simultaneously from both hemispheres [9, 10]. Several new focal and generalised seizure types were introduced, and are classified after their clinical appearance [11].

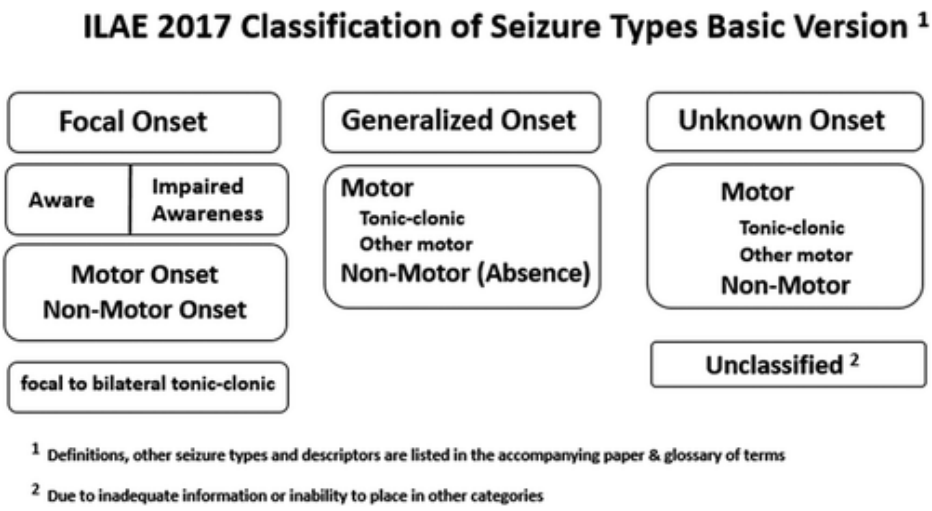

Figure 1.1 The basic classification of seizure types. ILAE introduced a revised classification of seizure types in 2017. The seizure types are divided into three categories: focal onset, generalised onset, and unknown onset. Each category contains subgroups of epilepsy types. The figure is obtained from [10].

The revisions provided by ILAE have faced criticism for being confusing, convoluted and incorrect, as well as the overzealousness of implementing these adjustments before the classifications were validated [12]. The revisions has of 2017 been translated to Norwegian for implementation by Norsk Epilepsiselskap (NES), the Norwegian branch of ILAE [11].

1.2.2 Pregnancy and antiepileptic drugs

While most women with epilepsy will experience uncomplicated pregnancies, both the mother and the foetus are at an increased risk for a range of perinatal complications compared to the general population [13, 14]. Perinatal complications are difficulties relating to the period starting a few weeks before childbirth, including birth, and a few weeks after birth [15].

Their children are at a 3-10% risk of developing major congenital malformations (neuronal tube defects, congenital heart, and oral clefts), and impaired cognitive and behavioural development (autism, and autism spectrum) owing to the exposure to an AED [13, 14]. Seizures are also believed to be detrimental, particularly convulsive seizures. Foetal bradycardia (abnormally low foetal heart rate) has been documented during maternal seizures, and additional risks include injury to the foetus, placental abruption (placental separation from the uterus), or foetal loss due to maternal trauma sustained during a seizure. The occurrence of five or more convulsive seizures (generalised tonic-clonic convulsive) during pregnancy, has been observed to be linked with delayed development in children in a study [13].

Findings across different pregnancy studies have found that different AEDs result in substantially contrasting levels of risks. Lamotrigine (LTG) carries a risk of malformations similar as for the general population (2-4%), whereas valproic acid (VPA) is associated with a several-fold increase. Nevertheless, polytherapy is the biggest risk factor, particularly a regimen including VPA [13, 14].

In addition to the specific AED in monotherapy or polytherapy, the gestational timing of the exposure and the dose of the AED are likely to be important. This has been mostly associated with VPA. The International Registry of Antiepileptic Drugs and Pregnancy (EURAP) analysed the dose at the time of conception, and reported a dose-dependent increase in major malformation rates for monotherapy with carbamazepine, phenobarbital, VPA and LTG [13].

1.3 Antiepileptic drugs

AEDs are roughly classified by their principal mode of action. These are: affecting ion channels (Na^+-, Ca^{2+}-, and K^+ channels), gamma-aminobutyric acid (GABA)-mediated inhibition, and glutamate-mediated excitation, as seen in figure 1.2 for VPA and LTG. With this being said, there are AEDs that have multiple mechanisms of action, or other mechanisms than listed [16].

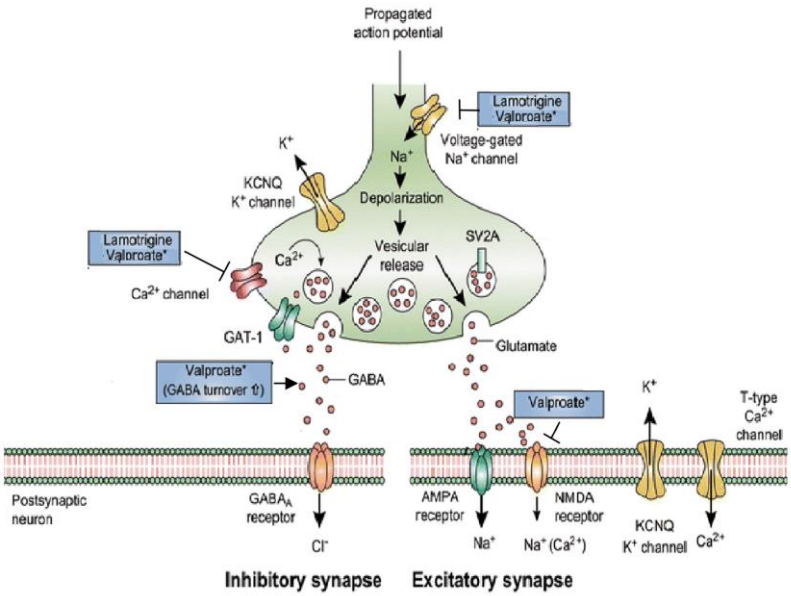

Figure 1.2 Some of the most important modes of action for VPA and LTG. VPA inhibits voltage-gated Na^+-, Ca^{2+} channels, increases GABA turnover, and may inhibit glutamatergic excitation through a blockade of NMDA receptors. LTG inhibits voltage-gated Na^+- and Ca^{2+} channels. The asterisk (*) by VPA indicate that it has multiple modes of action. This figure is obtained and modified from [17].

1.3.1 Valproic acid

VPA is a synthetic fatty acid derivative (propylpentanoic acid, figure 1.3) with antiepileptic properties. It also has mood stabilisation, potential antineoplastic, and anti-angiogenesis activities. VPA is a broad-spectrum antiseizure drug used to treat generalised- and focal seizures through monotherapy and polytherapy [16, 18].

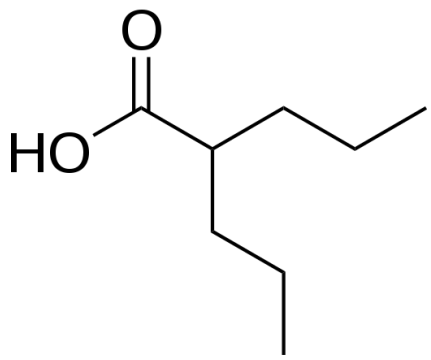

Figure 1.3 Chemical structure of valproic acid

In spite of its wide use over several years, the mechanism of action for VPA is still not completely established, and its antiepileptic action is likely due to a combination of various effects in the CNS. These effects encompass suppression of high-frequency, repetitive neuronal firing by blocking voltage-dependent Na^+ channels, and acting against T-type Ca^{2+} currents. GABA is an inhibitory neurotransmitter that is widely distributed throughout the CNS. Its activity is enhanced by VPA through affecting presynaptic $GABA_B$ receptors, as well as inhibiting nerve terminal GABA transaminase (GABA-T), and increasing GABA synthesis by activating glutamic acid decarboxylase (GAD). The synthesis of GABA is dependent upon the enzyme GAD, whilst the metabolism of GABA to succinate occurs in presynaptic neurons and glia by means of the enzyme GABA-T [16].

A theorised mechanism of the antineoplastic and anti-angiogenesis activities that VPA displays, is the inhibition of histone deacetylases (HDAC) [19]. HDAC is a family of enzymes involved in the regulation of DNA transcription. Histones are proteins with the ability to bind and pack DNA to chromatin. This packed chromatin structure with DNA and protein inhibits access to transcription due to its compressed state. HDACs are responsible of deacetylating histones wherein the chromatin structure stays tightly condensed, making DNA unavailable for transcription factors. Histone acetyltransferases (HATs) are responsible for acetylation in which

DNA becomes exposed [20]. A recruitment of HDACs leads to transcriptional repression, therefore the inhibition promoted by VPA would reverse HDAC activity and lead to a re-expression of genes (figure 1.4) [21]. *In vivo* studies have shown that HDAC inhibition of VPA is likely to be the cause of its teratogenicity [22].

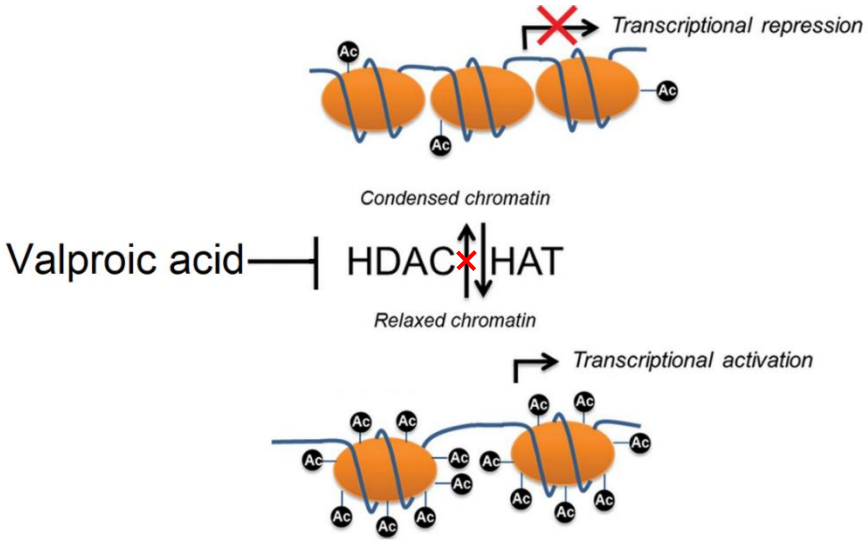

Figure 1.4 The mechanism by which gene expression is regulated by HDAC and HAT, and altered by VPA. HDACs condense chromatin, and repress transcription through deacetylation. HATs relax chromatin, and activate transcription through acetylation. VPA is an inhibitor of HDAC, and this inhibition results in a re-expression of genes. This figure is obtained and modified from [23].

VPA exposure *in utero* is associated with major malformations and other adverse effects of neuronal tube-like defects (spina bifida) in foetuses. Additional patterns of teratogenicity associated with first-trimester VPA exposure include oral clefts, as well as cardiovascular, and urogenital malformations, which are independent of any contribution of the epilepsy syndrome itself [13].

If possible, it is recommended to avoid VPA in pregnancy, and use it with restriction in fertile women. The spectrum of teratogenic effects has grown. The general understanding of effects goes further than increased risks of major congenital malformations, and includes impaired cognition and behavioural development [24, 25].

In 2014, EMA decided to strengthen the warnings of VPA use in childbearing women. These statements were among EMA's Pharmacovigilance Risk Assessment Committee's (PRAC) recommendations:

1. *"Only prescribe valproate medicines for epilepsy (and bipolar disorders) if other treatments are ineffective or not tolerated."*

2. *"Consider alternative treatments if a female patient becomes or plans to become pregnant during valproate treatment. Regularly review the need for treatment and re-assess the balance of the benefits and risks for female patients taking valproate and for girls reaching puberty."*

Epileptologists and others treating epileptics have expressed serious concerns to these recommendations. They fear that these restrictions will give rise to women and girls enduring unnecessary drug use before VPA is prescribed. This would be problematic for patients with genetic idiopathic generalised epilepsy (revised to genetic generalised epilepsy), where VPA currently is the more efficacious AED [25, 26]. Another apprehension is how these exacting recommendations could lead to a discontinuation of VPA in women who already use VPA before or during pregnancy. Without a suitable replacement, not only do they endangering themselves, but also the foetus [26].

In 2018, after concerns about how the earlier steps were insufficient to raise awareness about, and reduce the use of VPA during pregnancy, PRAC decided to introduce further measures [27-29]. VPA should not be prescribed to childbearing women or girls, unless there is no other applicable treatment. And if VPA is to be used in fertile women and girls, they should use effective contraception, and follow a strict pregnancy prevention programme [29]. The pregnancy prevention programme entails conversations to ensure that women understand the risks for major congenital malformations and neurological developmental disturbances. The programme also involves the need for regular pregnancy tests, and the use of an effective contraception during the entire treatment without deviations [30].

1.3.2 Lamotrigine

LTG is a synthetic phenyltriazine (figure 1.5) with antiepileptic, mood stabilising and analgesic properties [31, 32]. Its mode of action is not fully understood and it may also have multiple effects. LTG inhibits voltage-gated Na^+ channels, thereby blocking repetitive firing and hyperexcitability [16]. It might enhance the action of GABA, which can result in a reduction of pain-related transmission of signals along nerve fibres, as well as suppressing glutamate release,

and inhibiting serotonin reuptake [31]. It is used to treat focal seizures, and primary and secondary tonic-clonic seizures [32].

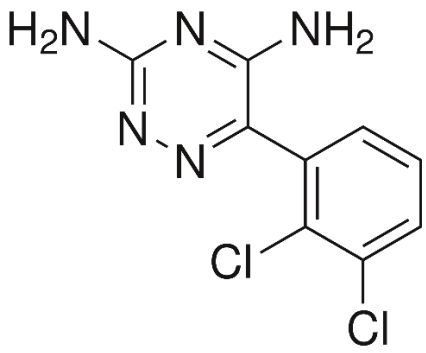

Figure 1.5 Chemical structure of lamotrigine

LTG is an AED considered safe to use during pregnancy. An observational cohort study from 2011 concluded that *in utero* exposure to LTG did not have a significant detrimental effect on child neurodevelopment as opposed to VPA. But there were still evidence of mild or significant developmental delay compared to the children in the control group [33].

Available data on the use of LTG during pregnancy are based on thousands of pregnancies that came to the conclusion that there is no increase of malformations, birth complications or delayed mental- or neuromotoric development [34]. However, the data regarding risk and dose of LTG have been conflicting.

International Lamotrigine Pregnancy Registry did not find effect on the incidence of major malformations with an LTG dose up to 400 mg/day, however the United Kingdom Epilepsy and Pregnancy Registry did observe a dose relationship. They suggested that doses higher than 200 mg/day might present a risk akin to VPA. North American Antiepileptic Drug Pregnancy Registry reported a higher than expected prevalence of cleft lip and/or cleft palate in infants exposed to LTG in the first trimester (8.9 per 1000 to the expected 0.7 – 2.5 per 1000) [13].

1.4 The central nervous system during development

The neural development is the process where the nervous system with all its components come to existence. It entails the cellular basis and the underlying mechanisms that guide the

developmental processes, including neural induction, cellular proliferation, migration, axonal guidance, and synapse formation [35]. This process initiates around the twentieth day of human embryogenesis, when the neural tube emerges giving rise to the brain and spinal cord [36]. A failure of the neuronal tube to fully close, results in functional deficits, such as spina bifida [37]. The cells from the neural tube are undifferentiated stem cells known as neural precursor cells. The anterior end of the neural tube starts to develop the components recognized as the forebrain, midbrain and hindbrain. The neural precursor cells migrate and eventually differentiate to neurons, mostly between the sixth and eighth week of gestation. Nearly all neurons are generated before the end of the second trimester, and with some exceptions, no new neurons are generated after birth [36].

After they reach their destination in the brain and spinal cord, neural precursor cells differentiate to distinctive cells types. After migration and differentiation, neurons initiate and project neurites to connect to other cells, and to transmit and receive the information that determines their ultimate function [36]. This process is called neurite outgrowth and occurs during development or regeneration of the nervous system [38]. Having reached the target cells, the axon endings form synapses [36].

As opposed to other tissues, the nervous system has a limited ability to repair injuries on neurons, since nerve cells lack the ability to regenerate themself in the CNS [39]. Therefore, a failing in CNS development may result in a variety of malformation or lead to motor/sensory, and cognitive dysfunctions [35].

1.4.1 The cerebellum

The cerebellum is a structure residing at the anterior end of the hindbrain, and is critical for the sensory-motor processing, as well as participating in cognitive and emotional functions. The cerebellum is a suitable structure to understand neuronal development, on account of its granule cells which undergo all the stages of neuronal development, such as proliferation, migration, differentiation and apoptosis in a limited time frame [40]. The cerebellar granule neurons (CGNs) are the smallest and most abundant neurons in the vertebrate brain, representing 80% of all neurons in the human brain [41].

The cerebellar cortex is composed of a very basic structure comprised of three layers, the molecular layer, the Purkinje layer and the granular layer where CGNs are packed (figure 1.6).

The external germinal layer (EGL) is a temporary population of proliferating cerebellar cells that produce CGNs. CGNs are glutamatergic, post-mitotic, and develop axons (parallel fibres) in the developing molecular layer (ML), while the somata migrate inward to the granular layer (GL, also known as internal granular layer (IGL)). ML thickens rapidly between 38 weeks of gestation and 1 year postnatally, whilst EGL disappears months postnatally [41].

CGNs migrate by extending vertically into ML, and there the CGNs elongate while migrating radially and reach the Purkinje cell layer (PCL). In GL, the CGNs migrate radially towards the white matter with the help of guidance cues [41].

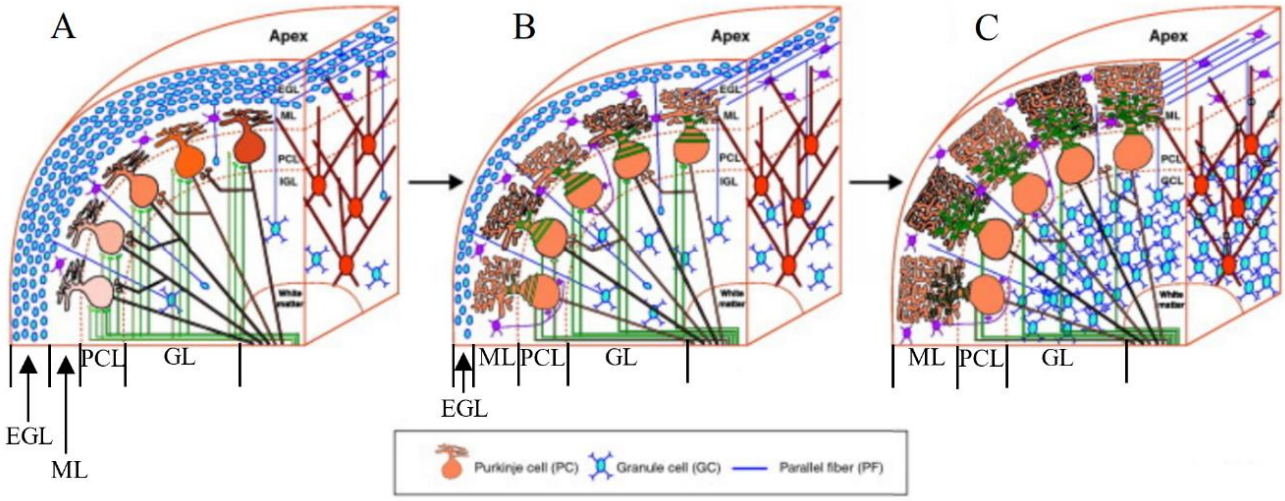

Figure 1.6 The cerebellum during development. A) CGNs proliferate in the temporary EGL, and extend axons and migrate through ML and PCL. **B)** CGNs reach GL, whilst EGL becomes smaller, and ML larger. **C)** EGL disappears, and ML and GL become larger. The figure is obtained and modified from [42].

The developing cerebellum is particularly vulnerable to clinical and environmental factors, since much of its growth in humans occurs in the third trimester and continues for a year after birth [43].

1.4.2 Molecules for neuronal development

Different molecules have been established to be of importance during neuronal development. The protein encoded by the proliferating cell nuclear antigen (*PCNA*) gene is found in the nucleus, and is a cofactor of DNA polymerase delta, which is required for DNA synthesis during replication [44, 45]. PCNA plays an important role in DNA metabolism, and is essential for DNA replication [46]. In response to DNA damage, this protein is ubiquitinated and is involved in DNA repair [44]. A mutation in *PCNA* can cause a DNA repair disorder with hearing loss, neurodegeneration, and premature aging as its characteristics [47]. The protein is present in all layers of the cerebellum during gestation, and can be used to study proliferation

in the developing human cerebellum, since its synthesis directly correlates with the proliferative state of cells [41, 48].

The paired box 6 (*PAX6*) gene belongs to a family that plays a critical role in the formation of tissues and organs during embryonic development, as well as maintaining the normal function of certain cells after birth. They do so by being transcription factors. During embryonic development, the PAX6 protein is thought to activate genes involved in the formation of the eyes, the CNS, and the pancreas [49]. Mutations resulting in a loss of *PAX6* function, have been observed to cause sight related defects including iris hypoplasia, as well as neurological and psychiatric conditions, encompassing nystagmus, impaired verbal working memory and auditory processing, autism and mental retardation [50]. In the cerebellum, *PAX6* is involved in the generation of almost all glutamatergic neurons including CGNs [41]. A disruption of *PAX6* affects neurite extension and cell migration in the cerebellar system [51].

Matrix metalloproteinase 9 (MMP9) is a member of a family of proteins that are involved in the breakdown of extracellular matrix in normal physiological processes, such as embryonic development, reproduction, wound repair, and tissue remodelling. They are also involved in physiological cellular processes, such as arthritis and metastasis. The expression and secretion of MMP9 are up-regulated in cancer and chronic inflammation [52, 53]. For an optimal function of MMP9, its level should be in a balance. Its expression is important in inducing neurite outgrowth, where low levels are associated with low regenerative capacity of CNS axons, which is heightened during embryonic development [54, 55]. The expression of the *MMP9* gene is modulated by PAX6 [56].

The brain-derived neurotrophic factor (*BDNF*) gene provides instructions for making BDNF, a growth factor found in the CNS [57]. The BDNF protein plays a role in the growth, differentiation, and maintenance of neurons by promoting their survival. In the brain, BDNF positively regulates the proliferation and migration of CGNs, as well as being active at the synapses [41, 57]. Synapses can change and adapt over time in response to experience referred to as synaptic plasticity, which the BDNF protein helps to regulate. This is important for learning and memory [58]. A dysregulation of BDNF has been implicated in neurodegenerative diseases, such as Alzheimer's disease, Parkinson's disease, and multiple sclerosis. A deficiency may contribute to an accelerated cell damage [57].

Glutamate ionotropic receptor NMDA type subunit 2B gene (*GRIN2B,* also known as *NR2B)* provides instructions for making a protein called GluN2B. GluN2B is a subunit of NMDA receptors which acts as an agonist binding site for glutamate found in neurons in the brain, primarily during embryonic development. NMDA receptors are ionotropic, and the attachment of glutamate and glycine to the receptor, allows cations to flow through. The flow of cations excites neurons to depolarise and leads to the production of an action potential. The cation flow of Ca^{2+} plays a role in differentiation. NMDA receptors are involved in normal brain development, synaptic plasticity, learning, and memory [59]. Naturally occurring mutations in *GRIN2B* have been associated with neurodevelopmental disorders including autism spectrum disorder (ASD), attention deficit hyperactivity disorder (ADHD), epilepsy, and schizophrenia [60].

Gamma-aminobutyric acid receptor subunit rho-1 (GABRR1) is a member of the rho subunit family, which are seen as a subunit of $GABA_A$ receptors. It is an ionotropic Cl^- channel [61]. A GABA mediated activation of this receptor promotes Cl^- efflux, leading to a hyperpolarisation. At an early developmental stage in the CNS, GABA acts in an excitatory manner, leading to a depolarisation through Cl^- influx. An activation of $GABA_A$ in immature neurons stimulates the opening of voltage-gated Ca^{2+} channels, which exerts trophic effects through a triggering of BDNF synthesis and release [62, 63]. This is implicated in proliferation, migration, differentiation, and synaptogenesis [63].

The excitatory effects GABA displays during embryonic development, are associated with the levels of transporters, NKCC1 ($1Na^+/2Cl^-/1K^+$) and KCC2 ($1K^+/1Cl^-$) co-transporter (figure 1.7) [64, 65]. In the immature neuron, NKCC1 transporter is highly expressed, promoting a high intracellular Cl^- concentration, thereby causing a depolarisation when GABA is activating its Cl^- channels [64, 65]. Solute Carrier Family 6 Member 13 (SLC6A13, also known as GAT-2) is a Na^+- and Cl^--dependent GABA transporter that keeps the extracellular levels of the neurotransmitter low, as well as providing amino acids for metabolic purposes [66, 67]. GAT-2 terminates GABA action by reuptake into presynaptic terminals or glial cells [68]. The transporter has been proposed to have a role in development because of its abundance in neonatal mice brains and how it can be found in the cerebellum [69].

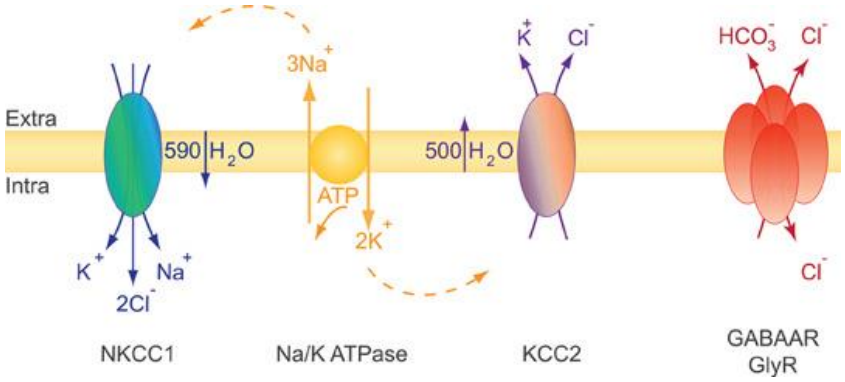

Figure 1.7 The transport properties of the co-transporter NKCC1 and KCC2 in relation to $GABA_A$. NKCC1 and KCC2 use energy to trigger an influx of $1Na^+$, $1K^+$, and $2Cl^-$ (NKCC1) or an efflux of $1K^+$, and $1Cl^-$ (KCC2). NKCC1 predominates during development, and leads to a depolarising effect of GABA via an efflux of Cl^- through $GABA_A$ receptors. The figure is obtained from [70].

1.5 Model systems

To explore the effects of LTG and VPA on the developing nervous system, *in vivo* experiments were performed in chicken embryo cerebella and brain exposed to LTG and VPA *in ovo*. *In vitro* studies were also employed, using chicken embryo cerebella cultures and PC12 cells.

1.5.1 The chick embryo model

A classic model to observe developmental processes in a higher vertebrate, is the chicken embryo. In early stages, the chicken embryo morphology is similar to humans, and experiments in chicken have elucidated the underlying mechanisms of human genetic diseases, and provided a basis for testing novel therapies [71].

There are several advantages for adopting the chicken embryo model. Fertilised eggs can be obtained from poultry farms, thereby eliminating the necessity to breed and house adult animals in facilities. The ability to order the exact amount of eggs needed for each experiment contributes to 3R (reduce, replace, refine) in ethical guidelines pertaining testing on animals [71]. The eggs are self-sustained, and are of a convenient size. They have a short 21-day incubation time, in addition to originating from different mothers, thereby introducing a genetic variation between the chicken embryos [72]. The fact that the eggs develop almost entirely outside the mother, excludes the hens from the experiments as well.

1.5.2 The PC12 model

PC12 cells are an established cell line derived from a pheochromocytoma of the rat adrenal medulla. It has been used to create artificial nervous system tissue models to study neurodegeneration [73, 74].

PC12 cells have an ability to undergo neuronal differentiation (neurite outgrowth and arrested proliferation) in response to nerve growth factor (NGF) [75, 76]. The cell line has been the subject of numerous studies, and is therefore vastly studied with respect to its properties. Advantages of employing PC12 cells are their capacity for proliferation, where they can be produced in a large amount with minimum effort, and they permit rapid experiments. Since they are derived from a single progenitor, they represent a relatively homogenous population that can be used to replicate cultures [76].

1.6 The aim of the study

An epileptic seizure during pregnancy can cause severe consequences for both the woman and the foetus. It is therefore vital to continue the use of AEDs during gestation. Nonetheless, some AEDs are teratogenic. LTG is considered as the safer option, but some reports claim that the risks are higher than initially believed. VPA is an AED with extensive documentation of an elevated risk of developing major malformations. But then again, with its broad spectrum, it might be the only option for certain epilepsies. The aim of this thesis is to examine how these two AEDs affect neuronal development.

Secondary objectives have been:

1. Examining the distribution of the AEDs to the brain of chicken embryos after injection into the brain.

2. Exploring if the AEDs affect *PAX6*, *PCNA*, *BDNF*, *GRIN2B*, *SLC6A13*, and *GABRR1* gene expression in RT-qPCR, and if the PAX6, PCNA and GluN2B effects can be reproduced through western blotting, including MMP9.

3. Exploring how the AEDs affect PAX6 and MMP9 promotor activity with both PC12 cells, and chicken CGNs.

4. Exploring effects of the AEDs on neurite outgrowth in CGNs.

2 Materials and methods

2.1 Overview of chemicals, biological products, and equipment

Table 2.1 Chemicals and biological products

Product:	**Supplier:**
2-mercaptoethanol	Sigma-Aldrich, St. Louis, USA (now MERCK)
Adenosine triphosphate (ATP)	Sigma-Aldrich, St. Louis, USA (now MERCK)
Anti-B-actin	Sigma-Aldrich, St. Louis, USA (now MERCK)
Anti-MMP9 (Lot 3-T6879)	Enzo Life Science Inc, Farmingdale/New York, USA
Anti-NR2B (Lot GR3183264-1)	Abcam, UK
Anti-PAX6 (rabbit polyclonal) (Lot 2776793)	Millipore Corporation, Billerica, USA (now MERCK)
Anti-PCNA	Dako Denmark A/S, Glostrup,
BioWhittaker's® DMEM (Dulbecco's Modified Eagle's Medium)	Lonza, Verviers, Belgium
Bovine serum albumin (BSA)	Sigma-Aldrich, St. Louis, USA (now MERCK)
Bromophenol blue	MERCK KGaA, Darmstadt, Tyskland
Calcium chloride ($CaCl_2$)	MERCK KGaA, Darmstadt, Tyskland
Cellstoff 20x20 cm	Mediq Norge AS, Kløfta, Norway
Cytosine β-D-arabinofuranoside (AraC)	Sigma-Aldrich, St. Louis, USA (now MERCK)
Deoxyribonuclease I (DNase I)	Sigma-Aldrich, St. Louis, USA (now MERCK)
Dimethyl sulfoxide (DMSO)	Sigma-Aldrich, St. Louis, USA (now MERCK)
Dithiothreitol (DTT)	Sigma-Aldrich, St. Louis, USA (now MERCK)

D-Luciferin free acid (Lot 6C014615)	PanReac AppliChem ITW Reagents, USA
Dry milk	Normilk AS, Levanger, Norway
Elfo buffer	Bio-Rad Laboratories Inc, USA
Goat anti-mouse IGG-HRP	Bio-Rad Laboratories Inc, USA
Hoechst 33342	Invitrogen Molecular Probes™, Oregon, USA
Immobilon® Classico Western HRP Substrate	Millipore Corporation, Billerica, USA (now MERCK)
Immobilon® Crescendo Western HRP Substrate	Millipore Corporation, Billerica, USA (now MERCK)
K2® Transfection system	Biontex, Germany
Lamotrigine	Sigma-Aldrich, St. Louis, USA (now MERCK)
Lamotrigine isethionate	Tocris Bioscience, Bristol, UK
Leupeptin	Sigma-Aldrich, St. Louis, USA (now MERCK)
L-glutamine	Sigma-Aldrich, St. Louis, USA (now MERCK)
Luminata™ Crescendo Western HRP Substrate	Millipore Corporation, Billerica, USA (now MERCK)
Luminata™ Forte Western HRP Substrate	Millipore Corporation, Billerica, USA (now MERCK)
Mouse anti-rabbit IgG-HRP	Santa Cruz Biotechnology
MTT (3-(4,5-dimethylthiazol-2-yl)-2,5-diphenyltetrazolium bromide)	Thermo Fisher Scientific, Waltham, MA, USA
Na_3VO_4 (sodium orthovanadate)	Sigma-Aldrich, St. Louis, USA (now MERCK)
Penicillin-Streptomycin	Invitrogen Company, California, USA
Pepstatin A	Sigma-Aldrich, St. Louis, USA (now MERCK)
Phenylmethylsulfonyl fluoride (PMSF)	Sigma-Aldrich, St. Louis, USA (now
Poly-L-lysine hydrobromide (PLL) (Lot SLBJ7844V)	Sigma-Aldrich, St. Louis, USA (now MERCK)
Ponceau S	Sigma-Aldrich, St. Louis, USA (now

Precision Plus Protein All Blue Standards	Bio-Rad Laboratories Inc, USA
Precision Plus Protein™ Dual Color Standards	Bio-Rad Laboratories Inc., USA
Restore™ Western Blot Stripping Buffer	Thermo Fischer Scientific, Rockford, USA
Sodium chloride (NaCl)	VWR BDH Chemicals, Belgium
Sodium dodecyl sulfate (SDS)	Sigma-Aldrich, St. Louis, USA (now
Trans-blot buffer	Bio-Rad Laboratories Inc, USA
Tris/Glycine/TGS, 10X	Bio-Rad Laboratories Inc, USA
Trypsin	Sigma-Aldrich, St. Louis, USA (now MERCK)
Trypsin inhibitor	Sigma-Aldrich, St. Louis, USA (now MERCK)
Tween® 20	Sigma-Aldrich, St. Louis, USA (now MERCK)
Valproic acid sodium salt	Sigma-Aldrich, St. Louis, USA (now MERCK)

Table 2.2 Equipment	
Product:	**Supplier:**
2720 Thermal Cycler	Applied Biosystems
Alkotip®	Medguard, Ireland
Bio-Rad Power Pac 300	Bio-Rad Laboratories Inc, USA
Biosphere® Filter Tips	Sarstedt, Germany
ChemiGenius Bio Imaging System	Syngene, VWR International
CLARIOstar®	BMG Labtech, Germany
Corning Centristar centrifugation tubes	Corning Inc, NJ, USA
Costar® Cell lifter	Corning incorporated, NY, USA
CPA225D Laboratory Balance	Sartorius, Germany
Cryotube™ Nunc™ Vials	Thermo Scientific, Rockford, USA
Disposable scalpel	Swann-Morton Ltd., Sheffield, England
Disposable syringe	Terumo Europe, Leuven, Belgium

Disposable syringe	B. Braun, Germany
Eppendorf tubes	Eppendorf AG, Hamburg, Germany
Holten LaminAir, model 1.2 LAF bench	Eco Holten AS, Denmark
IncuCyte®	Essen BioScience, USA
IncuCyte® ImageLock Plates	Essen BioScience, USA
Kubota 2010 Centrifuge	Kubota Corp., Japan
LightCycler ® 480	Roche, Switzerland
Lumat LB 9507 Luminometer	EG&G, Germany
Mini-PROTEAN® TGX™ Gel (4-20%)	Bio-Rad Laboratories Inc, USA
MQ water apparatus (MilliQ 5)	Merck, Darmstadt, Germany
Multiply® µStrip (0.2 mL)	Sarstedt, Germany
Neubauer 0.100 mm Tiefe Depth Profondeur	Assistant, Germany
Nunc™ Cell culture dishes (8.8 cm^2)	Thermo Scientific, Waltham, MA, USA
Nunc™ Cell culture flask (75 cm^2)	Thermo Scientific, Waltham, MA, USA
Nunc™ Clear 96-well Plates	Thermo Scientific, Waltham, MA, USA
Ova Easy Advance II series incubator	Brinsea®, USA
Pellet pestle®	Kimble Chase, USA
Pierce™ BCA Protein Assay Kit	Thermo Scientific, Rockford, USA
Pipette Boy Costar Corning	Corning Inc, NJ, USA
Pipette tips (Optifit tips)	Sartorius Biohit, Finland
Qiagen Kit	Qiagen, USA
Sterile filter (0.2 µm)	Whatman, Germany
Stuart™ Roller Mixer SRT9	Bibby scientific Ltd., Staffordshire, UK
Sub Aqua 12 water bath	Grant, England
ThermForma Steri-Cycle CO_2-incubator	Thermo Scientific, Waltham, MA, USA
Trans-Blot® RTA Transfer Kit Blotting equipment	Bio-Rad Laboratories, USA
Trans-Blot® Turbo™ Transfer System Blotting machine	Bio-Rad Laboratories Inc, USA
Whirl mixer	Terumo lab AS, Sweden

2.2 Chicken embryo

Fertilised chicken eggs (*Gallus gallus*) from Nortura in Våler were kept in an incubator (Ova Easy Advance II series ®) at 37 °C. Optimal humidity (45%) was sustained by adding water to an associated chamber, and the eggs, placed in racks, were mechanically tilted, mimicking the brooding of a hen.

2.2.1 *In ovo* exposure of chicken embryos

VPA and LTG were injected on embryonic day 16 (E16), as well as embryonic day 13 (E13) for pharmacokinetics. Firstly, the eggs were transilluminated to determine viability, as well as identifying a suitable point for injection. The injection point was proximal to blood vessels to ensure a thorough distribution within the eggs, yet distant enough to prevent accidental puncturing.

The injection point was punctured with a small pick after the area was sterilized with 70% isopropyl alcohol swab (Alkotip®). With a volume equivalent to 1 µL/gram egg of the desired exposure (table 2.3), the eggs were injected with a sterile needle (30G) and incubated until harvest.

Table 2.3 Exposure of chicken embryos

Exposure	**Final concentration in the egg**
Valproic acid (900-1000 mM stock solution)	0.9-1 µM, 9-10 µM, 90-100 µM, 450-500 µM, 900-1000 µM
Lamotrigine isethionate (5 mM stock solution)	5 µM
Lamotrigine (42 mM stock solution)	4.2 µM, 10 µM, 25 µM
DMSO	0.1%
Saline	0.0009%

2.2.2 Harvesting of the entire brain

The exposure of chicken embryos for pharmacokinetics was in accordance to the procedure formerly described in section 2.2.1, and shown in table 2.4. An assortment of eggs was injected on E13, whilst a second was injected on E16. The brains of the embryos were extracted after exposure to VPA dissolved in saline, LTG isethionate dissolved in saline or LTG dissolved in DMSO, after certain time-points. Postdoctoral Fellow, Mussie Ghezu Hadera from Section for Pharmacology and Pharmaceutical Biosciences injected VPA on E13, and performed the subsequent harvest.

On E13, the eggs were injected with a brain isolation after 15 minutes, 30 minutes, 1 hour, 2 hours, 4 hours, 6 hours, 12 hours, 48 hours, and 72 hours. On E16, eggs were injected with a brain isolation after 5 minutes, 15 minutes, 30 minutes, 1 hour, 2 hours, 4 hours, 6 hours, 12 hours, and 24 hours. The chicken embryos were sedated through submergence in crushed ice for 7 minutes, however, brains exposed for 5 minutes were unable to be anaesthetised on account of how the 7 minutes are included in the exposure time. The eggs were cracked in a 14 cm sterile petri dish with the embryos decapitated with a sterile scalpel. The brain was isolated with the use of scissors, tweezers and a spatula.

The extracted brain was washed in saline to remove excess drug and dried with paper ahead of transfer to a cryotube. The cryotube was put in a Styrofoam box containing liquid nitrogen (-196 °C), before storage in -80 °C.

Table 2.4 Exposures for pharmacokinetics

Exposure	**Final concentration in the egg**
Valproic acid (100 mM and 1000 mM stock solution dissolved in saline)	100 µM, 500 µM, 1000 µM
Lamotrigine isethionate (5 mM stock solution dissolved in saline)	5 µM
Lamotrigine (42 mM stock solution dissolved in DMSO)	4.2 µM, 10 µM, 25 µM

2.2.3 Harvesting of the cerebellum

Chicken embryos where the cerebellum was isolated for western blotting (section 2.5) or RT-qPCR (section 2.6), were exposed on E16. On embryonic day 17 (E17), the eggs were

submerged in crushed ice for 7 minutes to anesthetize the embryos through hypothermia before the isolation. The eggs were cracked in a 14 cm sterile petri dish with the embryos decapitated with a sterile scalpel. Scissors, tweezers and a spatula were utilised for the cerebella extraction. After removing the meninges, the cerebella were transferred to a cryotube and temporarily stored in liquid nitrogen (-196 °C) for instant freezing. The samples were stored in -80 °C.

2.2.4 Preparing of CGN culture

Chicken embryo cerebella were also used to make cerebellar granular neurons (CGNs) for transfection (section 2.7) and neurite outgrowth (section 2.8). Since CGNs have a difficulty adhering to dishes and plates, the adherence was enhanced by precoating them with poly-L-lysine (PLL). Whilst adsorbed PLL forms a polycationic layer in the dishes and plates, cells have a polyanionic surface. Their interaction leads to the adhesion of cells [77].

A 0.5 mg/mL PLL solution was prepared by adding 10 mL MQ-water to 5 mg PLL. The solution was diluted to 0.01 mg/mL, before 1 mL of this solution was added to dishes, and 100 µL in each well for 96-well plates. PLL was removed after 30-60 minutes, and if the dishes/plates were going to be plated with the CGN the following day, the dishes/plates were left partially open in the hood. If they were to be plated on Monday, then the dishes/plates were left closed in the hood with the air speed at maximum strength on Friday the week before.

To make CGNs, eggs from E17 were sunk in 70 % ethanol to sterilize the surface before decapitation. After decapitating the embryos, the heads were transferred to a laminar air flow (LAF) bench.

In the LAF bench, the cerebella were extracted and placed in a petri dish were the meninges were removed using tweezers. The cerebella were piled in the middle of the dish and chopped with a scalpel in two perpendicular directions.

To the petri dish containing the chopped cerebella, 10 mL of solution 1 (table 2.5) was added, and the mixture was transferred to a 50 mL tube. The tube containing the mixture was centrifuged at 1000 rpm for 1 minute with a Kubota 2010 Centrifuge. Solution 1 is a physiological solution containing Mg^{2+} and Krebs-Ringer solution (table 2.6). Mg^{2+} is an essential mineral with, reportedly, a fundamental role in cellular processes including

proliferation, survival, and differentiation of cell cultures. Krebs-Ringer solution preserves an optimal pH range, and contains several salts for tissue maintenance [78].

The supernatant resulting from the centrifugation was removed, and 8 mL of solution 2 (table 2.5) was added. Solution 2 contains trypsin, an enzyme that cleaves proteins, and helps to produce a suspension of neuronal cells from the cerebella [79]. The pellet, resultant from the centrifugation, was dispersed with a pipette. The suspension was transferred to a trypsinizing flask with the cap loosely attached, and placed in a water bath for 15 minutes at 37 °C. This was to further convert the tissue to a cell suspension, and was enhanced by periodically shaking the flask to agitate the tissue [80].

The suspension was transferred to a 50 mL tube containing 15 mL of solution 4 (table 2.5). Solution 4 is a mixture of solution 1 and 3 (table 2.5), with the latter containing a trypsin inhibitor and DNase I. The trypsin inhibitor prevents further destruction of proteins, whilst DNase I removes DNA from protein preparations, and reduces cell clumping [81, 82]. The tube was centrifuged at 1000 rpm for 2 minutes. If the supernatant was non-translucent, a small amount of solution 3 was added and the centrifugation was repeated. An equal amount of the supernatant was removed before an amount of solution 3 was added.

The clear supernatant was removed from the tube, and 3 mL of solution 3 was added to disperse the pellet by trituration with a glass pipette. Afterwards, the suspension was left to stand for the tissue to sediment. The newly formed supernatant containing single cells, was transferred to a sterile tube containing 15 mL of solution 5 (table 2.5). Solution 5 is solution 1 including more Mg^{2+} and Ca^{2+}. Ca^{2+}, as Mg^{2+}, is also an essential mineral, and is important for metabolic processes, replication and enzyme activities [83]. An amount of solution 3 (2 mL) was added to the original tube containing the sedimented cells, and left to sediment to reduce more cell clumping. The supernatant was transferred to the tube containing solution 5 until there were no visible clumps.

The tube containing the supernatants in solution 5 was centrifuged at 900 rpm for 7 minutes, and 10 mL of the plating medium (table 2.7) was added. To count the number of cells, 10 µL of this solution was diluted to 100 µL, wherein 20 µL was transferred to a Neubauer counting chamber.

After the cell counting, the cell suspension with the plating medium was diluted to ensure that the cells were plated at a density of 1.7-1.9 x 10^6/mL. Dishes for transfection (section 2.7) and plates for neurite outgrowth (section 2.8) were plated as detailed in table 2.9.

The dishes and plates with cells in plating medium, were incubated at 5% CO_2 and 37 °C overnight before the plating medium was replaced with a defined feeding medium (table 2.8) for transfection (section 2.7), or exposed with treatment for the measurement of neurite outgrowth (section 2.8).

Table 2.5 Solutions used for the preparation of chicken cerebellar granule neurons

Solution	**Reagent**	**Quantity**
Solution 1	Bovine serum albumin (BSA)	1.5 g
	10X Krebs-Ringer solution (table 2.6)	50 mL
	$MgSO_4$ (38.2 mg/mL distilled water)	4 mL
	Distilled water	ad 500 mL
Solution 2	Trypsin	25 mg
	Solution 1	100 mL
Solution 3	Trypsin inhibitor	26 mg
	DNase 1	6.2 mg
	$MgSO_4$ (38.2 mg/mL distilled water)	0.5 mL
	Solution 1	ad 50 mL
Solution 4	Solution 1	100 mL
	Solution 3	16 mL
Solution 5	Solution 1	40 mL
	$MgSO_4$ (38.2 mg/mL distilled water)	320 µL
	$CaCl_2$ (12.0 mg/mL distilled water)	320 µL
Solutions were made right before use. **Solutions 1 was made in an Erlenmeyer flask with a magnetic stirrer.** **Solution 1-5 were sterile filtered using 0.2 µm filters.** **The volumes are for cell cultures with up to 80 chicken embryo cerebella.**		

Table 2.6 10X Krebs-Ringer solution	
Reagent	**Final concentration**
NaCl	1.21 M
Glucose	0.14 M
$NaHCO_3$	0.25 M
KCl	48 mM
KH_2PO_4	12 mM
Phenol red	0.28 mM
Distilled water	ad 500 mL
The solution was sterile filtered 0.2 µm, and stored at 2-8 °C for up to 6 months.	

Table 2.7 Plating medium for chicken cerebellar granule neurons		
Reagent	**Final concentration in medium**	**Quantity**
Basal Medium Eagle (GIBCO)	-	500 mL
Warm inactivated chicken serum, Biowest	7.5 %	37.5 mL
KCl	22 mM	825 mg
Glutamine sigma G-8540	2 mM	146 mg
Penicillin-Streptomycin (10 000 U/mL – 10 mg/mL)	1%	5 mL
Insulin 16634 (Sigma)	100 nM	50 µL from 1 mM stock (5.7335 mg dissolved in 1 mL distilled water with pH 2.0)
KCl and Glutamine were weighed in a 50 mL tube, dissolved in the medium and sterile filtered 0.2 µm back to the medium bottle. The plating medium was stored at 2-8 °C.		

Table 2.8 Feeding medium for chicken cerebellar granule neuronal cells		
Reagent	**Final concentration in medium**	**Quantity**
Basal Medium Eagle (GIBCO)	-	500 mL
KCl	22 mM	825 mg
Glutamine sigma G-8540	2 mM	146 mg
Penicillin-Streptomycin (10 000 U/mL – 10 mg/mL)	1%	5 mL
h-Transferrin T-0665 (Sigma)	100 µg/mL	50 mg
Putrescin P-5780 (Sigma)	60 µM	4.8 mg
Insulin 16634 (Sigma)	25 µg/mL	12.5 mg dissolved in 6.25 mL distilled water with pH 2.0
Triiodothyronine (T_3)	1 nM	17 µL from 20 µg/mL stock solution
Sodium selenite (Na_2SeO_3)	30 nM	150 µL from 100 µM stock solution
Dry matter was weighed in a 50 mL tube, dissolved in the medium, and sterile filtered 0.2 µm back to the medium bottle. The feeding medium was stored at 2-8 °C.		

Table 2.9 Plating of CGN			
Analysis	**Type of plate**	**Volume of the medium**	**Cell density**
Neurite outgrowth	96 well-plate	100 µL	1.7-1.9 x 10^6/mL
Transfection	Small dishes (8.8 cm^2)	1 mL	1.7-1.9 x 10^6/mL

2.3 PC12 cells

PC12 cells were cultivated in a 75 cm^2 cell culture flask in an incubator at 37 °C, and 5% CO_2. The cells were spilt in a LAF bench twice a week when the PC12 cells reached confluency for maintenance or for plating in dishes/plates for experiments. During splitting, the media in the flask was replaced with a new PC12 medium (table 2.10) before the cells were dislodged by

hitting the flask. The resulting cell suspension was triturated with a pipette until there were no noticeable clumps visible under the microscope. After removing the cell suspension, the original and a new flask were added with 20 mL of PC12 medium, and 1.5 mL of the cell suspension before incubation (37 °C and 5% CO_2).

Proceeding the splitting, PC12 cells could be plated for experiments. For this, 20 µL of the cell suspension was transferred to a Neubauer counting chamber. There, three 4x4 fields were counted to estimate the density, and furthermore, estimate the required volume to add $7x10^4$ cells/mL in each dish for transfection, and $3.5x10^4$ cells/mL in each well for both MTT assay (section 2.9) and Hoechst staining (section 2.10). Table 2.11 details the density and volume used for PC12 cells experiments. The dishes and plates were incubated (37 °C and 5% CO_2) for 24 hours before transfection (dishes), or 48 hours before exposure for MTT assay and Hoechst staining (plates). Experiments were performed on undifferentiated PC12 cells from passage 5-25.

Table 2.10 PC12 medium

Reagent	**Final concentration in medium**	**Quantity**
Dulbeccos Modified Eagles Medium with L-Glutamine (DMEM)	-	500 mL
Fetal bovine serum (FBS), Biowest	10 %	50 mL
Horse serum (HS), Gibco™	5 %	25 mL
Penicillin-Streptomycin (10 000 U/mL – 10 mg/mL) (PS)	1%	5 mL
Sodium Pyruvate (P)	1 mM	5 mL
Reagents were added to DMEM in a LAF-bench. The PC12 medium was stored at 2-8 °C.		

Table 2.11 Plating of PC12 cells			
Experiment	**Type of plate**	**Volume of the medium**	**Cell density**
Transfection	Small dishes (8.8 cm^2)	1 mL or 2 mL	$7x10^4$/mL
MTT-analysis	96 well-plate, clear	200 µL	$3.5x10^4$/mL
Hoechst staining	96 well-plate, black bottomed	200 µL	$3.5x10^4$/mL

2.4 Pharmacokinetics

Pharmacokinetics is the study of the movement of drugs into, through, and out of an organism. This entails the time course of its absorption, distribution into blood and tissue, conversion to active or inactive metabolites and lastly, the elimination from the organism [84]. Through pharmacokinetics, one can establish the relation between dose, plasma or tissue concentrations, and therapeutic or toxic effects of a drug [85].

2.4.1 Homogenisation

Isolated brains were individually weighed to estimate the amount of MQ-water needed for homogenisation. The volume (mL) of MQ-water per brain equated the weight in mg in the ratio 1:2 (brain:MQ water). Brains in cryotubes were added cold MQ-water and homogenised with an electric, rotating pestle (Pellet pestle®). The homogenate (100 µL) was added to two 5 mL tubes, and instantly frozen with liquid nitrogen (-196 °C). The tubes were corked and temporarily placed in -20 °C before storage in -80 °C.

2.4.2 GC/MS

Gas chromatography mass spectrometry (GC/MS) was used to analysed the samples exposed to VPA. GC/MS is an analysis method for small and volatile molecules. GC/MS begins with gas chromatography, where the sample is vaporised (gas phase) and its various components separated using a capillary column packed with a stationary (solid) phase. The compounds are propelled by an inert carrier gas, and as the components become separated, they elute from the column at different times, referred to as their retention time. After passing through the GC column, the components are ionised by the mass spectrometer using electron or chemical

ionisation sources. Ionised molecules are then accelerated through the instruments mass analyser and it is here that the ions are separated by their different mass-to-charge (*m/z*) ratios [86].

This analysis was performed by Gerd-Wenche Brochmann at The Department of Forensic Science at Oslo University Hospital, as well as the sample preparation. For details about the conditions of the GC/MS analysis, see Appendix I.

VPA sample preparation

For the standard and the control (Appendix I) to have the same conditions as the samples, 50 µL were added to 50 µL negative (untreated) chicken brain homogenates, whilst 50 µL MQ-water was added to the blank sample (0-sample). Of the internal standard, cyclohexanecarboxylic acid (800 µM), 50 µL was added to all the samples before they were mixed with a multimixer. Thereafter, 1 mL 0.2 M hydrochloric acid (HCl), and 500 µL hexane were added for extraction. The samples were corked and turned up and down for 15 minutes before a 10-minute centrifugation (4500 rpm and 4 °C). Following the centrifugation, 200 µL of the organic phase was transferred to brown autosampler glasses, and 50 µL of N-Methyl-N-(trimethylsilyl)trifluoroacetamide (MSTFA) was added to the samples. The samples were left to stand for 15 minutes before injection in GC/MS.

2.4.3 LC-MS/MS

Liquid chromatography tandem mass spectrometry (LC-MS/MS) was used to analyse the samples exposed to LTG. LC-MS/MS is an analytical technique that combines separation from liquid chromatography with the highly selective mass analysis capability of mass analyser (quadruple) mass spectrometry. Firstly, a sample solution containing analytes of interest flows through a stationary phase (LC column) with a mobile phase at high pressure. After elution, the effluent is directed to the mass spectrometer. This mass spectrometer has an ionisation source where the effluent becomes nebulised, desolvated, and ionised. The charged particles migrate through a series of two of quadruples. The first quadruple targets a specific precursor ion, excluding other particles with differing *m/z*. The precursor ion is fragmented into product ions by a collision of an inert gas. The final quadruple targets specific product ion fragments which is then quantified [87].

The preparation of the samples, and the analysis, was performed by Gerd-Wenche Brochmann at The Department of Forensic Science at Oslo University Hospital. For details about the conditions of the LC-MS/MS analysis, see Appendix II.

LTG sample preparation

LTG was extracted from the brain homogenate through a precipitation reaction. For the standards and control (Appendix II) to have the same conditions as for the samples, 100 µL was added to 100 µL of negative chicken brain homogenate. The 0-sample did not contain any chicken brain homogenate. In a fume hood, 100 µL 5mM ammonium acetate buffer with pH 3.1 in methanol (MeOH) (50:50), was added to all the samples, including the 0-sample. This step was to extract LTG from the brain homogenate. All the samples were kept in an ice bath throughout the sample preparation.

With a Multipette®, 50 µL of the internal standard, methaqualone (5 µM), was added in a fume hood before the samples were mixed with a multimixer (0-sample did not contain methaqualone). Each sample was added 500 µL of cold acetonitrile (ACN)/MeOH solution (85:15) before immediately mixing with a whirl mixer. The samples were further agitated on a multimixer for 1 minute before storage in -20 °C for 10 minutes. A 10-minute centrifugation (4500 rpm at 4 °C) ensued before 100 µL MQ-water was added, and 100 µL of the ACN/MeOH phase was transferred to auto sampler vials for LC-MS/MS analysis.

2.5 Western blot

Western blot or western blotting is a method used for detecting and analysing proteins extracted from cells or tissue [88]. This method detects specific proteins by its molecular weight and binding specificity of antibodies to the proteins. The samples are transferred to a gel, and further to a membrane for the proteins to be identified and quantified (figure 2.1).

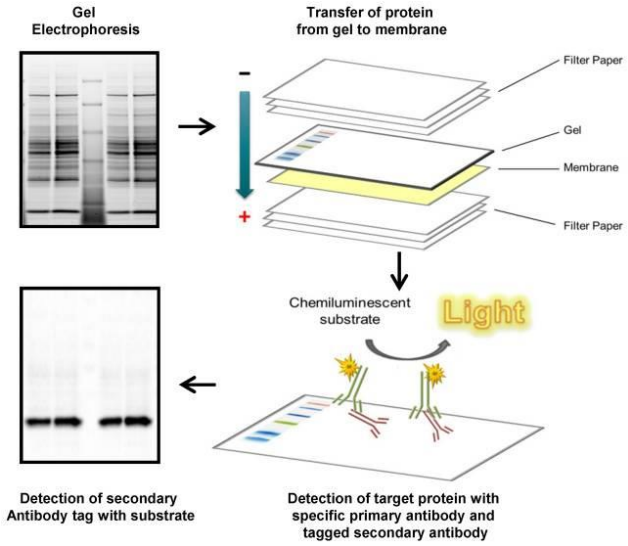

Figure 2.1 The process of western blot. Western blot requires samples to be transferred to a gel, where the proteins are separated through gel electrophoresis based upon their molecular mass. Afterwards, the proteins from the gel is transferred to a membrane arranged between two stacks of filters. The membrane is incubated with a primary antibody for a specific protein, before incubation with a secondary antibody to detect the primary antibody. The secondary antibody catalyses an enzymatic reaction with a horseradish peroxidase substrate, which can be detected by a digital imager. The figure is obtained from [89].

2.5.1 Sample preparation

The sample preparation consisted of homogenisation of the cerebellum and measuring of the amount of protein. The Eppendorf tubes containing the cerebellum, was added 300 µL of TE-buffer with protease inhibitors (table 2.12), before homogenisation with Pellet pestle®. Protease inhibitors prevent natural degradation of the samples. Afterwards, 300 µL of TE-buffer with 4% sodium dodecyl sulphate (SDS) (table 2.12) was added, and the homogenate was further homogenised with a needle (21G) and a syringe. The homogenate was boiled for 2 minutes at 95 °C, before a dilution (1:20) was made with TE-buffer: 10 µL of the sample and 190 µL of the TE-buffer.

Pierce™ BCA Protein Assay Kit was used to determine the amount of protein in the diluted samples. From the kit, a working reagent was prepared with 50 parts reagent A and 1 part reagent B. A standard solution of 0.5 mg/mL bovine serum albumin (BSA) was made by diluting 2 mg/mL BSA with PBS.

In a clear 96-well plate (Thermo Scientific®), an increasing volume of the standard solution was added to 14 wells in duplicates: 0 µL; 1.25 µL; 2.5 µL; 5 µL; 10 µL; 20 µL; 40 µL, followed by 5 µL of the samples in the ensuing wells in triplicates. Added to the wells containing the

samples and the standard, was 200 µL of the working reagent. Then the plate was incubated for 1 hour (60-75 minutes) at 37 °C and 5% CO_2.

The absorbance of the samples in the plate was measured in a CLARIOstar® plate reader, and the values from the increasing amount of the standard was used to make a standard curve. With the standard curve, the amount of protein in each sample was determined.

Table 2.12 Solutions used for homogenisation of cerebella

Solution	Reagent	Quantity
Tris-EDTA (TE)-buffer	Tris-HCl solution, pH 8	0.5 mL
	0.5 M EDTA	0.1 mL
	MQ-water	ad 50 mL
TE-buffer with 4% sodium dodecyl sulphate (SDS)	20% SDS	5 mL
	TE-buffer	15 mL
TE-buffer with protease inhibitor (ribonuclease-, phosphatase- and protease-inhibitor)	5 mg/mL Leupeptin	8 µL
	100 mM PMSF	24 µL
	1 mg/mL Pepstatin A	40 µL
	10 mM Na_3VO_4	80 µL
	TE-buffer	4 mL
TE-buffer was sterile filtered 0.2 µm and kept in room temperature. TE-buffer with protease inhibitors was made right before use, and kept on ice.		

2.5.2 Gel electrophoresis

The samples were boiled at 95 °C for 2 minutes after the protein measurement. A 400 µL sample was made containing 25 µg protein/15 µL of the samples, 25% 4X Laemmli buffer with bromophenol blue (table 2.13), 5% 2-mercaptoethanol, and MQ-water.

The gel was prepared and put in an electrophoresis tank filled with Elfo buffer (table 2.14), where 5 µL of the standard, Precision Plus Protein All Blue Standards®, was added to the first well in the gel. This was followed by 15 µL of the samples (7.5 µL added twice). The gel electrophoresis ran for 45-60 minutes at 150 V to secure a sufficient separation of the protein bands.

Table 2.13 4X Laemmli buffer		
Reagent	**Final concentration**	**Quantity**
20% SDS	2 %	25 mL
Glycerol 87%	20 %	14.7 mL
0.5 M Tris-HCl pH 6.8	300 mM	9.4 mL
MQ-water	-	0.9 mL
Bromophenol	-	A few grains
The solutions were stored in room temperature.		

Table 2.14 1X Tris-Glycin-SDS (TGS)-Elfo buffer	
Reagent	**Final concentration**
Tris	25 mM
Glycine	192 mM
SDS with pH 8.3	0.1 % (v/w)
Distilled water	-

2.5.3 Blotting to membrane

To prepare for blotting, two stacks of filter (containing six filters each) and a nitrocellulose membrane, were wetted with 1X Trans-Blot® buffer in a fume hood. The 1X Trans-Blot® buffer consisted of 1 part Trans Blot® Turbo™ 5X transfer buffer, 1 part ethanol and 3 parts distilled water. The gel, two stacks of filters and a nitrocellulose membrane were arranged in this following order: First stack of filter (containing six filters), nitrocellulose membrane, the gel, and the second stack of filter. Air bubbles were removed with a plastic roller, and the gel was blotted onto the nitrocellulose membrane at 25 V, 2.5 A for 10 minutes with Trans-Blot® Turbo™ Transfer System blotting machine.

2.5.4 Ponceau-colouring of membrane

To verify that proteins were transferred during blotting, the nitrocellulose membrane was submerged in a tray containing Ponceau S. Ponceau S is a dye that stains proteins on the membrane the colour red. Following the staining, the membrane was immersed in distilled

water to rinse off surplus, and a picture was taken of the membrane with the developer Chemi Genius Bio Imaging® system with the programme Genesnap from SynGene.

2.5.5 Antibody probing

Before adding any antibodies, the membrane had to be blocked with 5% dry milk to inhibit nonspecific binding on the membrane. The membrane was placed in a 50 mL tube (protein side facing inwards) with an addition of 5 mL of 5% dry milk before incubation on Stuart™ Roller Mixer for 1 hour. The blocking solution was discarded, and a primary antibody mixed with 5% dry milk in its correct dilution (table 2.15), was added before the membrane was incubated on the roller mixer overnight at 2-8 °C.

The solution was discarded the following day, and a wash cycle ensued with 5 mL 1xTBS Tween (TBS-T) (table 2.16) for 10 minutes on the roller mixer, three times, in room temperature. A secondary antibody was added to the membrane after the wash cycle by mixing the secondary antibody with 5% dry milk (table 2.15). The membrane was further incubated for a minimum of 1 hour on the roller mixer at room temperature before another wash cycle ensued.

Table 2.15 Antibodies used for Western blot

Primary antibodies	**Ratio**	**Lot.nr**	**Catalogue number**	**Supplier**
Anti-PCNA	1:1000	00083603	M0879	Agilent Dako
Anti-PAX6	1:5000	2776793	AB2337	Millipore (now MERCK)
Anti-NR2B	1:1000	GR3183264-1	AB28373	Abcam
Anti-MMP9	1:5000 1:3000 1:1000	3-T6879	BML-SA680-0100	Enzo Life Science
Anti-β-actin	1:10 000	12M4755	A5316	Sigma-Aldrich (now MERCK)
Secondary antibodies	**Ratio**	**Lot.nr**	**Catalogue number**	**Supplier**
Mouse anti-rabbit IgG-HRP	1:10 000	D0617	SC-2357	Santa Cruz Biotechnology

Goat anti-mouse IgG-HPR	1:10 000	310007187	1706516	Bio-Rad Laboratories

Table 2.16 10X Tris buffered saltwater (TBS) with 0.1 % Tween (TBS-T)	
Reagent	**Concentration**
Tris base	2.45 g/L
NaCl	8.0 g/L
Tween 20	0.1 %
MQ-water	ad 1 L
The solution was pH-adjusted to pH 7.6 with NaOH/HCl	

2.5.6 Detection and imaging

The membrane was developed after the wash cycle, where 1-1.5 mL of a developing substrate for horseradish peroxidase (HRP), Immobilon™ Western HRP Classico, Luminata™ Western HRP Crescendo or Forte was used to cover the membrane. The membrane was incubated with the substrate for 1 minute or 5 minutes, depending on the protein to be detected. The horseradish peroxidase enzyme linked to the secondary antibody catalyses a reaction that generates a signal that can be detected.

GeneSnap from SynGene was the programme used to develop the membrane following a 30 second – 7 minutes exposure. The protein bands were quantified with the programme ImageJ, where the number of measured pixels equated the light signal.

A shorter wash cycle ensued the developing of the membrane, with 5 mL 1xTBS-T for 5 minutes, three times, on the roller mixer in room temperature. Afterwards, another primary antibody was added or the membrane was stored in a plastic tube filled with 1xTBS-T at 2-8 °C.

2.5.7 Stripping of the membrane

If necessary, the membrane can be stripped with a stripping buffer. The stripping buffer loosens antibodies on the membrane from earlier antibody probing. This way, previously detected proteins with a similar molecular weight with the current protein to be determined, will not

interfere with the quantification. A disadvantage of this is that some of the proteins from the samples are also removed.

The membrane was washed for 5 minutes with 5 mL 1xTBS-T before 5 mL of Restore™ Plus Western blot Stripping Buffer was added to the membrane. The membrane was incubated for 5 minutes on the roller mixer before the stripping buffer was discarded. Thereafter, another wash cycle followed before a continuation from section 2.5.5.

2.6 RT-qPCR

Quantitative reverse transcription polymerase chain reaction (RT-qPCR) is a technique were a specific DNA sequence is amplified and measured to estimate a change in expression in mRNA. The method used for the quantification of gene expression was the two-step model; total RNA extracted from the embryos were transcribed into cDNA, and this cDNA was aliquoted and further used as the template for qPCR amplification [90].

2.6.1 Isolation of total RNA from cerebella

Total RNA isolation was performed with Beata Urbanczyk Mohebi, the head engineer from the Section for Pharmacology and Pharmaceutical Biosciences, at University of Oslo. RNeasy® Plus Mini Kit was used to process the cerebella for RT-qPCR, with minor modifications marked with an ‘’*’’. Harvested cerebella from section 2.2.2 were homogenised with 120 µL TE-buffer with protease inhibitors (table 2.12) with Pellet pestle®. Half of the homogenate was transferred to an Eppendorf tube where either 350 or 700 µL* (the kit states 350 or 600 µL) of RLT Plus Buffer (QIAGEN®) was added to lyse the cells. RLT Plus Buffer contains a highly denaturing guanidine-isothiocyanate which instantly inactivates RNases to ensure isolation of intact RNA. An amount equivalent to 10 µL B-mercaptoethanol/1 mL RLT Plus Buffer was added to RLT Plus Buffer before application to provide appropriate binding conditions for RNA [91]. The lysate was then centrifuged at 10-13 000 rpm (equivalent to ≥ 8000 gravitational acceleration (g)) for 3 minutes with Heraeus Pico 17 centrifuge (Thermo Scientific®).

The supernatant resulting from the centrifugation was added to a gDNA Eliminator spin column; a column designed to effectively remove genomic DNA contamination [92]. The spin column was centrifuged for 30 seconds at ≥ 8000 g. The column was discarded and an equal volume of 70% ethanol (350 or 700 µL) was added to the flow-through (lysate). The lysate with

70% ethanol were mixed with a pipette before 700 µL was transferred to an RNeasy spin column. With this column, RNA binds to the membrane and contaminants can be washed away [92]. The column was centrifuged for 15-20* (the kit states 15 seconds) seconds at ≥ 8000 g, followed by a discarding of the eluate.

The column was washed with 700 µL of RW1 Buffer with the eluate discarded after a 15-20* second centrifugation at ≥ 8000 g. This was also repeated with 500 µL of RPE Buffer per the same conditions. The column was further washed with 500 µL of RPE Buffer, except with a 2-minute centrifugation, to ensure that all the salt residue from RW1 Buffer was effectively removed. To dry the membrane, the RNeasy spin column was transferred to a new collection tube and centrifuged at ≥ 8000 g for 1 minute.

The RNeasy spin column was transferred to an Eppendorf tube were 30 µL RNase-free water was added directly to the membrane and centrifuged at ≥ 8000 g for 1 minute to eluate the RNA. The elution was either repeated with the eluate or a second addition of 30 µL RNase-free water to dilute the RNA. The samples were stored at -80 °C.

2.6.2 Quantification of RNA concentration

Quantification of RNA concentration was performed by Beata Urbanczyk Mohebi, the head engineer at University of Oslo, from the Section for Pharmacology and Pharmaceutical Biosciences. The concentration and purity degree (OD) of the samples were determined with NanoDrop™ Lite Spectrophotometer at an absorbance of 260/280 nm. The OD ranged from 2.0-2.1. A value ~2.0 signifies a pure, uncontaminated RNA [93]. A blank (1 µL of RNA-free water) was measured before 1 µL of each sample was added to NanoDrop™ and the concentrations were measured (ng/µL).

2.6.3 Reverse transcription of RNA to cDNA

Reverse transcription was performed by Beata Urbanczyk Mohebi, the head engineer at University of Oslo, from the Section for Pharmacology and Pharmaceutical Biosciences. To convert RNA to cDNA, the kit High Capacity RNA-to-cDNA Kit® from Applied Biosystems, was employed (table 2.17). The RNA samples were added to miniature Eppendorf tubes, Multiply®-µStrip, with a volume equivalent of 2-3 µg of total RNA from each sample. The tubes were filled with RNA-free water up to 10 µL. The tubes were added 10 µL of 2xRT Buffer

and 1 µL 20X Enzyme mix before the samples were incubated for 1 hour at 37 °C for the reverse transcription. Negative controls were included to check for any contaminant DNA that could generate a signal during qPCR.

The reaction was stopped by increasing the temperature to 95 °C, that was kept for 5 minutes, followed by a decrease to 4 °C, with Applied Biosystems™ 2720 Thermal Cycler.

Table 2.17 High Capacity RNA-to-cDNA	
Reagent	**Amount**
2X RT buffer	10.0 µL
20X Enzyme mix	1.0 µL (left out in the negative control)
RNA sample	Up to 9 µL
RNA-free H_2O	ad 20.0 µL
Total per reaction	20.0 µL
The samples were stored at -20 °C after being diluted (1:10).	

2.6.4 qPCR

qPCR was performed by Beata Urbanczyk Mohebi, the head engineer at University of Oslo, from the Section for Pharmacology and Pharmaceutical Biosciences. Each cDNA sample was diluted (1:10) with RNA-free water. From the sample, 2 µL was further diluted in Multiply®-µStrip tubes, where 5 µL of 2X qPCR mix SYBR Green mixed with 3 µL of the primer mix for the specific gene, were added (table 2.18). Table 2.19 details the primers utilised. In a white 96-well plate (BIOplastics®), 10 µL of each sample prepared (qPCR master mix) were added in triplicates, before the real time qPCR was performed with the instrument LightCycler 480®, and the programme LightCycler® 480 SW.

Table 2.18 qPCR master mix		
Reagent	**Target final concentration**	**Volume per single 10 µL reaction**
2X qPCR mix SYBR Green	1X	5.0 µL

Primer mix (1.666 µM)	0.5 µM	3.0 µL
cDNA (dilution 1:10)	-	2.0 µL

Table 2.19 qPCR primers

Gene	Gene bank number	Primer
ACTB	NM205518.1	F: 5'-ATG GCT CCG GTA TGT GCA A-3' R: 5'-TGT CTT TCT GGC CCA TAC CAA-3'
GRIN2B	XM015289359.2	F: 5'-AGC TAT GGC CCT CAG TCT CA-3' R: 5'-AGA GCA GAC ACC CAT GAA GC-3'
BDNF	XM015286148.2	F: 5'-GAA AAG TCT GCA CAT GAG GGC-3' R: 5'-GTG TGG CAT TGC TGT AAG GG-3'
PCNA	NM204170.2	F: 5'-GGG CGT CAA CCT AAA CAG CA-3' R: 5'-AGA GCC AAC GTA TCC GCA TT-3'
PAX6	XM025150599.1	F: 5'-CCA CAT CCC CAT CAG CAG TA-3' R: 5'-TGA AAG AGG AAA CGG GGG TG-3'
GABRR1	XM426190.5	F: 5'-AAA ATC CCT GCC ATC TGA CG-3' R: 5'-AAT CTG GAC AGT GGG GAA ACG-3'
SLC6A13	XM025141585.1	F: 5'-AGT GGG GAA GGT CTC ATC TCT-3' R: 5'-GAG GGA TGC TCT GGG GGT A-3'
GAPDH	NM304305.1	F: 5'-GAT GGG TGT CAA CCA TGA GAA A-3' R: 5'-TGG TGC ACG ATG CAT TGC-3'

F: forward primer
R: reverse primer

2.7 Luciferase Dual Reporter Assay

The Luciferase Dual Reporter Assay is a tool used to study gene expression at the transcriptional level. Luciferases are a class of enzymes that enable organisms that express bioluminescence, to emit light [94]. To determine if a substance is able to activate or supress transcription of a gene of interest, recombinant DNA is constructed where the promoter of the gene is placed adjacent to a luciferase reporter gene. The luciferase for firefly (*Photinus pyralis*)

is most widely used [95, 96]. The construct of the recombinant DNA containing a promoter region of the gene of interest and luciferase reporter gene, is introduced into cultured cells, and exposed to a substance. If the substance is able to affect transcription, it will be detected by the production of luciferase. The amount of luciferase produced can be quantified using a luminometer [97]. *Renilla* luciferase (from sea pansy, *Renilla Reniformis*) is a distinct member of luciferases, and is used as an internal control to correct for sample handling and transfection efficiency [95, 98].

2.7.1 Transfection of CGNs

Transfection is a process were DNA or RNA are artificially introduced into cells. This can result in a change in gene function or protein expression, and can be studied in the context of the cell [99].

K2 multiplier reagent® (10 µL) was dropped onto dishes 48 hours after plating with CGNs. This was to ensure that any immune response exhibited by the cells, would be inhibited of activating defence mechanisms against the introduced plasmids (table 2.20) [100]. The dishes were incubated for 2 hours.

A transfection solution was prepared by making a plasmid solution and a K2 solution that were mixed together. DNA (1 µg) was whirlmixed with 50 µL of serum-free medium per dish. Of this 1 µg DNA, 0.8 µg consisted of the plasmid of interest, and 0.2 µg of *Renilla* luciferase (pRL-TK), the internal control. For the K2 solution, 1 µL of K2 transfection reagent® was mixed with 50 µL of serum-free medium per dish. The K2 solution could not be whirlmixed. DNA solution was added to the K2 solution, and incubated for 20 minutes in room temperature.

After the incubation, 100 µL of the transfection solution was gently dripped onto the cells, and the dishes were incubated (37 °C and 5% CO_2) for 5-6 hours. The cells were exposed with VPA or LTG in different concentrations (table 2.21), whilst changing the media.

Table 2.20 Plasmids for transfection of chicken cerebellar granule neurons		
Plasmid	**Abbreviation**	**Concentration per mL cell suspension in the dish**
Firefly luciferase reporter gene containing PAX6 promoter regions	PAX6-luc	0.8-0.9 µg
Firefly luciferase reporter gene containing MMP9 promoter regions	MMP9-luc	0.8-0.9 µg
Renilla luciferase reporter gene containing thymidine kinase promoter region	pRL-TK	0.1-0.2 µg

Table 2.21 Exposure of chicken cerebellar granule neurons for transfection	
Exposure	**Final concentration**
Valproic acid (1000 mM stock solution in saline)	0.9-1 µM, 90-100 µM, 450-500 µM, 900-1000 µM
Lamotrigine (42 mM stock solution in DMSO)	1 µM, 5 µM, 10 µM, 100 µM
Saline	0.0009%
DMSO	0.2%

2.7.2 Transfection of PC12 cells

After plating the dishes with sufficient PC12 cells, according to section 2.3, transfection could be performed after 24 hours. An extra step had to be included if the dishes were plated with 2 mL instead of 1 mL (table 2.11), since the transfection procedure is optimised for 1 mL of medium. Therefore, the media had to be removed, and 1 mL of the media was added back to the dishes.

The transfection procedure is similar as for CGNs. The cells were added 10 µL of K2 multiplier reagent® with the cells incubated for 2 hours to optimise the transfection. The DNA solution

and K2 solution were prepared equally as with CGNs, but the ratio of the 1 µg of DNA was different. The 1 µg of plasmid (table 2.22) consisted of 0.9 µg of the plasmid of interest and 0.1 µg of pRL-TK. The transfection solution (100 µL) was dropped onto the cells, and further incubated at 5% CO_2 and 37 °C. The PC12 cells were not exposed to treatment 5-6 hours after as for CGNs, however, the transfection continued overnight, as PC12 cells are more robust. Table 2.23 details what the PC12 cells were exposed to.

Table 2.22 Plasmids for transfection of PC12 cells

Plasmid	**Abbreviation**	**Concentration per mL cell suspension in the dish**
Firefly luciferase reporter gene containing PAX6 promoter regions	PAX6-luc	0.8-0.9 µg
Firefly luciferase reporter gene containing MMP9 promoter regions	MMP9-luc	0.8-0.9 µg
Renilla luciferase reporter gene containing thymidine kinase promoter region	pRL-TK	0.1-0.2 µg

Table 2.23 Exposure of PC12 cells for transfection

Exposure	**Final concentration**
Valproic acid (900-1000 mM stock solution in saline)	0.9-1 µM, 90-100 µM, 450-500 µM, 900-1000 µM
Lamotrigine (42 mM stock solution in DMSO)	1 µM, 5 µM, 10 µM, 100 µM, 500 µM
Trichostatin A (5 mM solution in DMSO)	1 nM, 10 nM, 100 nM
Saline	0.0009%
DMSO	0.1%, 0.2%, 1.2%

2.7.3 Harvesting cells for luciferase assay

CGNs were harvested 48 hours after transfection and exposure, whilst PC12 cells were harvested 24 hours after exposure. The media in the dish was removed with a pipette, and the dish was washed twice with 1 mL ice cold PBS (table 2.24). Gently added to the dishes was 125 µL of cold 0.1% LUC with 1 mM DTT (table 2.25) to prevent oxidation-reduction reactions, followed by a 5-minute incubation in room temperature.

A cell scraper was used in two perpendicular directions in the dishes to ensure a detachment of cells from the surface. The resulting suspension was transferred to an Eppendorf tube and centrifuged at 4 °C for 5 minutes, and ≥8000 g. To a new Eppendorf tube, 125 µL of the resulting supernatant was transferred.

Table 2.24 Phosphate buffered saltwater (PBS-solution)

Reagent	**Final concentration**
NaCl	138 mM
KCl	2.7 mM
KH_2HPO_4	2 mM
$Na_2HPO4 \times 2 H_2O$	10 mM
MQ-water	ad 4000 mL
The solution was pH-adjusted with HCl/NaOH, autoclaved, and stored at 2-8 °C.	

Table 2.25 Harvesting solution for luciferase assay 0.1 % LUC with 1 mM DTT

Reagent	**Final concentration**
Tris-1 M MES with pH 7.8	50 mM Tris-50 mM MES
Triton X-100	0.1 %
MQ-water	ad 100 mL
DTT	1 mM
The harvesting solution was stored at 2-8 °C.	

2.7.4 Measuring firefly luciferase activity

The amount of firefly luciferase is indicative of the activation in the cells. After the background light-intensity had been measured with 200 µL of LUC-cocktail (table 2.26), the sample measurement could commence. From the samples, 50 µL was mixed with 150 µL of LUC-cocktail in a cold glass tube. The glass tube was transferred to a luminometer (Lumat LB 9507 Luminometer), which adds 100 µL of Luciferin (table 2.27) through its dispenser, and the light-intensity was measured in 2 seconds. Each sample was measured once.

Table 2.26 LUC-Cocktail

Reagent Components	**Final concentration**
Adenosine-5-triphosphate (ATP)	2.4 mg/mL
1 M magnesium acetate	20 mM
1 M Tris-1 M MES with pH 7.8	83 mM Tris/83 mM MES
MQ-water	ad 100 mL
LUC-cocktail was stored at -20 °C, and kept on ice during measuring.	

Table 2.27 Luciferin solution

Reagent Components	**Final concentration**	**Quantity**
D-luciferin	1 mM	11 mg
MQ-water	-	36.7 mL
The luciferin solution was stored at 2-8 °C, and protected from light.		

2.7.5 Measuring *Renilla* luciferase activity

The values from the *Renilla* luciferase measuring, illustrates the efficiency of the transfection, and is used to normalise the firefly measurement. A reagent, Stop&Glo®, was diluted 100 times with MQ-water. From the samples, 5 µL was added in cold glass tubes mixed with 100 µL of the diluted S&G, before being measured in Lumat LB 9507 for 10 seconds. Each sample was measured a minimum of three times, since the *Renilla* readings could fluctuate. Therefore, if the values deviated more than 10% of each other, two additional measurements were included.

To validate the readings, 10 µL of the sample was measured at certain intervals to examine if this generated an approximate doubling in signal.

2.8 Neurite outgrowth

During development, neurons extend numerous projections that differentiate into dendrites and axons. These processes are critical for communication between neurons [101]. To analyse the progression of neurite outgrowth after exposure, the IncuCyte® system at Statens arbeidsmiljøinstitutt (STAMI) was employed. Neurite length and branch points were used as endpoints. The IncuCyte® system is a platform that allows for real-time quantitative live-cell imaging and analysis, as well as visualising and quantifying cell behaviour from hours to weeks. It does so by automatically gathering and analysing images [102].

IncuCyte® ImageLock Plates were plated with CGNs according to section 2.2.4, with a cell density of 1.7-1.9x10^6 cells/mL. The plating media (table 2.7) in the 96-well plate was replaced the following day with a defined feeding media (table 2.8) during exposure, as described in section 2.2.4. The only difference was the addition of Cytosine-beta-D-arabinofuranoside (AraC) in the media with a final concentration of 10 µM. AraC is a cytostatic that arrests proliferation. Table 2.28 details the exposure of CGNs for neurite outgrowth. Neurite outgrowth was assessed starting from the very day as exposure, and scanned and operated with the software IncuCyte® ZOOM in a 90-minute interval for 51 hours.

Table 2.28 Exposure of CGNs for neurite outgrowth

Exposure	**Final concentration**
Valproic acid (1000 mM stock solution in saline)	1 µM, 100 µM, 500 µM, 1000 µM
Lamotrigine (42 mM stock solution in DMSO)	1 µM, 5 µM, 10 µM, 100 µM, 500 µM
Saline	0.0009%
DMSO	0.2%, 1.2%

2.9 MTT assay

MTT (abbreviation of 3-(4,5-Dimethylthiazol-2-yl)-2,5-diphenyltetrazolium bromide), is a dye used for MTT assay, a colorimetric assay to detect viable cells. MTT is a positively charged compound that readily penetrates eukaryotic cells. Cells with an active metabolism convert MTT into a purple coloured formazan product, whilst dead cells lose this ability [103].

Handled as described in section 2.3, 200 µL of split PC12 cells were added into each well of a transparent 96-well plate before incubation (37 °C and 5% CO_2). After 48 hours, the wells were exposed to VPA in different concentrations, including a blank, a control and a vehicle control (table 2.29). After 48 hours, an MTT solution (5 mg MTT/mL PBS) was made and 10 µL were added to each well, excluding the blank column. Followed was a 3-4-hour incubation (37 °C and 5% CO_2). Afterwards, all the contents in the wells were replaced with 100 µL of DMSO accompanied by another 30-minute incubation (37 °C and 5% CO_2), before the absorbance was measured in CLARIOstar® at 570 nm.

Table 2.29 Exposure of PC12 cells for MTT assay and Hoechst staining

Exposure	**Final concentration**
Valproic acid (1000 mM stock solution in saline)	1 µM, 10 µM, 100 µM, 200 µM, 500 µM, 750 µM, 1000 µM, 2000 µM
Saline	0.0009%, 0.0018%

2.10 Hoechst staining

Hoechst 33343 is a blue fluorescent dye used to stain double-stranded DNA (dsDNA) to assess nuclear number and shape. The dye is cell permeable, it binds to DNA in live or fixed cells [104]. It is used to distinguish apoptotic cells from healthy or necrotic cells, by their nuclear condensation [105].

PC12 cells split as described in section 2.3, were added (200 µL) to a black bottomed 96-well plate. The cells were exposed with to VPA in different concentrations, as detailed in table 2.29, before incubation (37 °C and 5% CO_2). The PC12 medium was removed with the wells being washed with N-buffer (table 2.30), 48 hours after the incubation. To each well, 100 µL of N-buffer mixed with 1 mg/mL Hoechst (final concentration 4 µg/mL) was added. The plate was

then incubated for 1 minute protected from light before the solution was substituted with 100 µL of N-buffer.

The fluorescence was measured in a CLARIOstar® plate reader with an excitation of 350 nm, and emission of 461 nm.

Table 2.30 N-buffer

Reagent	**Final concentration**
NaCl 5 M	140 mM
KCl 1 M	3.5 mM
Tris-HCl 1 M pH 7	15 mM
Na_2HPO_4 x $Na_2H_2PO_4$ 0.1 M pH 7.4	1.2 mM
Glucose 1 M	5 mM
$CaCl_2$ 1 M	2 mM
MQ/Distilled water	Ad libitum (400 mL)

2.11 Statistical analysis and graphical presentation

Statistical significance was determined using GraphPad Prism 8.1 (Graph-Pad Software, La Jolla, CA, USA) with One Way Analysis of Variance (ANOVA) Dunnett's *post hoc* test, and a non-parametric Kruskal-Wallis Dunn's *post hoc* test for data that did not exhibit a Gaussian distribution. Statistical significance was also determined with an unpaired parametric t-test with Welch's correction, and a non-parametric Mann-Whitney test for data that did not exhibit a Gaussian distribution. All data are presented as either the mean + standard error of mean (SEM) or mean ± SEM. $P < 0.05$ was regarded as statistically significant. The graphical presentation was done using GraphPad Prism 8.1.

3 Results

The first of the secondary objectives for this thesis was to examine the distribution of VPA and LTG into the brain of chicken embryos. Pharmacokinetics experiments were performed with *in ovo* injections on E13 and E16 (section 3.1).

The second was to explore how being exposed to VPA and LTG might affect protein expressions of molecules important for neuronal development. Molecules included were PCNA, PAX6, MMP9 and GluN2B examined with a western blot analysis (section 3.2). In conjunction with the protein expression assessment, *PAX6, PCNA, BDNF, GRIN2B, SLC6A13,* and *GABRR1* gene expression was examined with RT-qPCR (section 3.2).

The third secondary objective consisted of exploring how a VPA and LTG exposure could affect PAX6 and MMP9 promoter activity *in vitro* in CGNs (section 3.2), and PC12 cells (section 3.3). This was performed with a luciferase assay.

PC12 cells were also employed for side projects. The first was to study cell viability after an exposure to VPA with an MTT assay and Hoechst staining (section 3.3). The second project was to examine if the inherent HDAC inhibition by VPA might have an effect on promoter activity (section 3.3).

The final objective was to see if CGNs exposed to VPA and LTG might affect neurite outgrowth (section 3.4). This differentiation process was observed with IncuCyte®.

3.1 Distribution of LTG and VPA into chicken embryo brains

There has not been conducted any studies to examine the distribution of LTG and VPA to the brain of chicken embryos. Therefore, it would be of interest to assess this after *in ovo* injection on E13 and E16.

Chicken embryos exposed to 100 µM VPA were done with a single injection in two independent experiments. The entire brain was isolated after a 5-minute-72-hour exposure. Each time-point consisted of 3-4 eggs. The selected time-points for the first experiment were 30-min., 1-hour,

4-hour, 6-hour, 12-hour, 24-hour, and 72-hour of exposures for E13. The time-points for the second experiment were 15-min., 30-min., 1-hour, 4-hour, 6-hour, and 24-hour exposures for eggs injected on E16. Two groups of 3 eggs were injected with 500 μM and 1000 μM for one time-point. To determine the concentrations, an GC/MS analysis was performed.

Chicken embryos exposed to LTG 4.2 μM where done with a single injection in two independent experiments. The entire brain was isolated after a 15-minute-72-hour exposure. Each time-point consisted of 3-4 eggs. The selected time-points for the first experiment were 2-hour, 4-hour, and 6-hour exposures, whilst 30-min., 24-hour, 48-hour, and 72-hour exposures for the second experiment. These were injected on E13. On E16, eggs were exposed for 30 min., and 4 hours, for the first experiment, and 15 min., 2 hours, 6 hours, and 24 hours on the second experiment. Two groups of 3 eggs were injected with 10 μM and 25 μM LTG at T_{max} on E16. The concentrations were determined through an LC-MS/MS analysis.

Chicken embryos were exposed to 5 μM LTG isethionate with a single injection in one experiment. The entire brain was isolated after a 15-min., 30-min., 1-hour, 2-hour, 4-hour, 6-hour, 12-hour, 24-hour, 48-hour, and 72-hour exposure for E13 injections. E16 time-points consisted of a 5-min., 15-min., 30-min, 1-hour, 2-hour, 4-hour, 6-hour, and a 24-hour exposure. E13 and E16 injections consisted of 2-4 eggs per time-point. The concentrations were determined through an LC-MS/MS analysis.

All the data was analysed by Fernando Boix Escolan, a Senior scientist at the Department of Forensic Sciences from the Section for Drug Abuse Research at Oslo University Hospital. The program used to analyse the data was Kinetica.

3.1.1 VPA injected on E13 result in relevant CNS concentrations

Figure 3.1A illustrates the measured concentrations for all the time-points after injecting eggs with VPA. The results show a rapid absorption and distribution to the brain. Figure 3.1B illustrates the fitted distribution of VPA, generated by Kinetica. The curves are visually similar, therefore the parameters calculated (table 3.1) are usable.

Table 3.1 Pharmacokinetic parameters for VPA E13

Parameter	**$VPA_{determined}$**	**$VPA_{generated}$**
C_{max} (μM)	28.67	28.82
T_{max} (hours)	4	4.38
AUC (μM×hour)		1230.23
K_a		0.809
K_{el}		0.027
$T_{1/2}$ (hours)		21.25

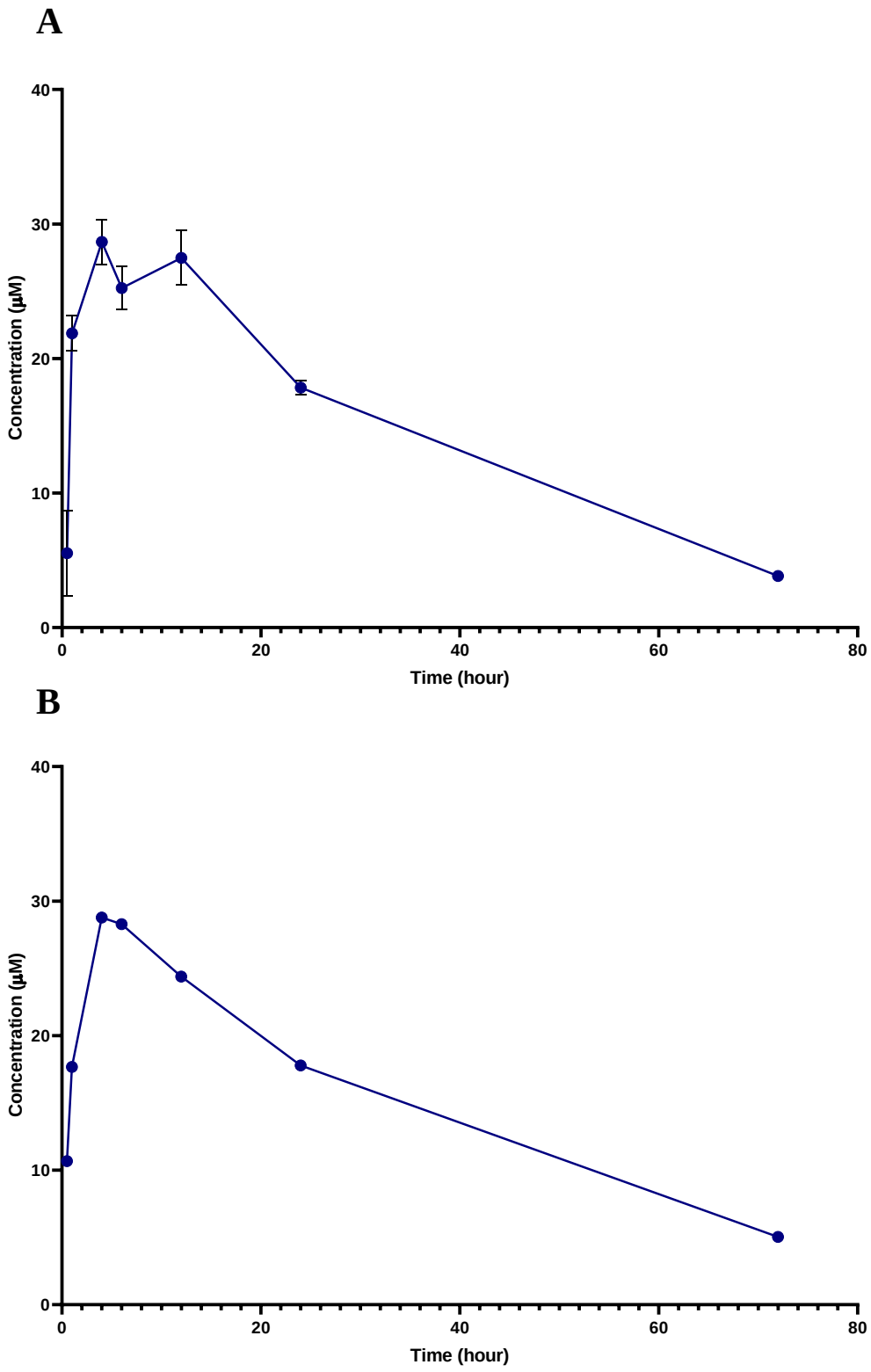

Figure 3.1 Concentrations of VPA in chicken embryo brains injected on E13. Chicken embryos were exposed *in ovo* to 100 µM VPA on E13 with 3-4 eggs per time-point. The entire brain was isolated after a 30-min, 1-hour, 4-hour, 6-hour, 12-hour, 24-hour, and a 72-hour exposure. The concentrations were determined through GC/MS. **A)** The measured concentrations in chicken embryo brains. The data is displayed as the average concentration (µM) ± SEM. **B)** The fitted distribution generated by Kinetica. The data is displayed as the average concentration (µM). N = 4 for the 6-hour, 12-hour, and 24-hour time-points. N = 3 for the 30-min., 1-hour, 4-hour, and 72-hour time-points.

3.1.2 VPA injected on E16 has a faster elimination

The measured concentrations following E16 injection as seen in figure 3.2A show a rapid absorption and distribution to the brain. There was a measurable concentration after a 15-min. exposure (31.03 μM). The elimination was faster on E16.

Two higher concentrations of VPA were also injected on E16 (500 μM and 1000 μM). The concentrations determined after a 4-hour exposure were 141.24 μM for 500 μM, and 357 μM for 1000 μM (not displayed). VPA concentration after a 4-hour exposure to 100 μM was 26.26 μM.

Figure 3.2B is the fitted distribution generated by Kinetica. The curves look similar, but the fitted C_{max} compared with the measured C_{max} are not. The model can be considered usable on account of their likeness, but with care due to the difference in C_{max}.

Table 3.2 Pharmacokinetic parameters for VPA E16

Parameter	**$VPA_{determined}$**	**$VPA_{generated}$**
C_{max} (μM)	39.39	35.33
T_{max} (hours)	0.50	0.58
AUC (μM×hour)		596.86
K_a		8.62
K_{el}		0.061
$T_{1/2}$ (hours)		13.41

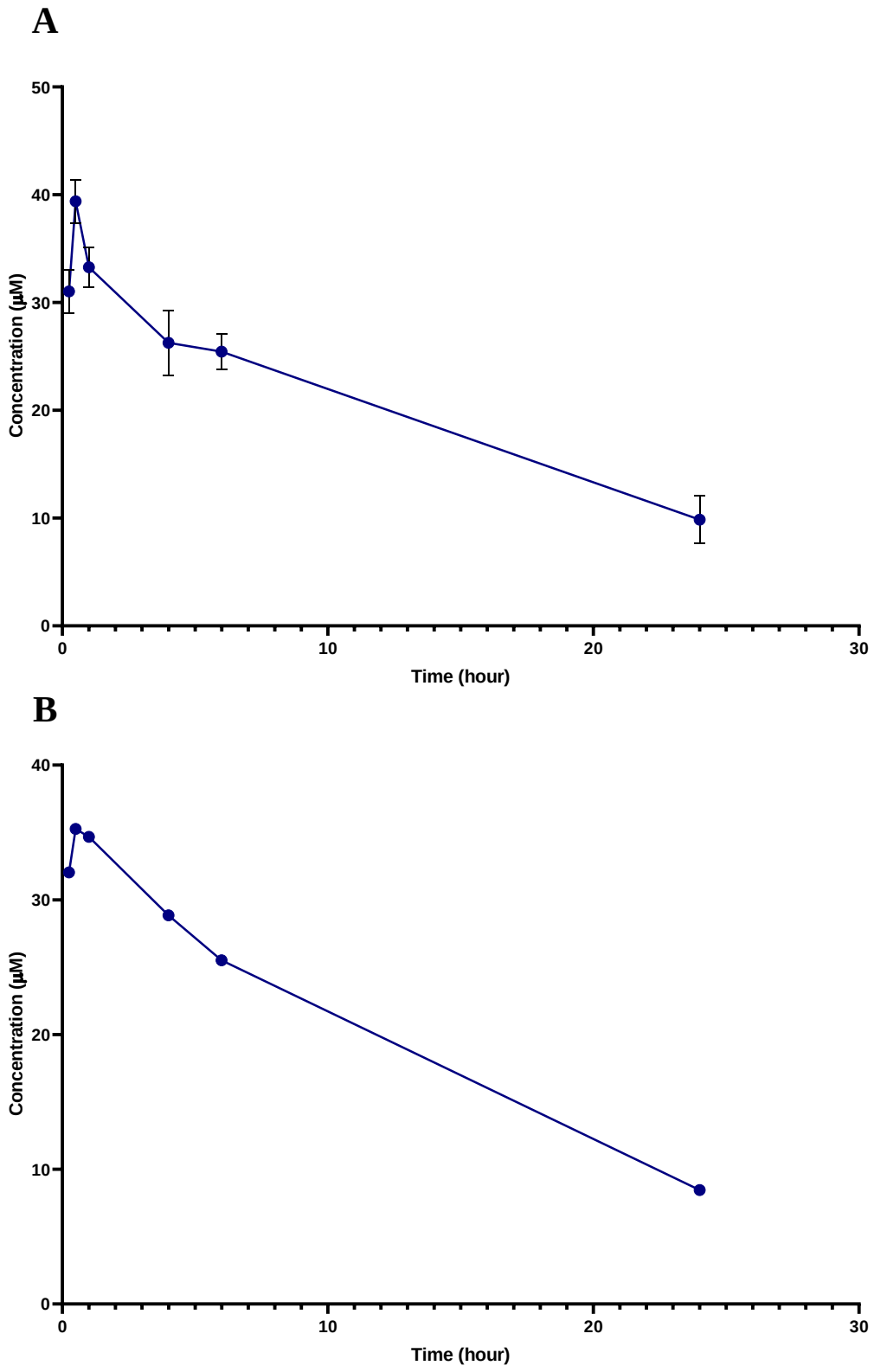

Figure 3.2 Concentrations of VPA in chicken embryo brains injected on E16. Chicken embryos were exposed *in ovo* to 100 µM VPA on E16 with 3 eggs per time-point. The entire brain was isolated after a 15-min., 30-min., 1-hour, 4-hour, 6-hour, and a 24-hour exposure. The concentrations were determined through GC/MS. **A)** The measured concentrations in chicken embryo brains. The data is displayed as the average concentration (µM) ± SEM. **B)** The fitted distribution generated by Kinetica. The data is displayed as the average concentration (µM). N = 3 for all the selected time-points.

3.1.3 LTG isethionate has a higher absorption than LTG injected on E13

Figure 3.3 illustrates the measured concentrations for all the time-points after exposing chicken embryos to 4.2 μM LTG and 5 μM LTG isethionate on E13. The absorption was rapid for both. The fitted distribution generated by Kinetica for LTG isethionate (figure 3.3B) was considered usable because of their likeness. This was not the case for the fitted curve for LTG (figure 3.3D). Table 3.3 details the calculated parameters.

Table 3.3 Pharmacokinetic parameters for LTG and LTG isethionate E13

Parameter	**$LTG_{determined}$**	**LTG $isethionate_{determined}$**	**$LTG_{generated}$**	**LTG $isethionate_{generated}$**
C_{max} (μM)	0.80	1.80	0.66	1.72
T_{max} (hours)	6	2	0.14	1.66
AUC (μM×hour)			92.53	59.77
K_a			62.77	0.91
K_{el}			0.007	0.058
$T_{1/2}$ (hours)			57.76	55.95

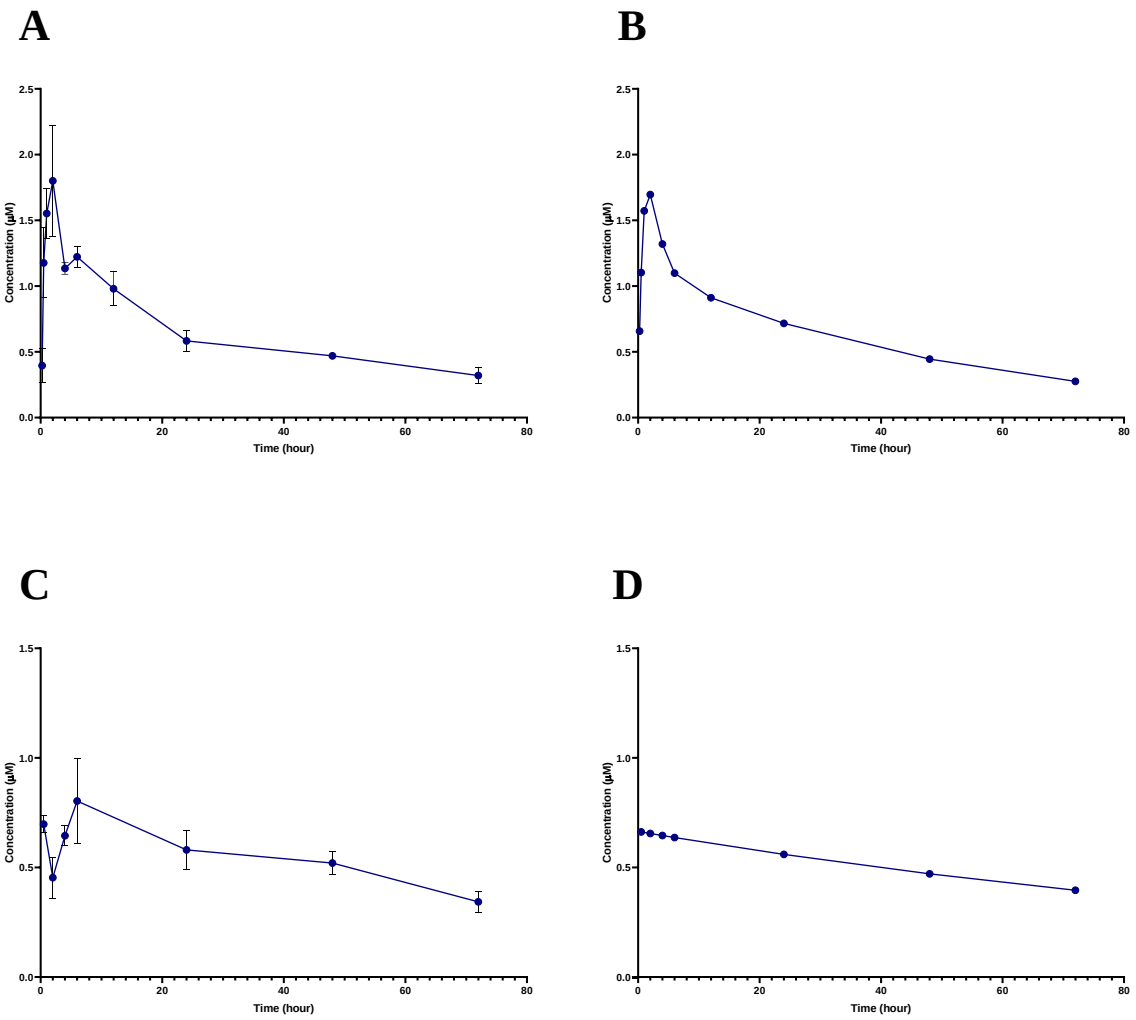

Figure 3.3 Concentrations of LTG isethionate and LTG in chicken embryo brains injected on E13. Chicken embryos were exposed *in ovo* to 5 μM LTG isethionate dissolved in saline or 4.2 μM LTG dissolved in DMSO on E13 with 2-4 eggs per time-point. The entire brain was isolated after a 15-min., 30-min., 1-hour, 2-hour, 4-hour, 6-hour, 12-hour, 24-hour, 48-hour, and 72-hour exposure from a single experiment for LTG isethionate. The entire brain was isolated after a 2-hour, 4-hour, and 6-hour exposure from one independent experiment, and 30-min., 24-hour, 48-hour, and 72-hour exposure from another independent experiment for LTG. The concentrations were determined through LC-MS/MS. **A)** The measured concentrations in chicken embryo brains after exposure to LTG isethionate. The data is displayed as the average concentration (μM) ± SEM. **B)** The fitted distribution generated by Kinetica after exposure to LTG isethionate. The data is displayed as the average concentration (μM). **C)** The measured concentrations in chicken embryo brains after exposure to LTG. The data is displayed as the average concentration (μM) ± SEM. **D)** The fitted distribution generated by Kinetica. The data is displayed as the average concentration (μM). N = 2 for the 12-hour, and 48-hour time-points. N = 3 for the 30-min., 2-hour, 24-hour, and 72-hour time-points. N = 4 for the 15-min., 1-hour, 4-hour, and 6-hour time-points for LTG isethionate. N = 3 for the 2-hour, 6-hour, and 72-hour time-points. N = 4 for the 30-min., 24-hour, and 48-hour time-points for LTG

3.1.4 LTG isethionate and LTG injected on E16 have a slower elimination

Figure 3.4 illustrates the measured concentrations for all the time-points after exposure to 4.2 μM LTG and 5 μM LTG isethionate. The absorption was rapid and the elimination was slow for both of the formulations.

Figure 3.4B illustrates the fitted curve generated by Kinetica for LTG isethionate. The results were deemed unreliable on account of their difference in curves. Kinetica was unable to generate a fitted curve from the LTG data, therefore no pharmacokinetic parameters were computed. Table 3.4 details the calculated parameters.

Two higher concentrations of LTG were injected on E16 (10 μM and 25 μM). They were exposed for 2 hours (T_{max}) with the subsequent concentrations 1.23 μM and 3.84 μM, respectively (not displayed).

Table 3.4 Pharmacokinetic parameters for LTG and LTG isethionate E16

Parameter	LTG	LTG isethionate$_{determined}$	LTG isethionate$_{generated}$
C_{max} (μM)	0.57	0.59	0.47
T_{max} (hours)	2	1	1.91
AUC (μM×hour)			46.02
K_a			2.97
K_{el}			0.010
$T_{1/2}$ (hours)			73.17

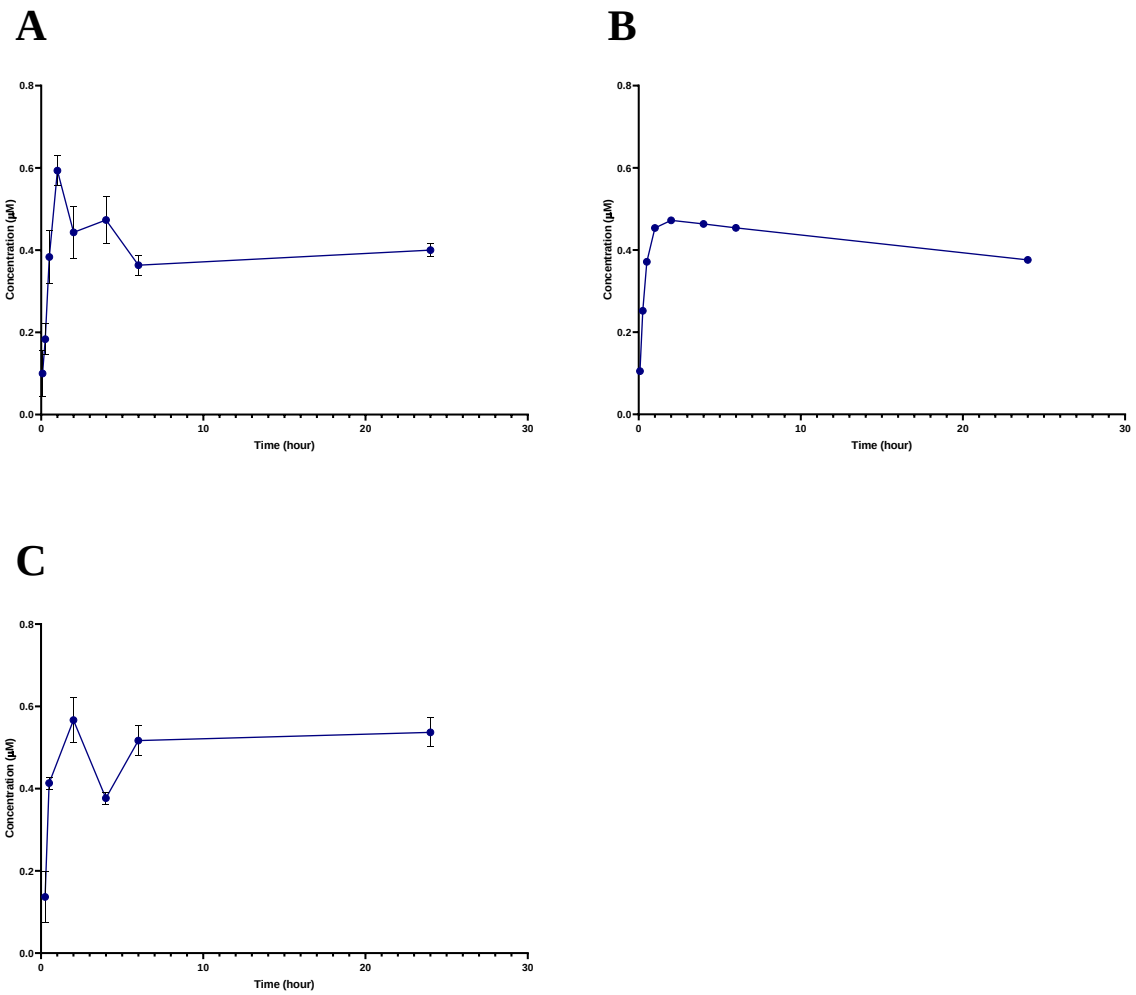

Figure 3.4 Concentrations of LTG isethionate and LTG injected on E16. Chicken embryos were exposed *in ovo* to 5 μM LTG isethionate dissolved in saline or 4.2 μM LTG dissolved in DMSO on E16 with 3-4 eggs per time-point. The entire brain was isolated after a 5-min., 15-min., 30-min, 1-hour, 2-hour, 4-hour, 6-hour, and 24-hour exposure from a single experiment for LTG isethionate. The entire brain was isolated after a 30-min. and 4-hour exposure from one independent experiment, and 15-min., 2-hour, 6-hour, and 24-hour exposure from another independent experiment for LTG. The concentrations were determined through LC-MS/MS. **A)** The measured concentrations in chicken embryo brains after exposure to LTG isethionate. The data is displayed as the average concentration (μM) ± SEM. **B)** The fitted distribution generated by Kinetica for chicken embryo brains exposed to LTG isethionate. The data is displayed as the average concentration (μM). **C)** The measured concentrations in chicken embryo brains after exposure to LTG. The data is displayed as the average concentration (μM) ± SEM. N = 3 for all the selected time-points.

3.2 Expression studies in chicken embryo cerebella

For western blot, VPA (1, 10, 100, 500, and 1000 μM) or LTG (10 and 25 μM) were injected in chicken embryos *in ovo* to evaluate PCNA, PAX6, MMP9, and GluN2B expression. This was performed on E16 with the cerebellum isolated on E17. The band strength from the western analysis was corrected with the internal standard β-actin (at 42 kDa, figure 3.5A-H).

For RT-qPCR, VPA 100 μM and 1000 μM, LTG 10 μM and 25 μM, and LTG isethionate 5 μM were injected in chicken embryos *in ovo* on E16. After the cerebella were harvested on E17, the genes *PCNA, PAX6, GRIN2B, BDNF, GABRR1,* and *SLC6A13* were determined. The results were corrected with the reference gene *ACTB.* One group of samples were corrected with another reference gene as well, *GAPDH,* due to a group of samples where the exposures affected *ACTB.* None of the LTG isethionate results are included, nor is VPA 100 μM results for *GABRR1,* and *SLC6A13* gene expression. This was the group of exposed chicken embryo cerebella significantly affecting *ACTB,* and were therefore excluded.

For luciferase assay in CGNs, the primary cell culture was prepared from chicken embryo cerebella from E17. Promoter activity of PAX6 and MMP9 were assessed with the reporter plasmids PAX6-luc and MMP9-luc through co-transfection with pRL-TK 48 hours after plating. CGNs were exposed to VPA (1, 100, 500, 1000 μM) or LTG (1, 5, 10, 100 μM) before harvest after 48 hours. The firefly luciferase activity was measured the very day as the harvest, and the samples were stored in -20 °C until *Renilla* luciferase was measured to correct the firefly luciferase values.

3.2.1 VPA does not significantly affect protein levels of PCNA, PAX6, MMP9, and GluN2B

The western blot analysis of homogenates from chicken embryo cerebella, showed a clear band for PCNA at 36 kDa (figure 3.5A), PAX6 at 48 kDa (figure 3.5C), and GluN2B at 176 kDa (figure 3.5G). The band for MMP9 at 92 kDa (figure 3.5E) was fainter. The result showed no significant change in protein levels after exposure.

There seemed to be a dose-dependent trend for PCNA. In the quantified graph of PCNA (figure 3.5B), higher concentrations reduced its expression. PAX6 (figure 3.5D) exhibited a Gaussian-shaped expression, were the lowest and highest concentration of VPA (1 μM and 1000 μM) resulted in a low protein expression, whilst the middle concentrations (10, 100, 500 μM) experienced a higher protein expression. GluN2B (figure 3.5H) seem to exhibit a dose-dependent trend as PCNA, but in a reversed manner. The quantified graph shows a higher protein expression with higher concentrations of VPA.

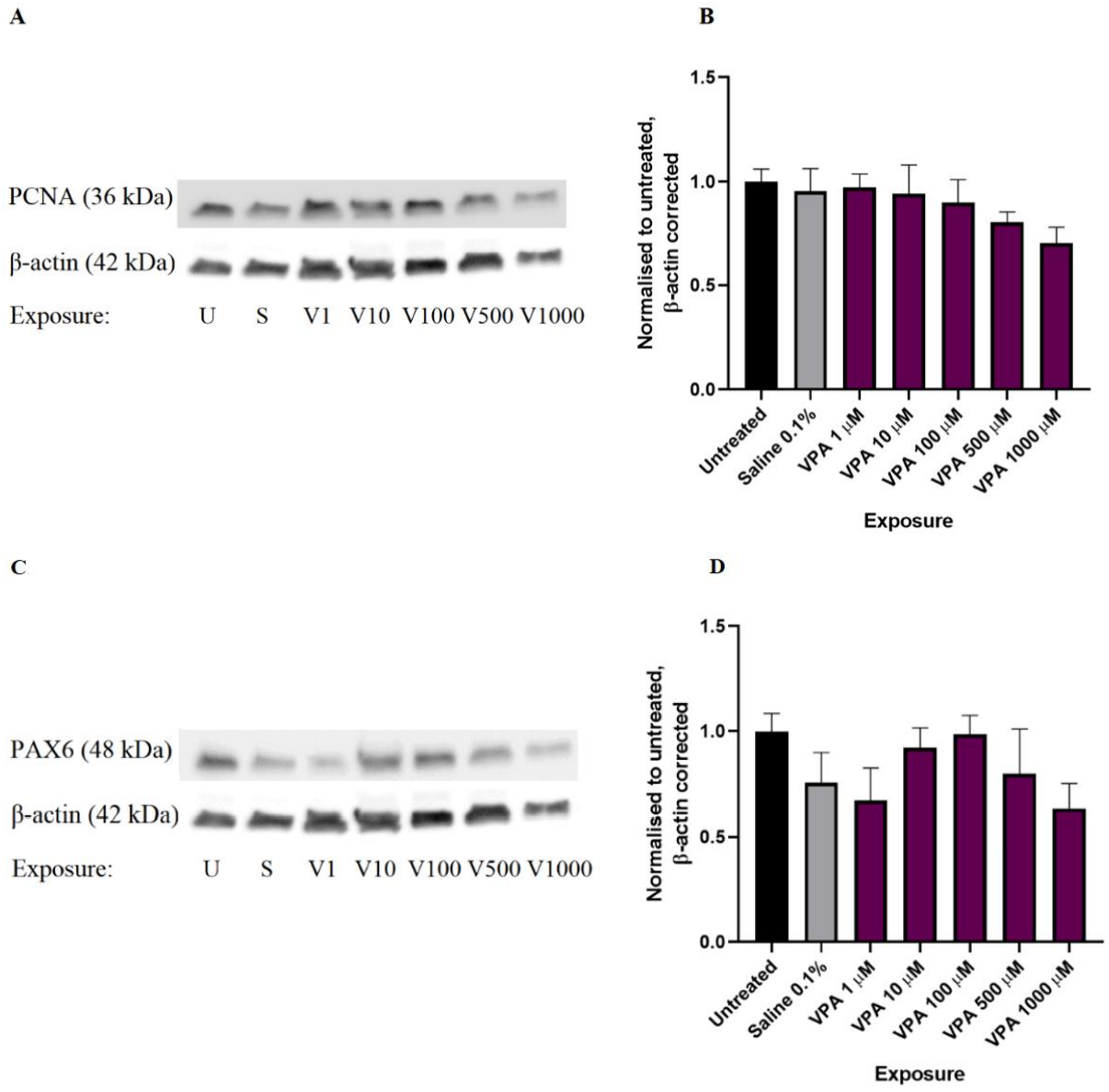

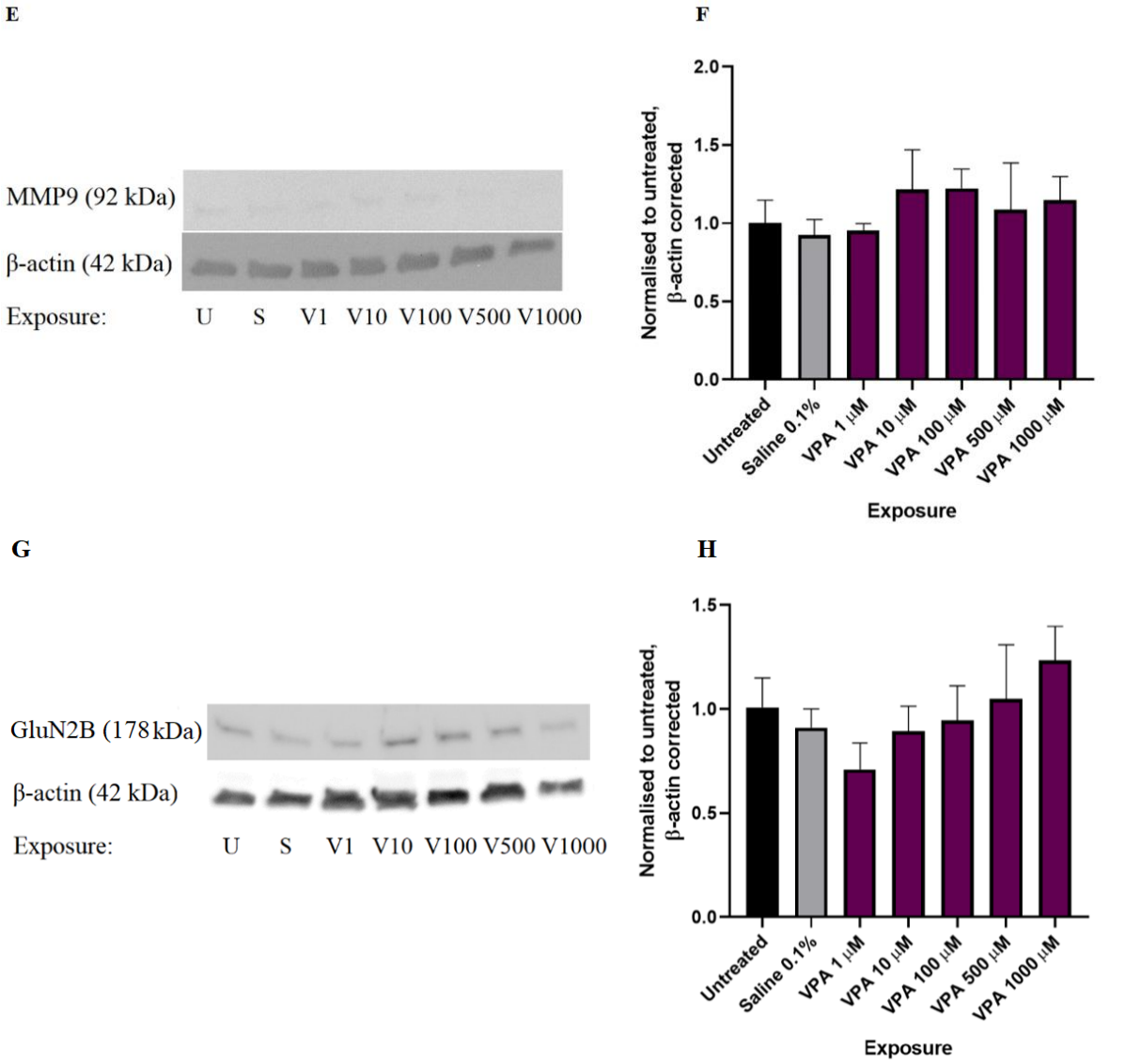

Figure 3.5 Protein expression is unaffected by VPA. Chicken embryos were exposed to VPA (1, 10, 100, 500, 1000 μM) or saline on E16. The cerebellum was harvested on E17 and studied through a western blot analysis. Eggs from two independent experiments were used with 4-5 chicken embryos per group. Groups: Untreated (U), saline (S), VPA 1 μM (V1), VPA 10 μM (V10), VPA 100 μM (V100), VPA 500 μM (V500), and VPA 1000 μM (V1000). The data is displayed as average band strength corrected with β-actin (internal standard), and normalised to untreated controls + SEM. **A)** PCNA western blot analysis of cerebellum from chicken embryos. **B)** Protein expression of PCNA in cerebellum from chicken embryos. **C)** PAX western blot analysis of cerebellum from chicken embryos. **D)** Protein expression of PAX6 in cerebellum from chicken embryos. **E)** MMP9 western blot analysis of cerebellum from chicken embryos. **F)** Protein expression of MMP9 in cerebellum from chicken embryos. **G)** GluN2B western blot analysis of cerebellum from chicken embryos. **H)** Protein expression of GluN2B in cerebellum from chicken embryos. Statistical analysis with One Way ANOVA Dunnett's *post hoc* test. N = 5 for untreated and VPA 1, 10, 100, 500, and 1000 μM, and n = 4 for saline.

3.2.2 VPA 100 µM significantly down-regulates *PAX6* expression, but does not affect *PCNA, BDNF, NR2B, SLC6A13* and *GABRR1*

The results from RT-qPCR show a reduction in *PCNA* expression, particularly by VPA 100 µM (figure 3.6A). *PAX6* expression was significantly reduced by the 100 µM exposure (figure 3.6B). *BDNF* (figure 3.6C) and *GRIN2B* (figure 3.6D) expression was reduced with 100 µM, whilst 1000 µM exposure resulted in an increase (figure 3.6C-D). *ACTB* data can be found in Appendix III.

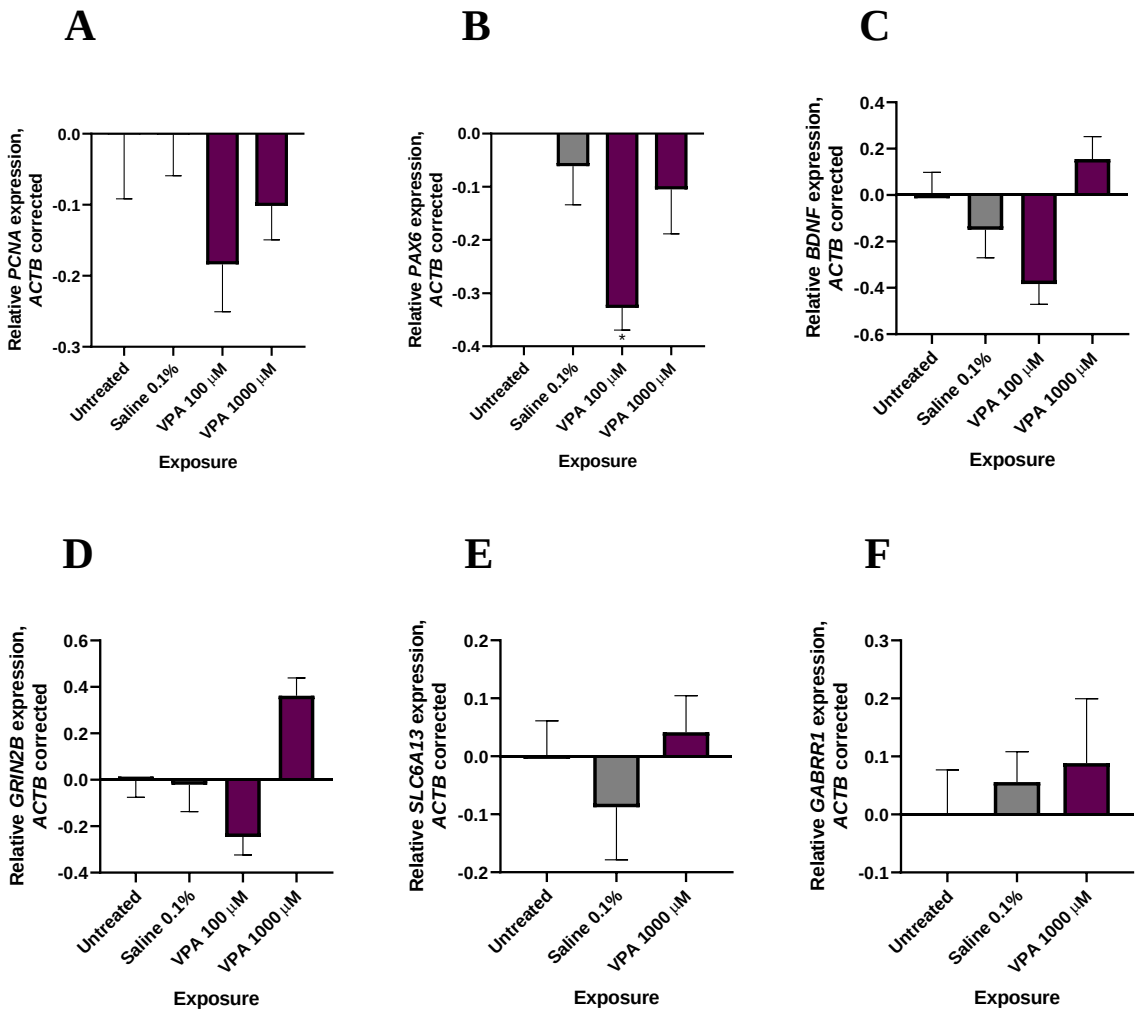

Figure 3.6 VPA 100 µM significantly decreases *PAX6* expression corrected with *ACTB*. Chicken embryos were exposed to VPA 100 µM, 1000 µM or saline on E16. The cerebellum was harvested on E17 and examined through RT-qPCR. Eggs from two independent experiments were used, with 4-6 chicken embryos per group. The data is displayed as *ACTB* corrected values normalised with cerebella from untreated chicken embryos + SEM. **A)** *PCNA* expression from chicken embryo cerebella. **B)** *PAX6* expression from chicken embryo cerebella. **C)** *BDNF* expression from chicken embryo cerebella. **D)** *GRIN2B* expression from chicken embryo cerebella. **E)** *SLC6A13* expression from chicken embryo cerebella. **F)** *GABRR1* expression from chicken embryo cerebella. Statistical analysis with One Way ANOVA Dunnett's *post hoc* test for A, B, E and F, and Kruskal-Wallis with Dunn's *post hoc* test for C and D. N = 10 for untreated, n = 9 for saline, n = 5 for VPA 100 µM, and n = 6 for 1000 µM. Significance is shown by: $p<0.05$ (*) compared to untreated cerebella. Note the values on the y-axis differ between graphs.

3.2.3 VPA does not significantly affect gene expression when corrected with *GAPDH*

One group of samples were noticed to significantly increase *ACTB* expression. For this reason, another group of samples where run again with a different reference gene, *GAPDH*. *BDNF*, *GABRR1* and *SLC6A13* expression (figure 3.7C, D and E) are the genes with an opposite result. *GAPDH* data can be found in Appendix III.

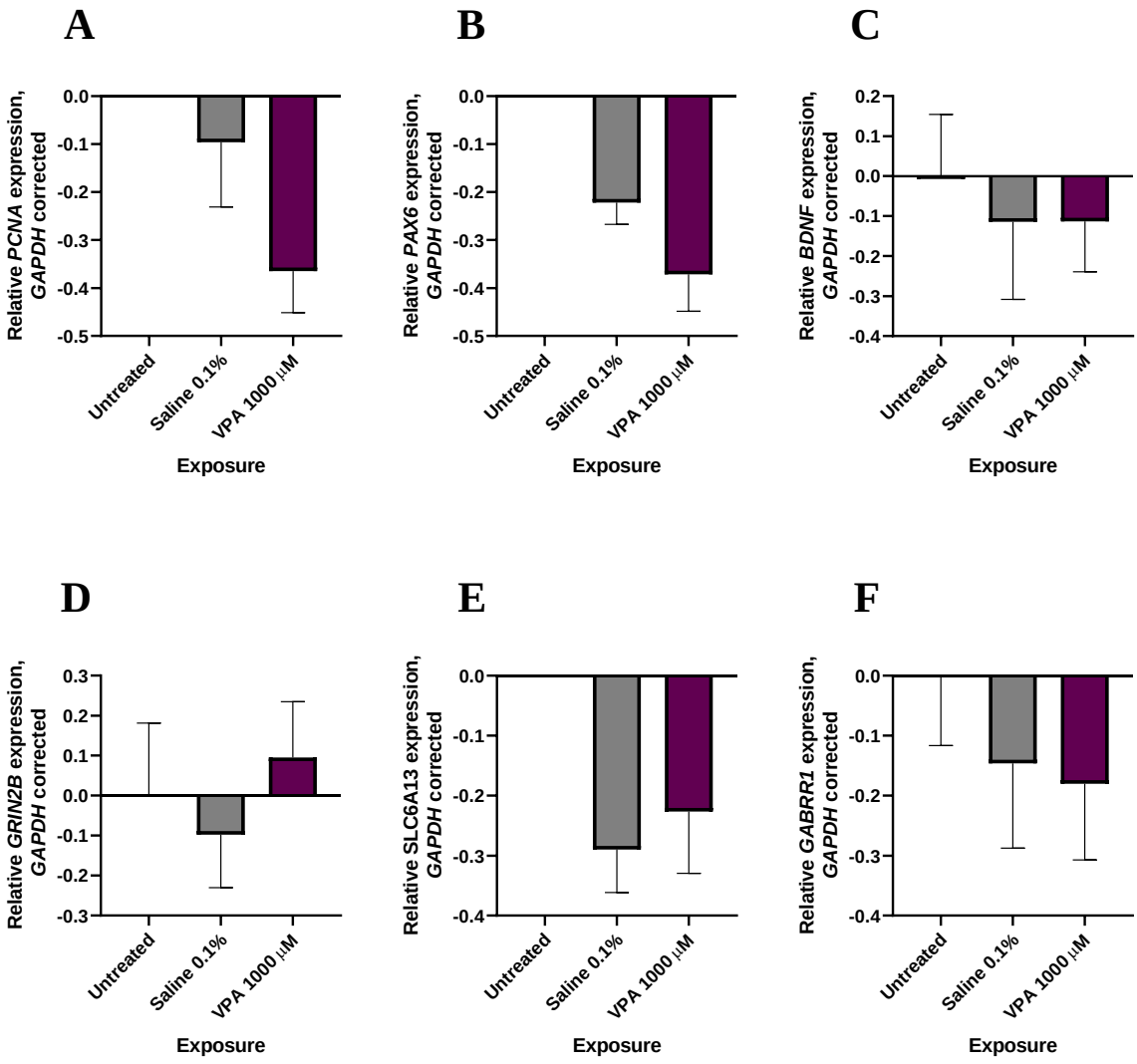

Figure 3.7 VPA does not significantly affect gene expression corrected with *GAPDH*. Chicken embryos were exposed to VPA 1000 μM or saline on E16. The cerebellum was harvested on E17 and examined through RT-qPCR. Eggs from one experiment was used, with 5-6 chicken embryos per group. The data is displayed as *GAPDH* corrected values normalised with cerebella from untreated chicken embryos + SEM. **A)** *PCNA* expression from chicken embryo cerebella. **B)** *PAX6* expression from chicken embryo cerebella. **C)** *BDNF* expression from chicken embryo cerebella. **D)** *GRIN2B* expression from chicken embryo cerebella. **E)** *SLC6A13* expression from chicken embryo cerebella. **F)** *GABRR1* expression from chicken embryo cerebella. Statistical analysis was performed with One Way ANOVA with Dunnett's *post hoc* test. N = 6 for untreated, n = 5 for saline, n = 6 for 1000 μM. Note the values on the y-axis differ between graphs.

3.2.4 High concentrations of VPA increases firefly and *Renilla* luciferase expression in CGN

Figure 3.8 illustrates the uncorrected firefly and *Renilla* luciferase. VPA significantly increased their expression. Figure 3.9 illustrates the *Renilla* corrected results, where there is an apparent significant reduction in PAX6 and MMP9 promoter activity after exposure to VPA in a dose-dependent manner. Firefly and *Renilla* luciferase data can be found in Appendix IV.

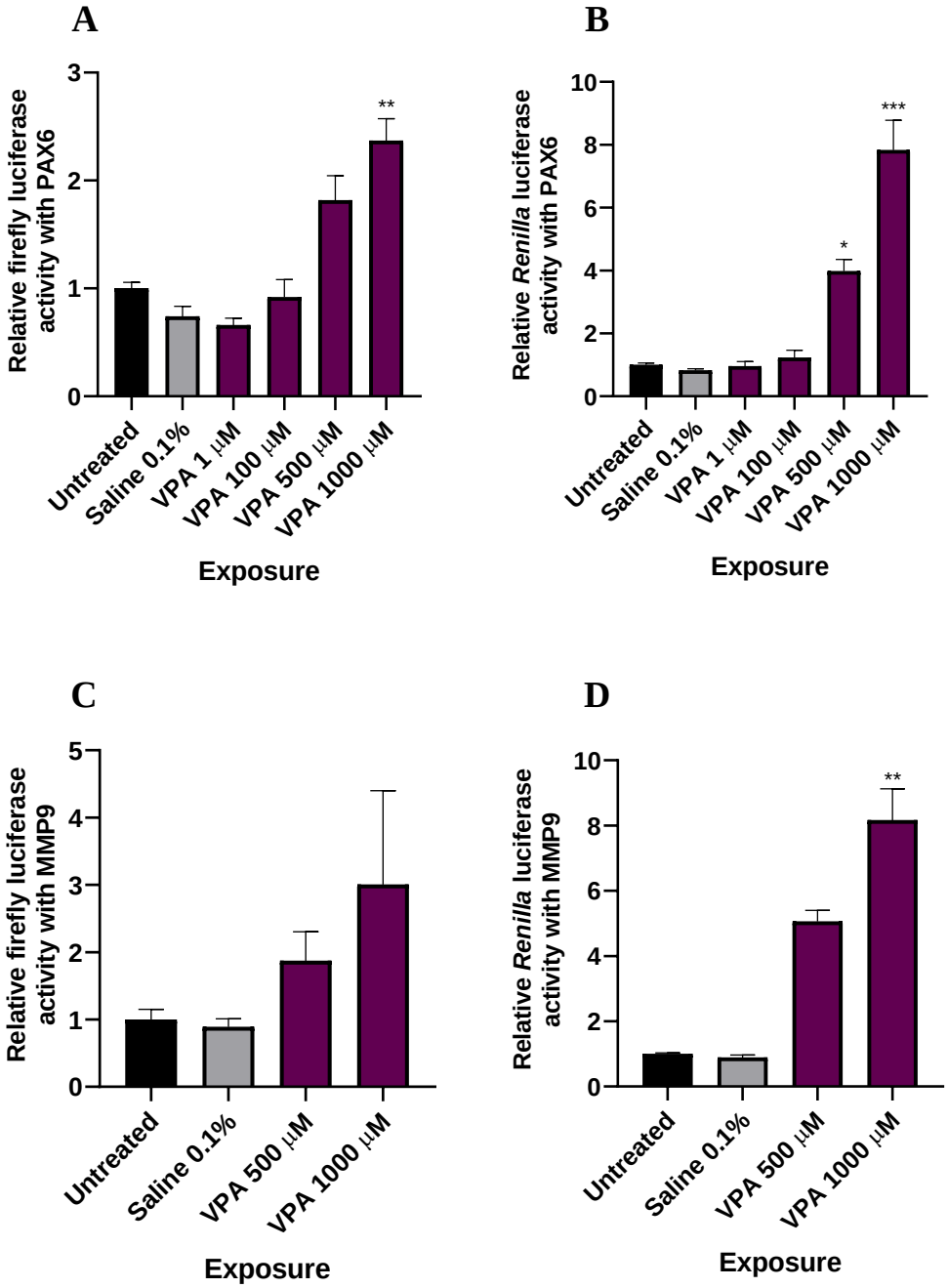

Figure 3.8 *Renilla* and firefly luciferase are significantly affected by VPA at high concentrations in CGNs. CGNs was prepared from extracted cerebella from chicken embryos on E17. CGN was co-transfected with a reporter plasmid (PAX6-luc or MMP9-luc) and an internal control (pRL-TK) 48 hours after plating. Same day as transfection, CGNs were exposed to VPA (1, 100, 500 and 1000 μM) or saline. Untreated dishes were used as a control. The cells were harvested, and the promoter activity was measured with firefly luciferase after 48 hours. *Renilla* luciferase was measured, and used to correct the firefly measurements. The data is displayed as relative luciferase values normalised with the untreated dishes + SEM. **A)** Uncorrected firefly luciferase results of PAX6 promoter activity from n = 12 from 4 experiments for untreated, n = 11 from 4 experiments for saline, n = 9 from 3 experiments for VPA 500 μM, and VPA 1000 μM. N = 6 from 2 experiments for VPA 100 μM, n = 3 from 1 experiment for VPA 1 μM. **B)** *Renilla* luciferase results from n = 12 from 4 experiments for untreated, n = 11 from 4 experiments for saline, n = 9 from 3 experiments for VPA 500 μM, and VPA 1000 μM. N = 6 from 2 experiments for VPA 100 μM, n = 3 from 1 experiment for VPA 1 μM. **C)** Uncorrected firefly luciferase results of MMP9 promoter activity from n = 6 from 2 experiments for untreated, saline, VPA 500 μM, and VPA 1000 μM. **D)** *Renilla* luciferase results from n = 6 from 2 experiments for untreated, saline, VPA 500 μM and VPA 1000 μM. Statistical analysis was performed with One Way ANOVA Dunnett's post hoc test for C, and Kruskal-Wallis Dunn's post hoc test for A, B, and D. Significance is shown by: $p<0.05$ (*), $p<0.01$ (**), $p<0.001$ (***) compared to untreated dishes. Note the values on the y-axis differ between graphs.

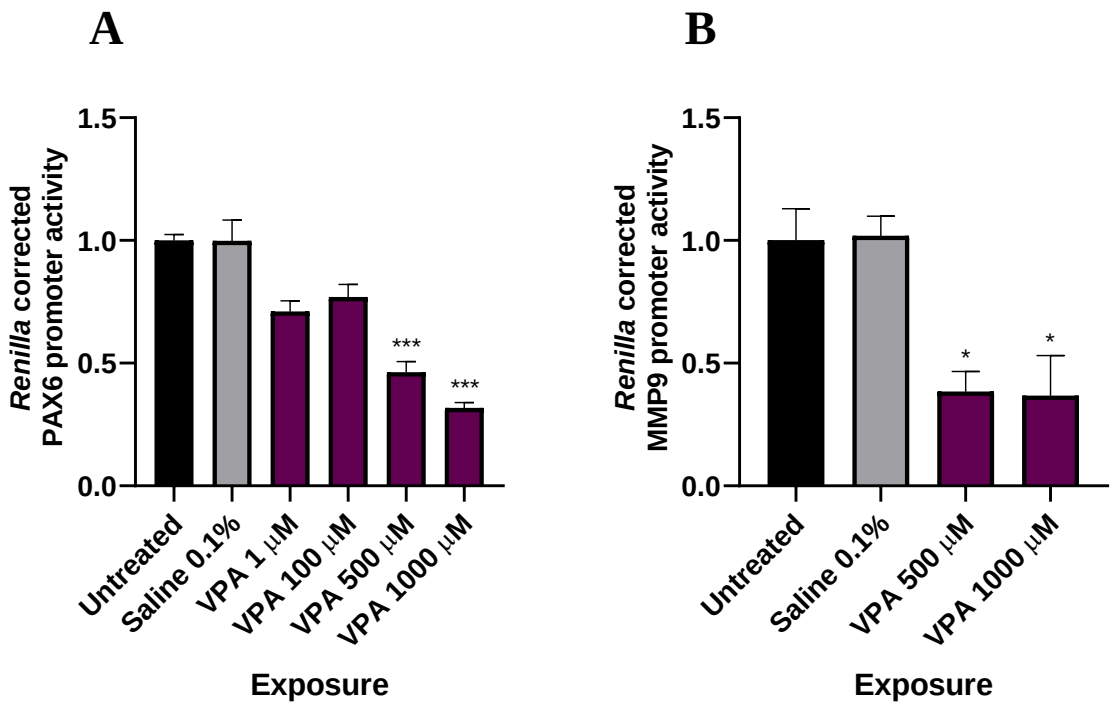

Figure 3.9 *Renilla* corrected PAX6 and MMP9 promoter activity in CGNs show an apparent significant reduction by VPA. CGNs were prepared from isolated cerebella from chicken embryos on E17. CGNs were co-transfected with a reporter plasmid (PAX6-luc or MMP9-luc) and an internal control (pRL-TK) 48 hours after plating. Same day as transfection, CGNs were exposed to VPA (1, 100, 500 and 1000 μM) or saline. Untreated dishes were used as a control. The cells were harvested, and the promoter activity was measured with firefly luciferase after 48 hours. *Renilla* luciferase was measured, and used to correct the firefly measurements. The data is displayed as *Renilla* corrected values normalised with the untreated dishes + SEM. **A)** PAX6 promoter activity with n = 12 from 4 experiments for untreated, n = 11 from 4 experiments for saline, n = 9 from 3 experiments for VPA 500 μM, and VPA 1000 μM, n = 6 from 2 experiments for VPA 100 μM, n = 3 from 1 experiment for VPA 1 μM. **B)** MMP9 promoter activity with n = 6 from 2 experiments for untreated, saline, VPA 500 μM and VPA 1000 μM. Statistical analysis was performed with One Way ANOVA Kruskal-Wallis Dunn's post hoc test. Significance is shown by: $p<0.05$ (*), $p<0.001$ (***) compared to untreated dishes.

3.2.5 LTG does not affect protein levels of PCNA, PAX6, MMP9, and GluN2B

The western blot analysis of homogenates from chicken embryo cerebella showed a clear band for PCNA at 36 kDa (figure 3.10A) and PAX6 at 48 kDa (figure 3.10C). The band for GluN2B at 176 kDa (figure 3.10G) and MMP9 at 92 kDa (figure 3.10E), appear fainter. The result showed no significant change in protein levels after exposure.

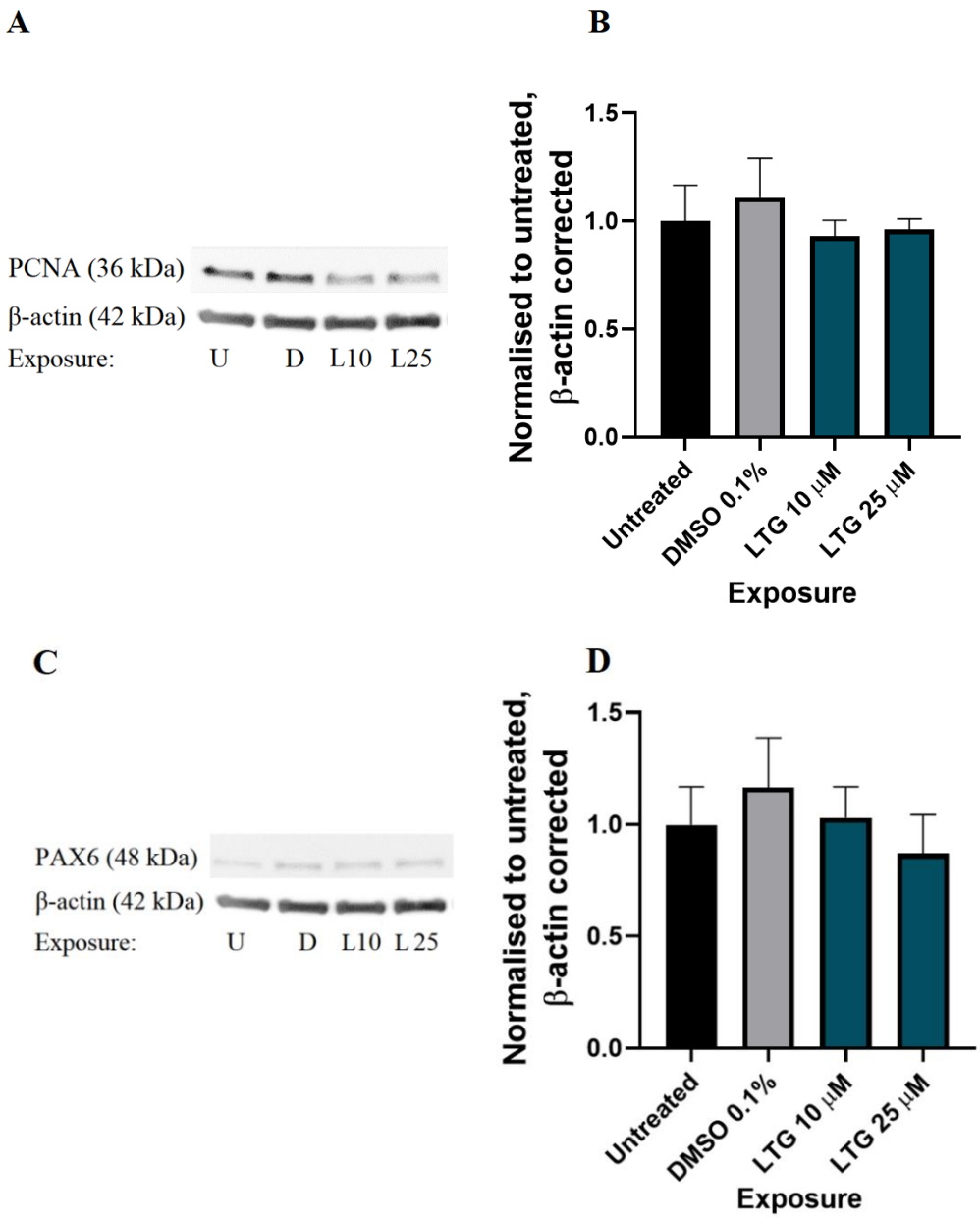

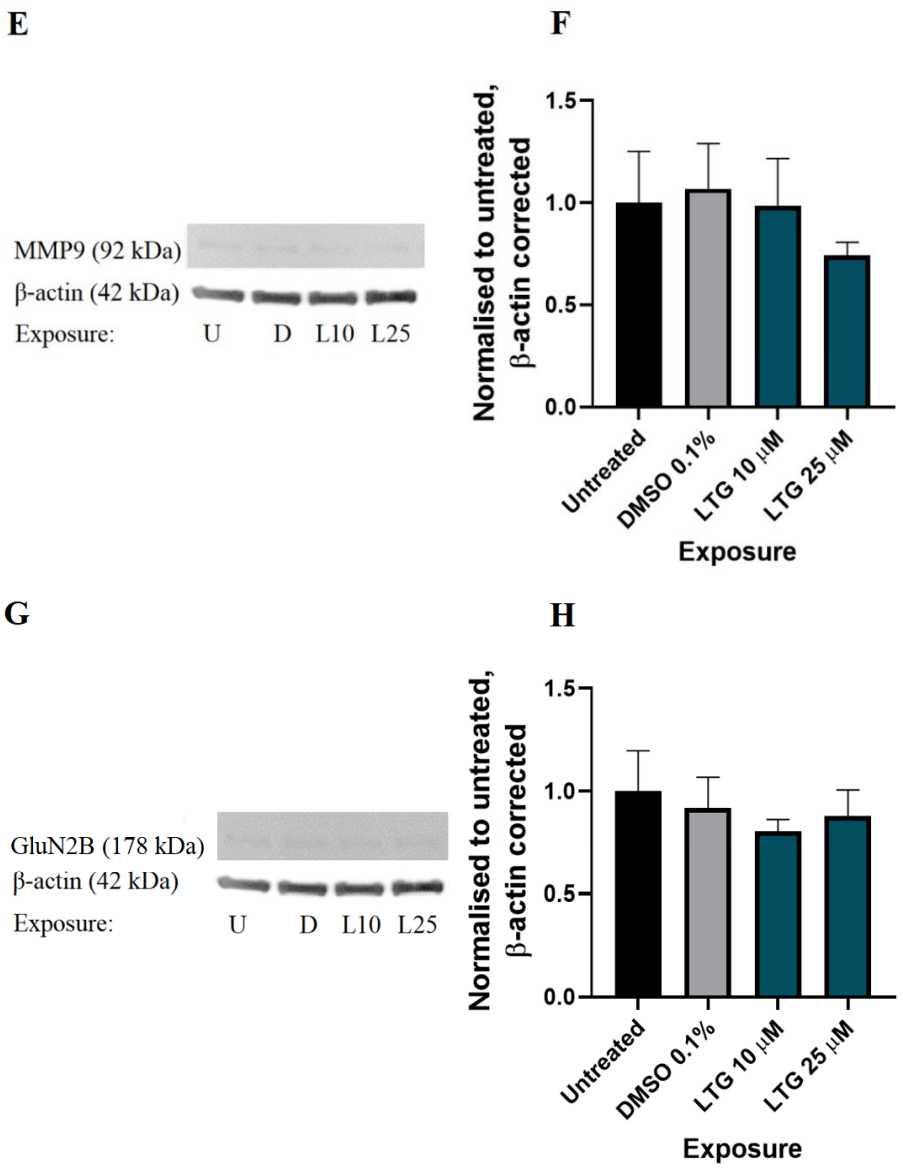

Figure 3.10 Protein expression is unaffected by LTG. Chicken embryos were exposed to LTG 10 μM, LTG 25 μM or DMSO 0.1% on E16. The cerebellum was harvested on E17 and studied through western blot analysis. Eggs from one experiment was used, with 5 chicken embryos per group. Groups: Untreated (U), DMSO 0.1% (D), LTG 10 μM (L10), and LTG 25 μM (L25). The data is displayed as average band strength corrected with β-actin (internal standard), and normalised to untreated controls + SEM. **A)** PCNA western blot analysis of cerebellum from chick embryo. **B)** Protein expression of PCNA in chicken embryo cerebellum after exposure. **C)** PAX western blot analysis of cerebellum from chick embryo. **D)** Protein expression of PAX6 in chicken embryo cerebellum after exposure. **E)** MMP9 western blot analysis of cerebellum from chick embryo. **F)** Protein expression of MMP9 in chicken embryo cerebellum after exposure. **G)** GluN2B western blot analysis of cerebellum from chick embryo. **H)** Protein expression of GluN2B in chicken embryo cerebellum after exposure. Statistical analysis was performed with One Way ANOVA Dunnett's *post hoc* test. N = 5.

3.2.6 LTG 25 µM significantly up-regulates *BDNF,* but does not affect *PCNA, PAX6, NR2B, SLC6A13* and *GABRR1*

In RT-qPCR, *BDNF* (figure 3.11C) was significantly increased for 25 µM exposure, whilst LTG 10 µM exhibited a decrease. For *GRIN2B* (figure 3.11D), 10 µM experienced an increase in gene expression, more than 25 µM (figure 3.11D). *ACTB* data can be found in Appendix III.

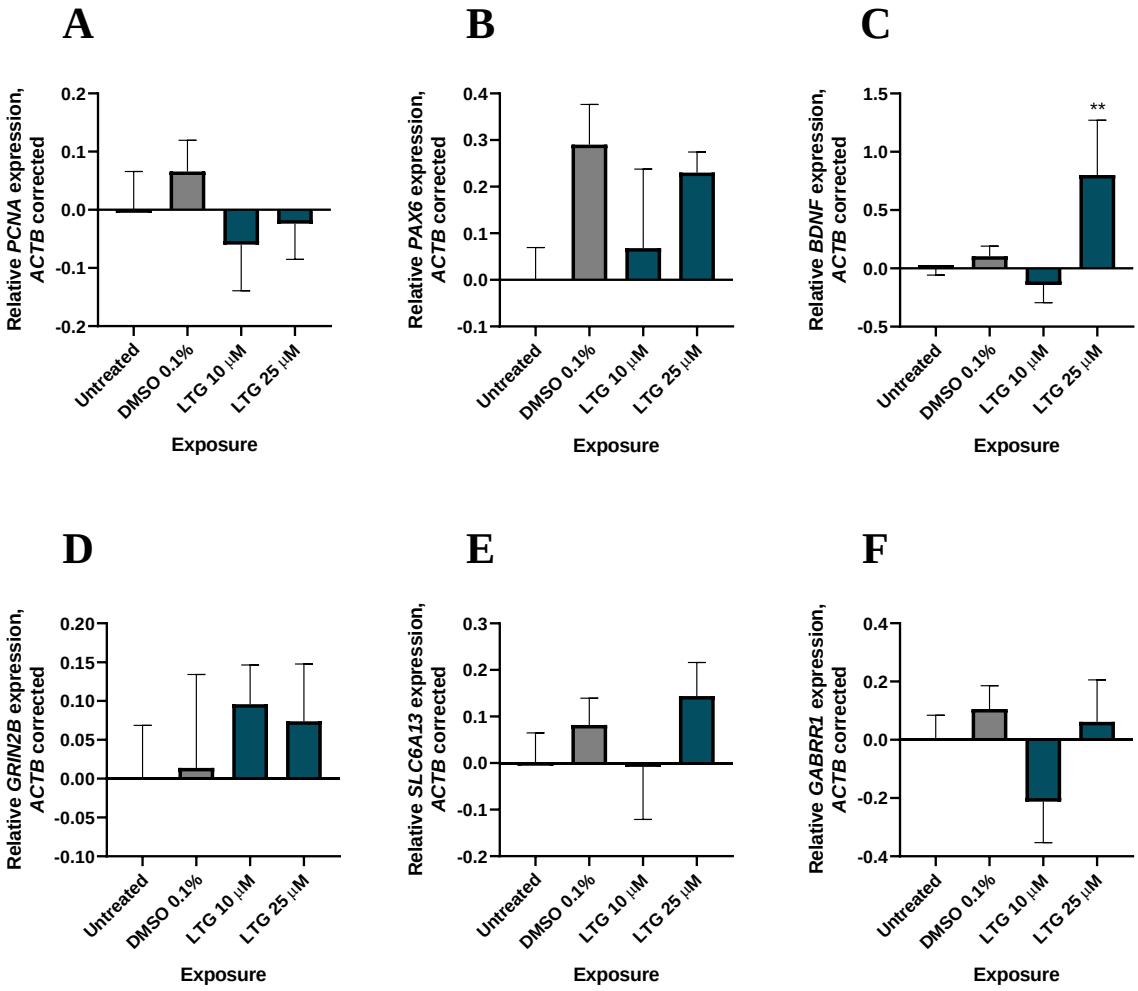

Figure 3.11 *BDNF* is significantly up-regulated by LTG 10 µM corrected with *ACTB*. Chicken embryos were exposed to LTG 10 µM, LTG 25 µM or DMSO 0.1% on E16. The cerebellum was harvested on E17 and studied through RT-qPCR. Eggs from 1 experiment was used, with 5 chicken embryos per group. The data is displayed as *ACTB* corrected values normalised with cerebella from untreated chicken embryos + SEM. **A)** *PCNA* expression from chicken embryo cerebella. **B)** *PAX6* expression from chicken embryo cerebella. **C)** *BDNF* expression from chicken embryo cerebella. **D)** *GRIN2B* expression from chicken embryo cerebella. **E)** *SLC6A13* expression from chicken embryo cerebella. **F)** *GABRR1* expression from chicken embryo cerebella. Statistical analysis was performed with One Way ANOVA Dunnett's *post hoc* test for B, and Kruskal-Wallis Dunn's *post hoc* test for A, C, D, E, and F. N = 5. Significance is shown by: p<0.01 (**) compared to untreated cerebella. Note the values on the y-axis differ between graphs.

3.2.7 LTG does not significantly affect gene expression when corrected with *GAPDH*

3.2.8 The solvent significantly affects PAX6 promoter activity

LTG was dissolved in DMSO, and the results from the luciferase assay illustrates that the vehicle significantly increases PAX6 promoter activity (figure 3.13A). LTG (5, 10 and 100 μM) was not significantly different from the vehicle control.

Figure 3.14 illustrates the uncorrected *Renilla* and firefly luciferase, which was mostly unaffected except by LTG 100 μM. Firefly and *Renilla* luciferase data can be found in Appendix IV.

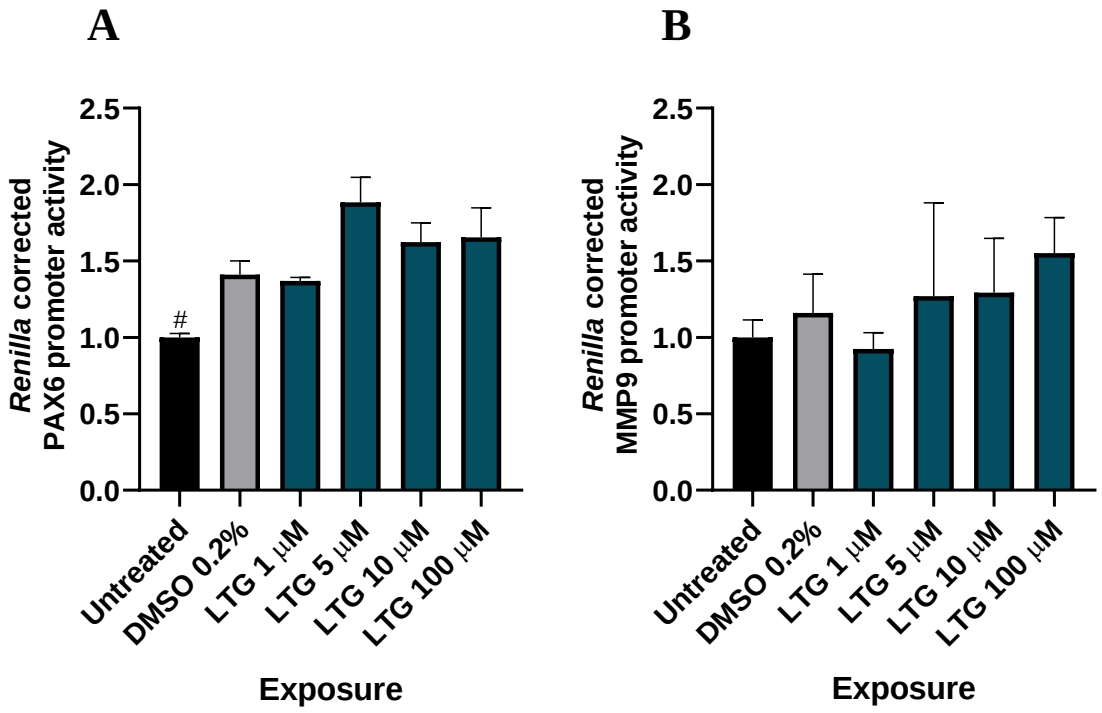

Figure 3.13 *Renilla* corrected PAX6 and MMP9 promoter activity in CGNs are affected by DMSO. CGNs were prepared from extracted cerebella from chicken embryos on E17. CGN was co-transfected with a reporter plasmid (PAX6-luc or MMP9-luc) and an internal control (pRL-TK) 48 hours after plating, and exposed with DMSO 0.2%, LTG (1, 5, 10, and 100 μM). Untreated dishes where used as a control. The cells were harvested, and the promoter activity was measured with firefly luciferase after 48 hours. *Renilla* luciferase was measured, which the firefly measurements were corrected with. The figure shows relative values normalised with the untreated dishes + SEM. **A)** *Renilla* corrected PAX6 promoter activity from n = 9 from 3 experiments for untreated, DMSO 0.2%, LTG 10 μM, and LTG 100 μM. N = 3 from 1 experiment for LTG 1 μM, and LTG 5 μM. **B)** *Renilla* corrected MMP9 promoter activity with from n = 9 from 3 experiments for untreated, and LTG 100 μM. N = 3 from 1 experiment for LTG 10 μM, and DMSO 0.2%. N = 2 for LTG 1 μM, and LTG 5 μM. Statistical analysis was performed with One Way ANOVA Kruskal-Wallis post hoc test for A, and Dunnett's post hoc test for B. Significance is shown by: $p<0.05$ (#) compared to DMSO.

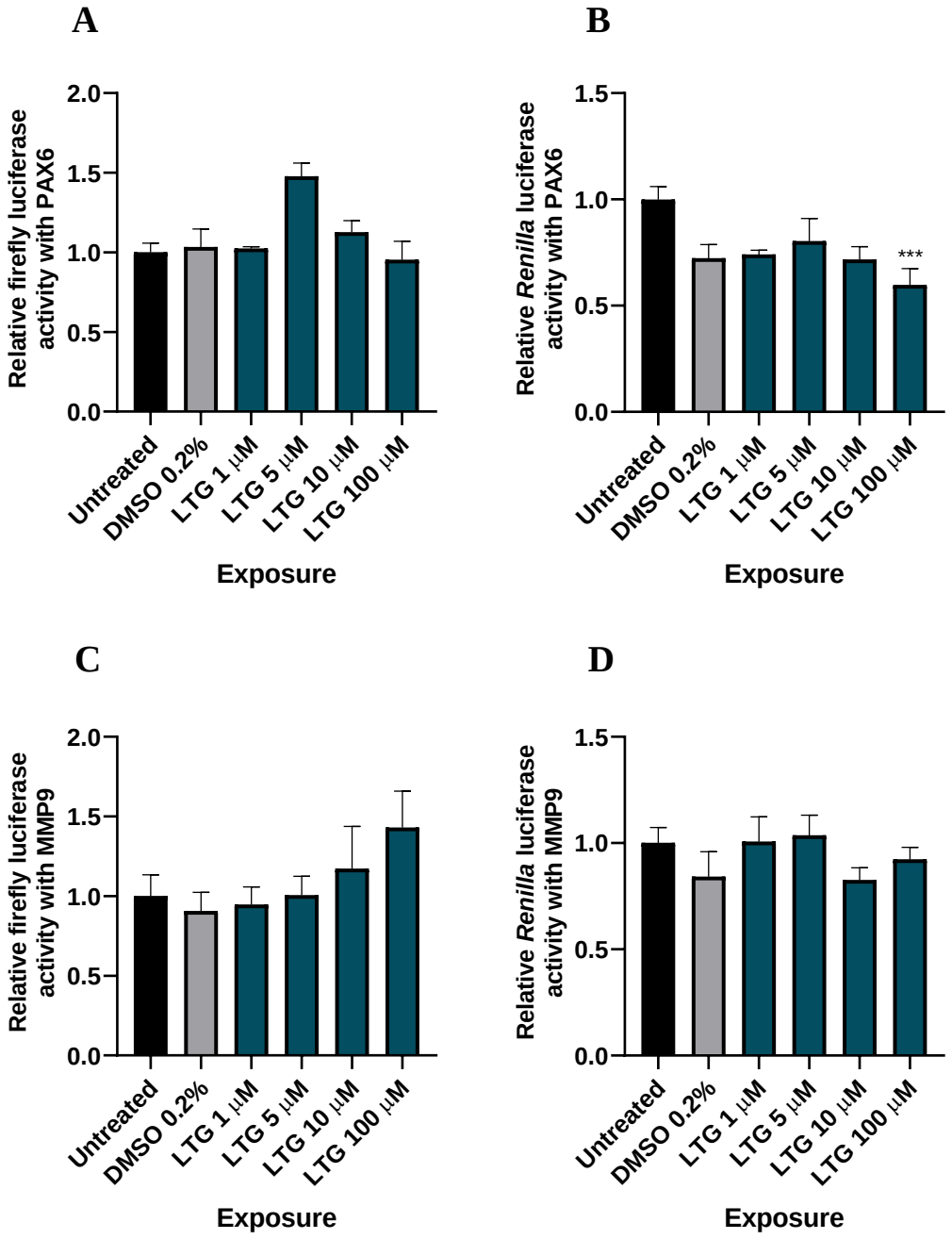

Figure 3.14 *Renilla* luciferase is significantly affected by 100 μM LTG with PAX6. CGNs were prepared from extracted cerebella from chicken embryos on E17. CGN was co-transfected with a reporter plasmid (PAX6-luc or MMP9-luc) and an internal control (pRL-TK) 48 hours after plating. Same day as transfection, CGNs were exposed to LTG (1, 5, 10 and 100 μM) or DMSO 0.2%. Untreated dishes were used as a control. The cells were harvested, and the promoter activity was measured with firefly luciferase after 48 hours. *Renilla* luciferase was measured and the firefly luciferase values were corrected. The data is displayed as relative luciferase values normalised with the untreated dishes + SEM. **A)** Uncorrected firefly luciferase results of PAX6 promoter activity from n = 9 from 3 experiments for untreated, DMS0 0.2%, LTG 10 μM and 100 μM, and n = 3 from 1 experiment LTG 1 and 5 μM. **B)** *Renilla* luciferase results of PAX6 promoter activity from n = 9 from 3 experiments for untreated, DMS0 0.2%, LTG 10 μM and 100 μM, and n = 3 from 1 experiment LTG 1 and 5 μM . **C)** Uncorrected firefly luciferase results of MMP9 promoter activity from n = 9 from 3 experiments for untreated, DMSO 0.2%, LTG 10 μM and 100 μM, n = 7 from 2 experiments for LTG 5 μM, and n = 6 from 2 experiments for LTG 1 μM. **D)** *Renilla* luciferase results of MMP9 promoter activity from n = 9 from 3 experiments for untreated, DMSO 0.2%, LTG 10 μM and 100 μM, n = 7 from 2 experiments for LTG 5 μM, and n = 6 from 2 experiments for LTG 1 μM. Statistical analysis was performed with One Way ANOVA Kruskal-Wallis Dunnett's post hoc test for A and B, Dunn's post hoc test for B, C, and D. Significance is shown by: $p<0.05$ (*), $p<0.001$ (***) compared to untreated dishes. Note the values on the y-axis differ between graphs.

3.3 Expression studies in PC12 cells

Promoter activity was assessed in PC12 cells with the reporter plasmids PAX6-luc and MMP9-luc through co-transfection with pRL-TK, 24 hours after plating. The cell culture was exposed to VPA (1, 100, 500, 1000 μM) and LTG (10, 100, 500 μM) after 24 hours, before the cells were harvested 48 hours after. Firefly luciferase was measured and the samples were stored in -20 °C until *Renilla* luciferase was measured to correct firefly luciferase.

To evaluate if VPA induced proliferation, an MTT analysis and Hoechst staining experiment were conducted. PC12 cells were exposed to 1, 10, 100, 200, 500, 750, 1000, and 2000 μM VPA 48 hours after plating, and analysed 48 hours after exposure for MTT analysis and Hoechst staining.

A promoter activity side project with PAX6-luc was performed with TSA (1, 10, 100 nM), an HDAC inhibitor, to establish if this was the mode of action for the affect VPA had on pRL-TK. A dose-response was performed before a final concentration was chosen.

The HDAC inhibition experiment was performed with PAX6-luc, pRL-TK, TSA 100 nM, and 10, 100, and 1000 μM VPA.

Firefly and *Renilla* luciferase can be found in Appendix IV.

3.3.1 High concentrations of VPA increases firefly and *Renilla* luciferase expression in PC12 cells

Figure 3.15 shows the uncorrected firefly and *Renilla* results, were there is a significant increase in their expression. The *Renilla* corrected results show an apparent reduction in promoter activity (figure 3.16).

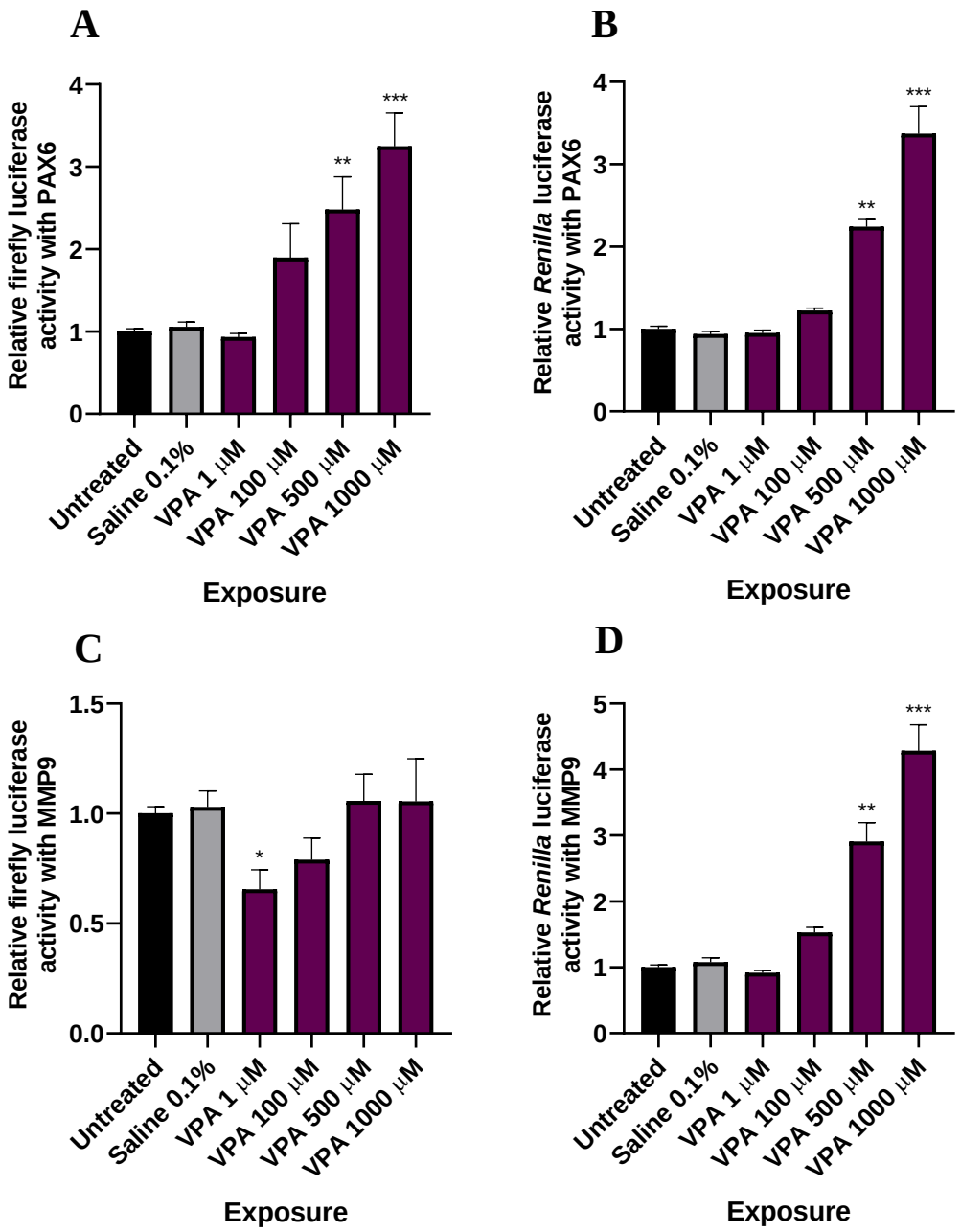

Figure 3.15 *Renilla* luciferase is significantly affected by VPA, and firefly luciferase increases with PAX6 at high concentrations, whilst decreases for MMP9 at low concentrations in PC12. PC12 cells were co-transfected with a reporter plasmid (PAX6-luc or MMP9-luc) and an internal control (*Renilla* luciferase, pRL-TK) 24 hours after plating. After 24 hours, the cells were exposed with saline or VPA (1, 100, 500 and 1000 μM). Untreated dishes were used as a control. The cells were harvested, and the promoter activity was measured with firefly luciferase 48 hours after exposure. *Renilla* luciferase was measured, and the firefly values were corrected. The data is displayed as relative luciferase values normalised with the untreated dishes + SEM. **A)** Uncorrected firefly luciferase results of PAX6 promoter activity from n = 9 values from 3 experiments for untreated, saline, VPA 100 μM, VPA 500 μM, and VPA 1000 μM. N = 6 values from 2 experiments for VPA 1 μM. **B)** *Renilla* luciferase results of PAX6 promoter activity from n = 9 values from 3 experiments for untreated, saline, VPA 100 μM, VPA 500 μM, and VPA 1000 μM. N = 6 values from 2 experiments for VPA 1 μM. **C))** Uncorrected firefly luciferase results of MMP9 promoter activity from n = 9 values from 3 experiments for untreated, and VPA 100 μM. N = 8 values from 3 experiments for saline. N = 6 values from 2 experiments for VPA 1 μM, VPA 500 μM, and VPA 1000 μM. **D)** *Renilla* luciferase results of MMP9 promoter activity from n = 9 values from 3 experiments for untreated, and VPA 100 μM. N = 8 values from 3 experiments for saline. N = 6 values from 2 experiments for VPA 1 μM, VPA 500 μM, and VPA 1000 μM. Statistical analysis with One Way ANOVA with Kruskal-Wallis Dunn's post hoc test. Significance is shown by: $p<0.05$ (*), $p<0.01$ (**), and $p<0.001$ (***) compared to untreated dishes. Note the values on the y-axis differ between graphs.

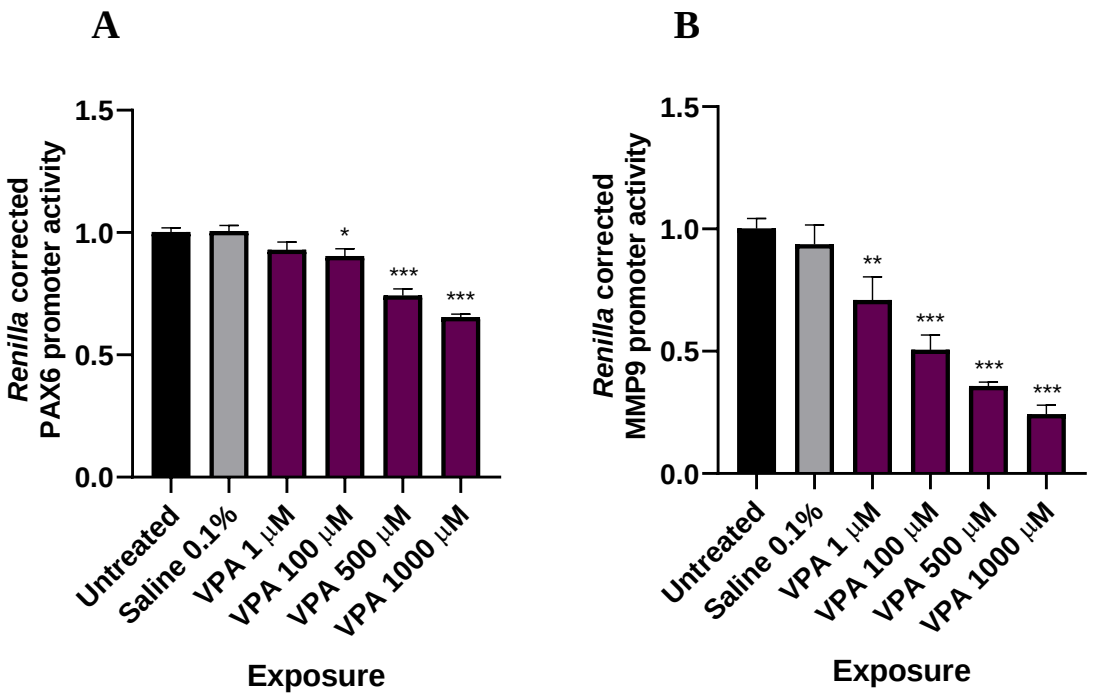

Figure 3.16 *Renilla* corrected PAX6 and MMP9 promoter activity in PC12 cells are affected by VPA PC12 cells were co-transfected with a reporter plasmid (PAX6-luc or MMP9-luc) and an internal control (pRL-TK) 24 hours after plating. After 24 hours, the cells were exposed with saline or VPA (1, 100, 500 and 1000 μM). Untreated dishes were used as a control. The cells were harvested, and the promoter activity was measured with firefly luciferase 48 hours after exposure. *Renilla* luciferase was measured, and the firefly luciferase values were corrected. The data is displayed as relative luciferase values normalised with the untreated dishes + SEM. **A)** *Renilla* corrected PAX6 promoter activity with n = 9 values from 3 experiments for untreated, VPA 1 μM. N = 6 values from 2 experiments for saline, VPA 100 μM, VPA 500 μM and VPA 1000 μM. **B)** *Renilla* corrected MMP9 promoter activity with n = 9 values from 3 experiments for untreated, saline, and VPA 100 μM. N = 6 values from 2 experiments for VPA 1 μM, VPA 500 μM, and VPA 1000 μM. Statistical analysis with One Way ANOVA with Dunnett's post hoc test for A, and Kruskal-Wallis Dunn's post hoc test for B. Significance is shown by: $p<0.05$ (*), $p<0.01$ (**), $p<0.001$ (***) compared to untreated dishes.

3.3.2 Cell viability was not increased, but significantly reduced by 2000 µM VPA

To assess cell viability, an MTT assay and Hoechst staining was performed. PC12 cells were exposed to VPA in different concentrations (1, 10, 100, 200, 500, 750, 1000, 2000 µM), or saline (combined results), where MTT was analysed 72 hours following the exposure. A dose-response curve of PC12 cells from MTT analysis show a significant decrease in cell viability after exposure to 2000 µM VPA (figure 3.17).

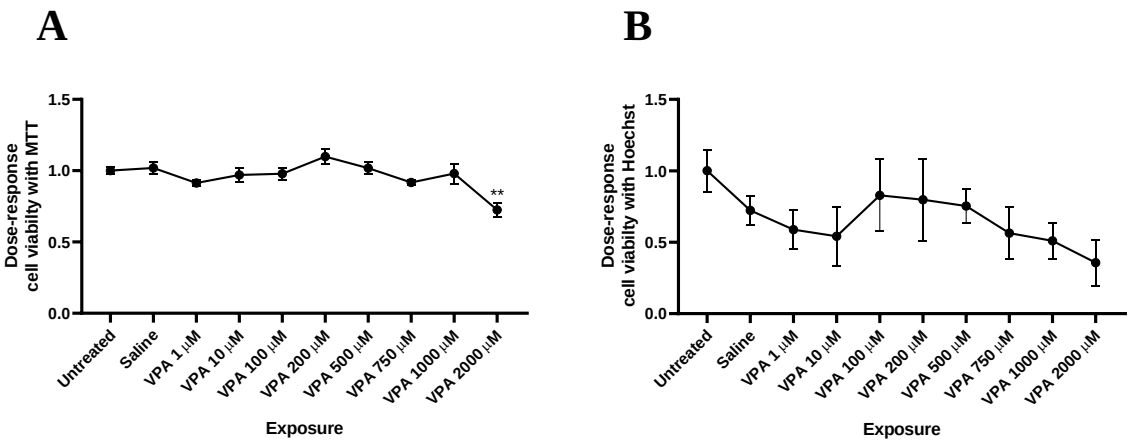

Figure 3.17 Dose-response curves following VPA exposure illustrates a significant decrease in cell viability for VPA 2000 µM. PC12 cells were exposed to VPA in different concentrations (1, 10, 100, 200, 500, 750, 1000, 2000 µM) 24 hours after plating, and analysed with MTT, or stained with Hoechst after 72 hours. The data is displayed as relative values normalised with the untreated wells ± SEM. **A)** PC12 cells analysed with MTT. **B)** PC12 cells analysed through Hoechst staining. N = 8 from 1 experiment. Statistical analysis with One Way ANOVA with Kruskal-Wallis Dunn's post hoc test for A, and Dunnett's post hoc test for B. Significance is shown by: $p<0.05$ (*) compared to untreated wells.

3.3.3 TSA significantly increases *Renilla* luciferase activity

To determine which concentration of TSA to use for the HDAC inhibition experiment, a dose-response experiment was performed. PC12 cells were co-transfected with PAX6-luc and pRL-TK 24 hours after plating. Then, the cells were exposed to TSA in different concentrations (1, 10, 100 nM) or DMSO 0.1% 24 hours later. The PC12 cells were harvested 48 hours after exposure and firefly luciferase was measured. *Renilla* luciferase was measured and used to correct firefly luciferase. *Renilla* luciferase was significantly increased by TSA compared to DMSO 0.1% treated cells (figure 3.18).

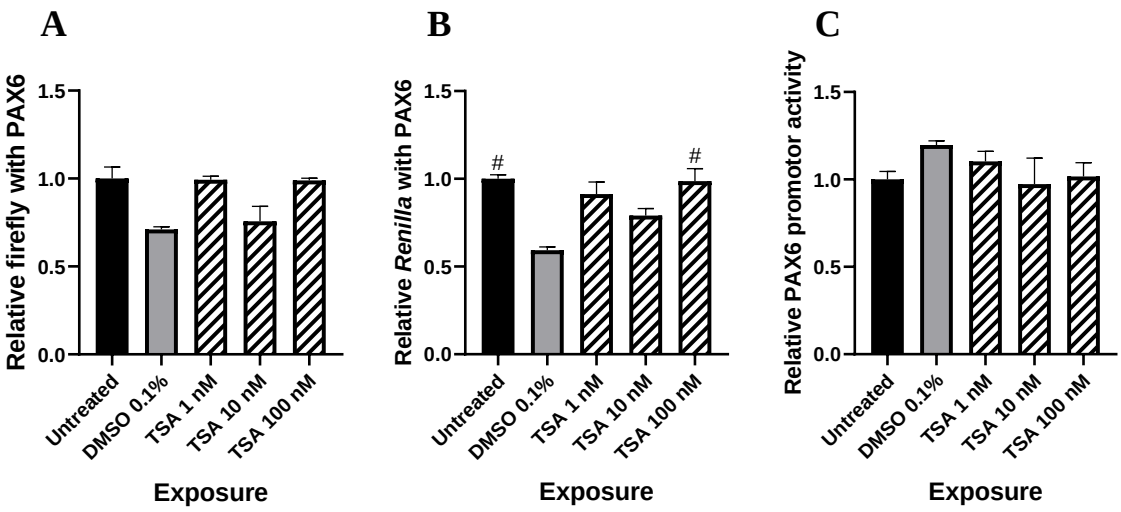

Figure 3.18 TSA significantly increases *Renilla* luciferase in PC12 cells. PC12 cells were co-transfected with the reporter plasmid, PAX6-luc, and an internal control (pRL-TK) 24 hours after plating. The cells were exposed to TSA (1, 10, and 100 nM) or DMSO 0.1% after 24 hours. Untreated dishes were used as a control. The cells were harvested, and the promoter activity was measured with firefly luciferase 48 hours after exposure. *Renilla* luciferase was measured, and the firefly luciferase values were corrected. The data is displayed as relative values normalised with the untreated dishes + SEM. **A)** Uncorrected firefly luciferase results on PAX6 promoter activity. **B)** *Renilla* luciferase results on PAX6 promoter activity. **C)** *Renilla* corrected PAX6 promoter activity. Statistical analysis with One Way ANOVA Kruskal-Wallis Dunn's test for A and B, and Dunnett's post hoc test for C. N = 3 from 1 experiment. Significance is shown by: $p<0.05$ (#) compared to DMSO.

3.3.4 TSA significantly increases *Renilla* luciferase in combination with VPA 10 μM

Renilla luciferase was significantly affected by VPA at higher concentrations. An HDAC inhibition experiment was conducted to determine if this could be ascribed to this mechanism. The TSA concentration selected from the dose-response experiment (100 nM, section 3.3.3), was chosen to see if it could mimic the response exhibited by VPA. Figure 3.19 shows that TSA 100 nM in combination seems to increase the firefly and *Renilla* luciferase. The combination of TSA and 10 μM is significantly increased compared to 10 μM alone (figure 19B).

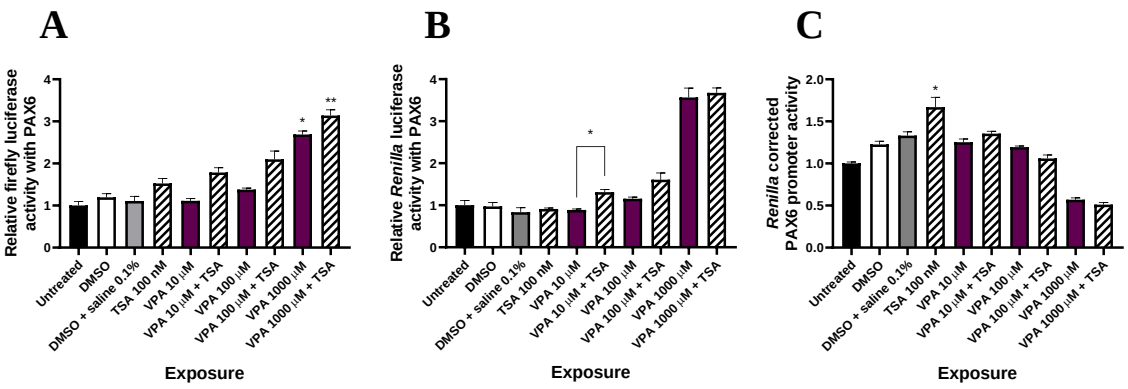

Figure 3.19 TSA significantly increases 10 μM *Renilla* luciferase in combination with TSA in PC12 cells. PC12 cells were co-transfected with the reporter plasmid, PAX6-luc, and an internal control (pRL-TK) 24 hours after plating. After 24 hours, the cells were exposed to DMSO 0.1%, DMSO 0.1% with saline, or TSA 100 nM, VPA 10, 100, 1000 μM alone or in combination. Untreated dishes were used as a control. The cells were harvested, and the promoter activity was measured with firefly luciferase 48 hours after exposure. *Renilla* luciferase was measured, and the firefly values were corrected. The data is displayed as luciferase values normalised with the untreated dishes + SEM. **A)** Uncorrected firefly luciferase results on PAX6 promoter activity. **B)** *Renilla* luciferase results on PAX6 promoter activity. **C)** *Renilla* corrected PAX6 promoter activity. Statistical analysis with One Way ANOVA Kruskal-Wallis Dunn's post hoc test. N = 3 from 1 experiment. Significance is shown by: $p<0.05$ (*), and $p<0.01$ (**) compared to untreated. Statistical analysis with Wilcoxon signed rank test and Welch's t-test. Significance is shown by: $p<0.05$ (*) compared to its VPA exposure. Note the values on the y-axis differ between graphs.

3.3.5 Solvent significantly induces promoter activity for PAX6

DMSO was seen to affect PAX6 promoter activity, more so with DMSO 1.2% (figure 3.20). There was no significant difference between the vehicle control compared with the other exposures. LTG 500 μM significantly reduced promoter activity (figure 3.20B), as well as firefly and *Renilla* luciferase (figure 3.21).

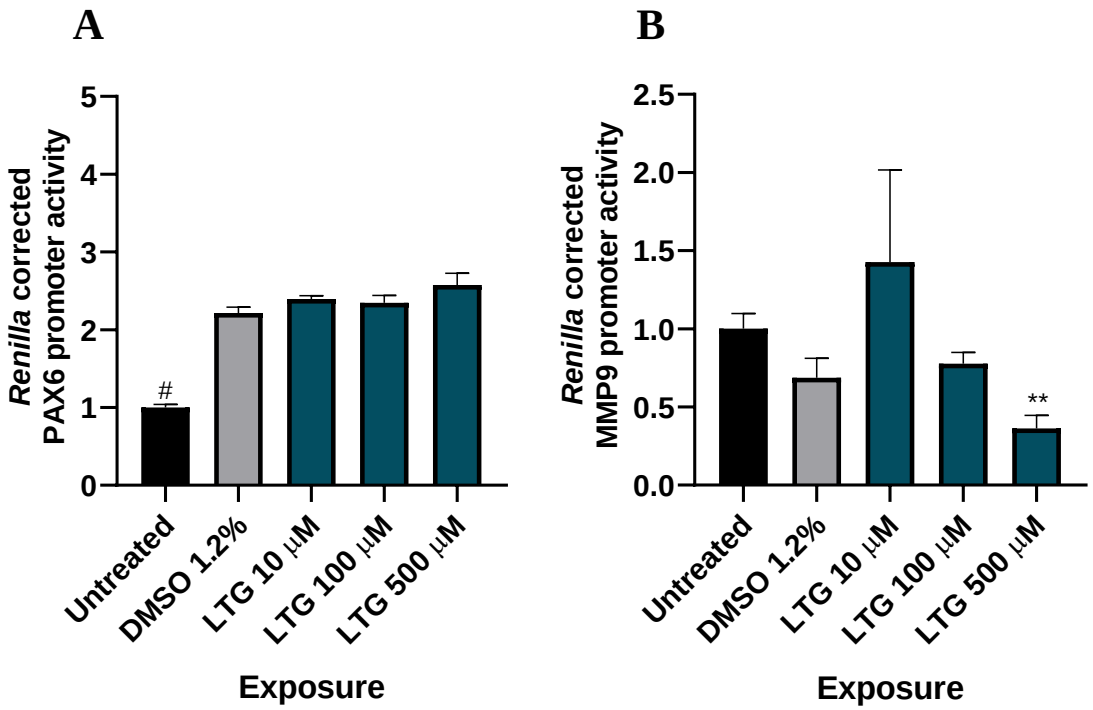

Figure 3.20 PAX6 and MMP9 promoter activity is significantly affected by DMSO 1.2% and LTG 500 μM, respectively. PC12 cells were co-transfected with a reporter plasmid (PAX6-luc or MMP9-luc), and an internal control (pRL-TK) 24 hours after plating. After 24 hours, the cells were exposed to LTG (10, 100, and 500 μM), DMSO 0.2% or DMSO 1.2%. Untreated dishes were used as a control. The cells were harvested, and the promoter activity was measured with firefly luciferase 48 hours after exposure. *Renilla* luciferase was measured, and the firefly values were corrected. The data is displayed as corrected *Renilla* luciferase values normalised with the untreated dishes + SEM. **A)** *Renilla* corrected PAX6 promoter activity with DMSO. N = 9 from 3 experiments for untreated, DMSO 1.2% and LTG 500 μM, n = 3 from 1 experiment for LTG 10 and 100 μM. **B)** *Renilla* corrected MMP9 promoter activity. N = 9 from 3 experiments for untreated and LTG 500 μM, n = 6 from 2 experiments for DMSO 1.2%, n = 3 from 1 experiment for LTG 10 and 100 μM. N = 6 from 2 experiments. Statistical analysis with One Way ANOVA Kruskal-Wallis Dunn's post hoc test. Significance is shown by: $p<0.05$ (#), compared to DMSO and $p<0.01$ (**) compared to untreated dishes. Note the values on the y-axis differ between graphs.

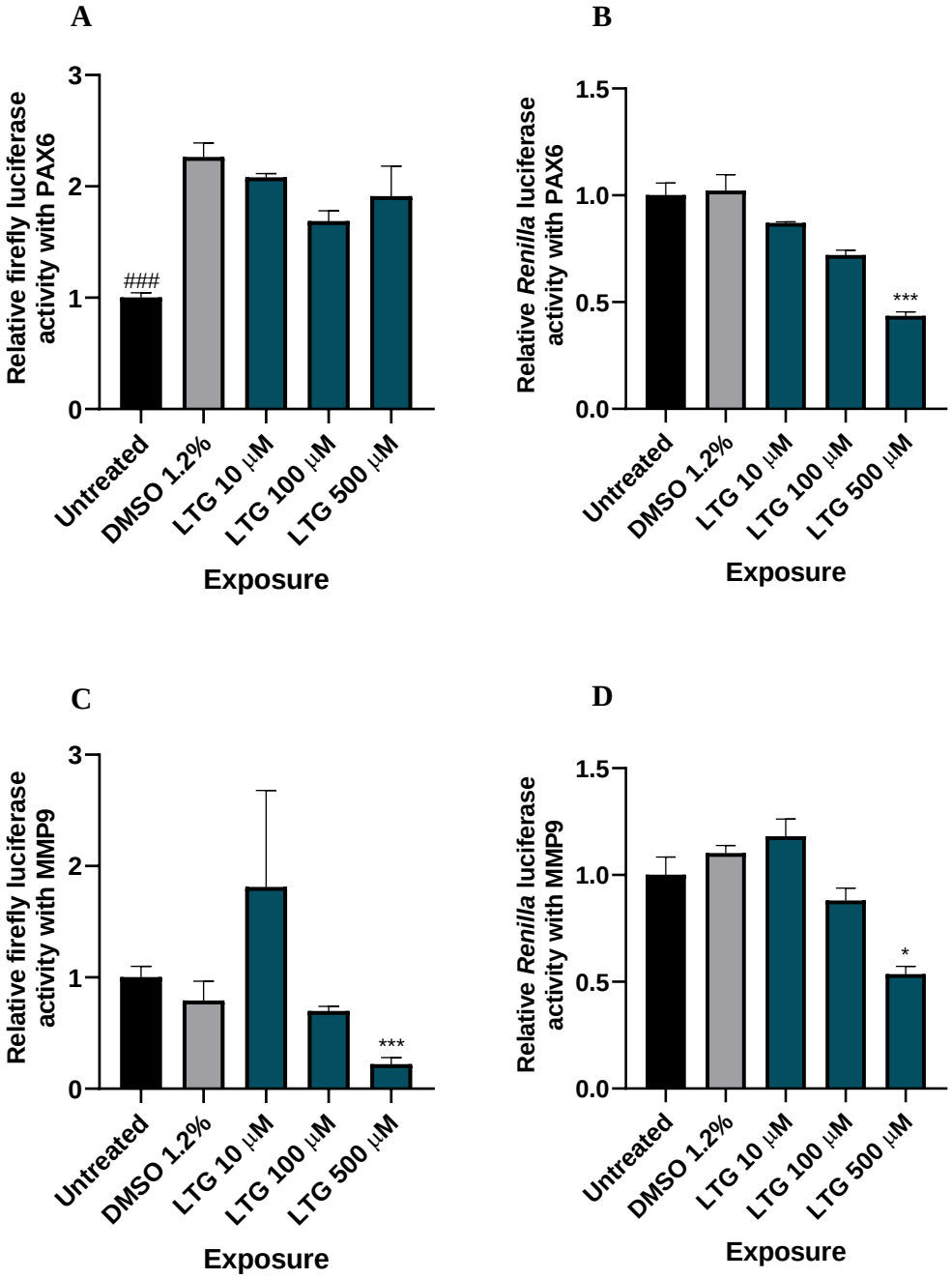

Figure 3.21 *Renilla* and firefly luciferase are significantly reduced by LTG 500 μM in PC12 cells. PC12 cells were co-transfected with a reporter plasmid (PAX6-luc or MMP9-luc), and an internal control (pRL-TK) 24 hours after plating. After 24 hours, the cells were exposed to LTG (10, 100, and 500 μM) or DMSO 1.2%. Untreated dishes where used as a control. The cells were harvested, and the promoter activity was measured with firefly luciferase 48 hours after exposure. *Renilla* luciferase was measured, and the firefly values were corrected. The data is displayed as luciferase values normalised with the untreated dishes + SEM. **A)** Uncorrected firefly luciferase results of PAX6 promoter activity. N = 9 from 3 experiments for untreated, DMSO 1.2% and LTG 500 μM, and n = 3 from 1 experiment for LTG 10 and 100 μM. **B)** *Renilla* luciferase results from PAX6 promoter activity. N = 9 from 3 experiments for untreated, DMSO 1.2% and LTG 500 μM, and n = 3 from 1 experiment for LTG 10 and 100 μM. **C)** Uncorrected firefly luciferase of MMP9 promoter activity. N = 9 from 3 experiments for untreated and LTG 500 μM, n = 6 from 2 experiments for DMSO 1.2%, n = 3 from 1 experiment for LTG 10 and 100 μM. **D)** *Renilla* luciferase results of MMP9 promoter activity. N = 9 from 3 experiments for untreated and LTG 500 μM, n = 6 from 2 experiments for DMSO 1.2%, n = 3 from 1 experiment for LTG 10 and 100 μM. Statistical analysis with One Way ANOVA Kruskal-Wallis Dunn's *post hoc* test. Significance is shown by: $p<0.05$ (*), $p<0.01$ (**), and $p<0.001$ (***) compared to untreated dishes. Note the values on the y-axis differ between graphs.

3.4 Neurite outgrowth

Neurite outgrowth was assessed with CGN culture. CGNs prepared from chicken embryo cerebella from E17, were plated and exposed to VPA (1, 100, 500, and 1000 μM), LTG (1, 5, 10, 100, and 500 μM), saline or DMSO (0.2% and 1.2%) 24 hours later. Neurite outgrowth was visually assessed with IncuCyte® the same day.

3.4.1 VPA does not significantly affect neurite length, nor branch points

Figure 3.22A-R illustrates the differentiation of CGNs exposed in 24-hour intervals to VPA (1, 100, 500, and 1000 μM), and saline. VPA does not significantly affect neurite outgrowth. It does seem to promote neurite length in a dose-dependent manner. Over time, the lower concentrations induced neurite length more than the higher concentrations (figure 3.23A-C). VPA exposure seems to increase neurite branch points (figure 3.24A-C). Curves in Appendix V illustrate the overall neurite length and branch point formation over time.

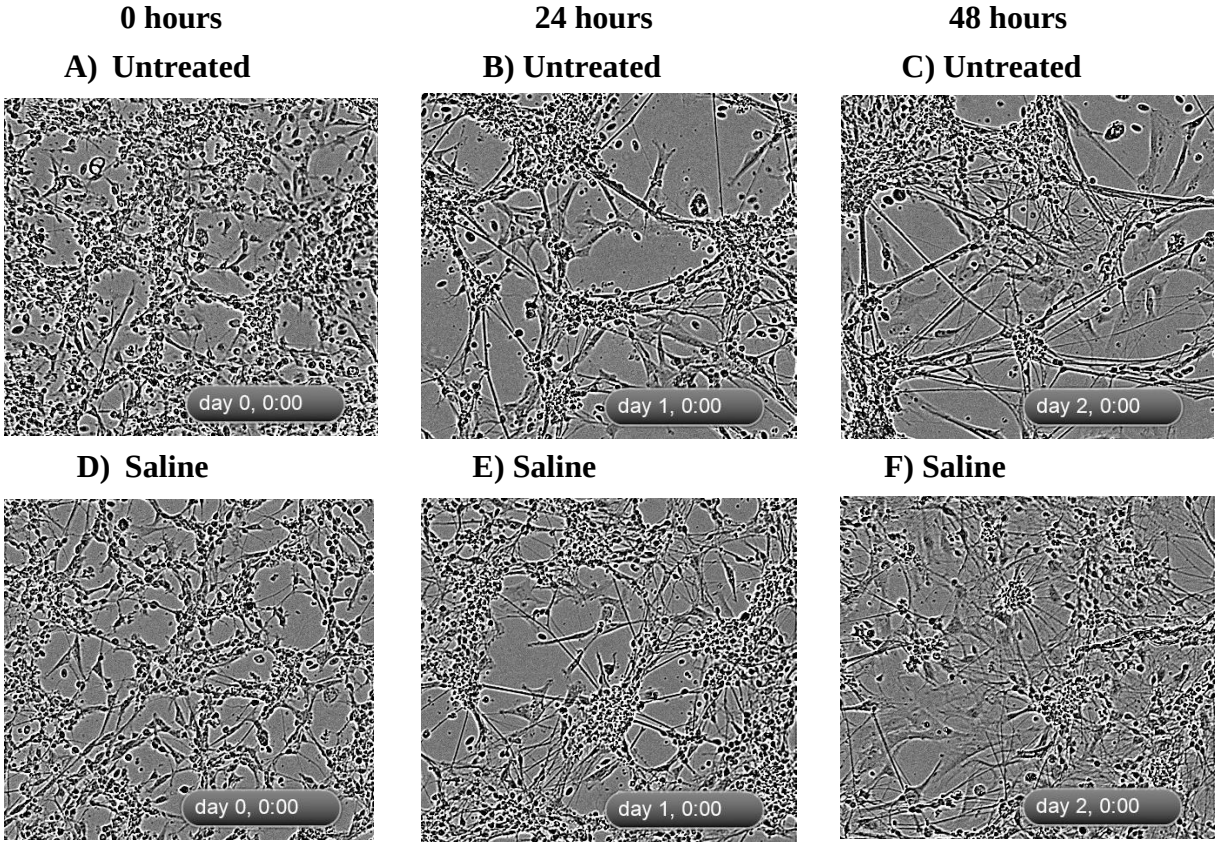

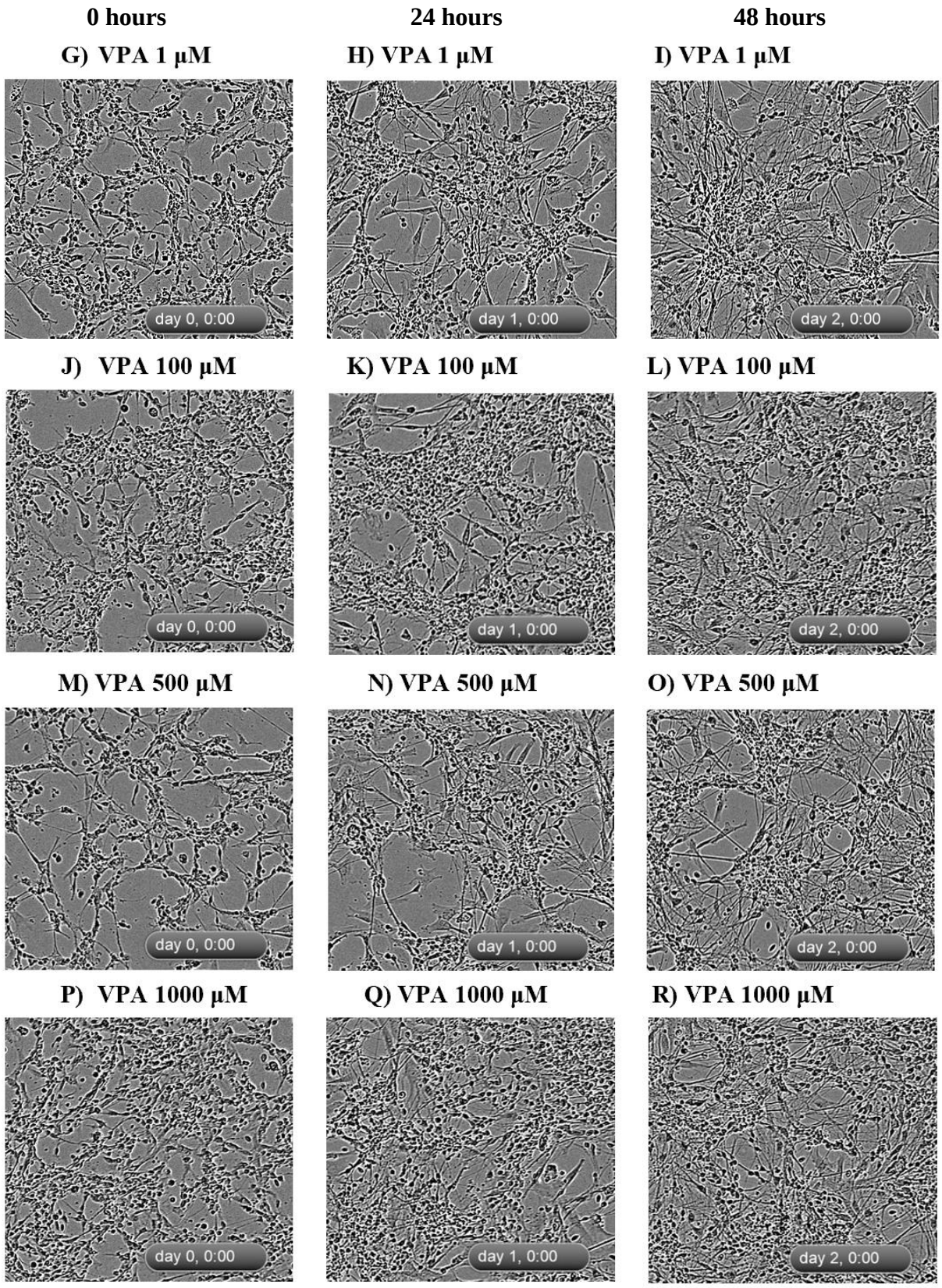

Figure 3.22 Neurite outgrowth of CGNs exposed to VPA. CGNs prepared from E17 chicken embryo cerbella were plated, and exposed to VPA (1, 100, 500, 1000 µM), or saline combined with AraC 24 hours later. That very day, neurite outgrowth was assessed with IncuCyte® over 51 hours. **A, D, G, J, M, P)** Neurite outgrowth at 0 hours. **B, E, H, K, N, Q)** Neurite outgrowth at 24 hours. **C, F, I, L, O, R)** Neurite outgrowth at 48 hours.

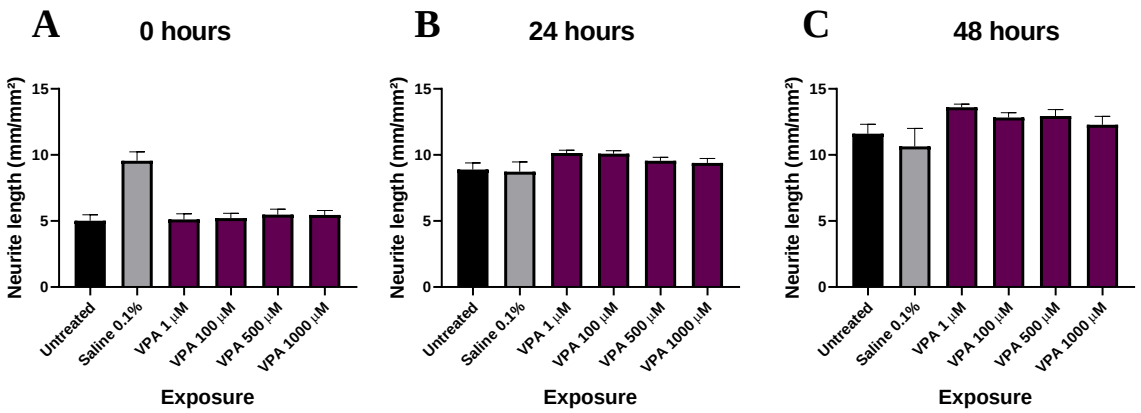

Figure 3.23 VPA does not affect neurite length. CGNs prepared from E17 chicken embryo cerbella were plated, before exposure to VPA (1, 100, 500, 1000 μM), or saline in combination with AraC, 24 hours later. Neurite outgrowth was assessed that very day with IncuCyte® over 51 hours. The data is displayed as the average ± SEM **A)** Neurite length of CGNs at 0 hours. **B)** Neurite length of CGNs at 24 hours. **C)** Neurite length of CGNs at 48 hours. N = 16 from 2 experiments. Statisical analysis with One Way ANOVA Kruskal-Wallis Dunn's *post hoc* test.

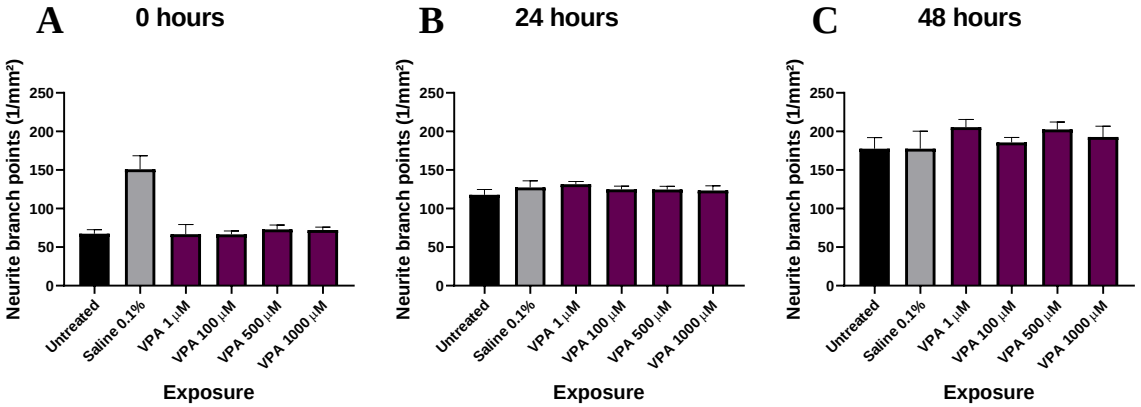

Figure 3.24 VPA does not affect neurite branch points. CGNs prepared from E17 chicken embryo cerbella were plated and exposed to VPA (1, 100, 500, 1000 μM), or saline in combination with AraC 24 hours later. Neurite outgrowth was assessed that very day with IncuCyte® over 51 hours. The figure shows the average ± SEM. **A)** Neurite branch points of CGNs at 0 hours. **B)** Neurite branch points of CGNs at 24 hours. **C)** Neurite branch points of CGNs at 48 hours. N = 16 from 2 experiments. Statisical analysis with One Way ANOVA Kruskal-Wallis Dunn's *post hoc* test.

3.4.2 DMSO affects neurite length at lower concentrations, but does not affect neurite branch points

Figure 3.25A-R illustrates the differentiation of CGN exposed to LTG (1, 5, 10, 100, 500 μM), DMSO 0.2%, and DMSO 1.2% in 24-hour intervals. DMSO 0.2%, LTG 1 μM, and 5 μM exhibit the same neurite length, as well as DMSO 1.2% and 500 μM. LTG 10 μM and LTG 100 μM depress and promotes neurite length, respectively (figure 3.26).

Regarding neurite branch points, different concentrations of LTG was not significantly affected compared to the solvent control. Curves in Appendix V illustrate the overall neurite length and branch point formation over time.

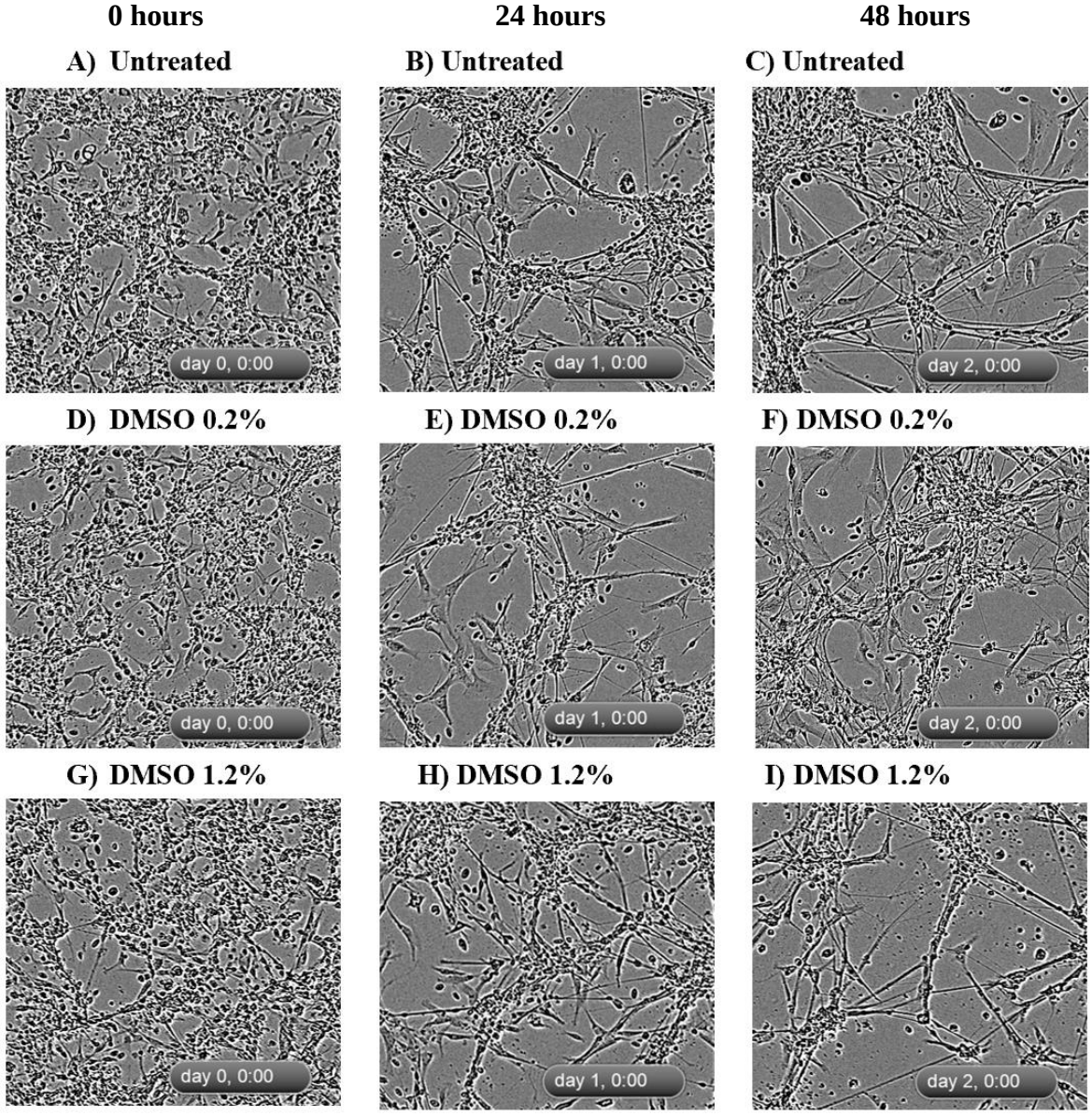

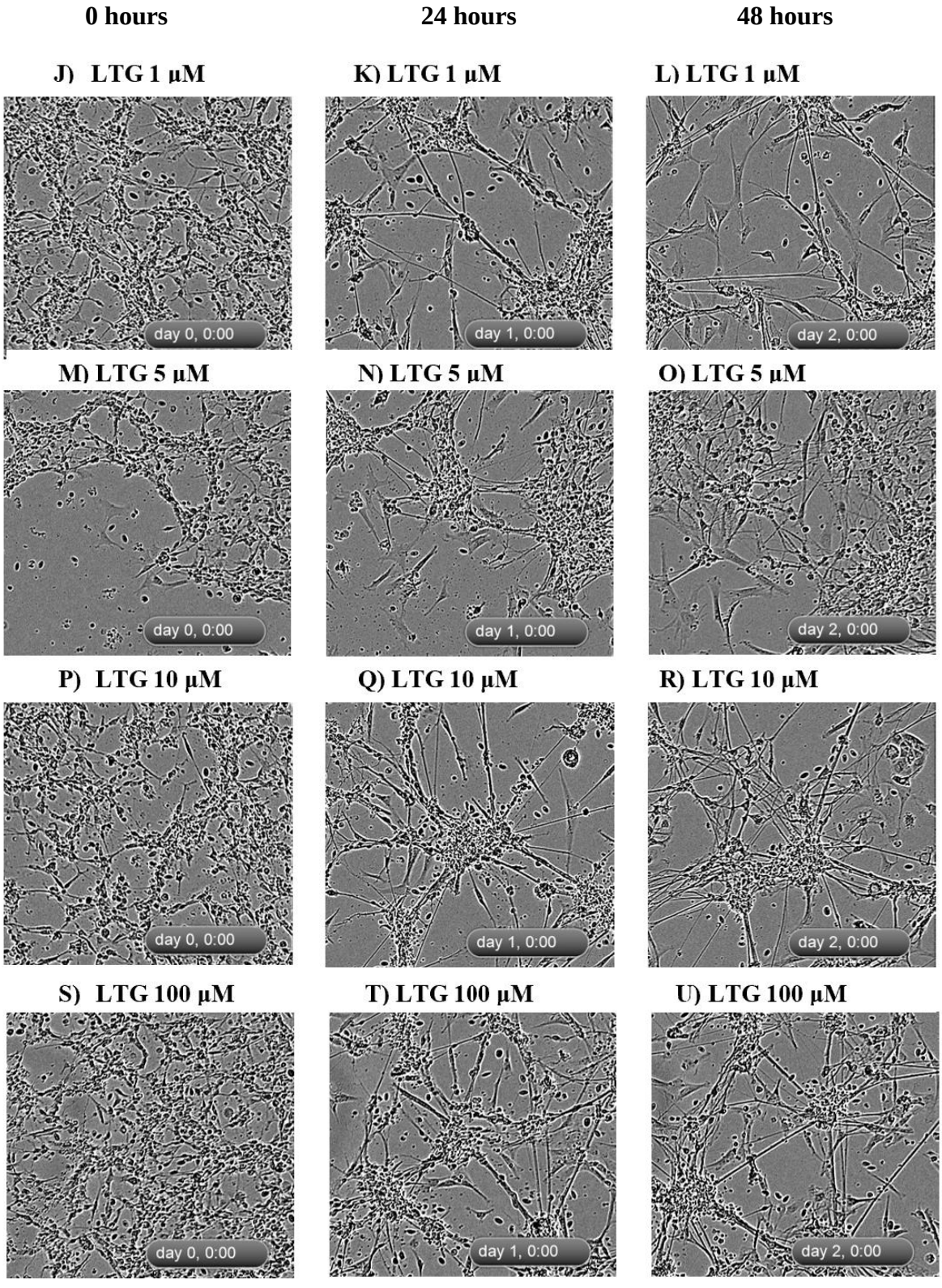
0 hours
24 hours
48 hours
J) LTG 1 µM
K) LTG 1 µM
L) LTG 1 µM
day 0, 0:00
day 1, 0:00
day 2, 0:00
M) LTG 5 µM
N) LTG 5 µM
O) LTG 5 µM
day 0, 0:00
day 1, 0:00
day 2, 0:00
P) LTG 10 µM
Q) LTG 10 µM
R) LTG 10 µM
day 0, 0:00
day 1, 0:00
day 2, 0:00
S) LTG 100 µM
T) LTG 100 µM
U) LTG 100 µM
day 0, 0:00
day 1, 0:00
day 2, 0:00

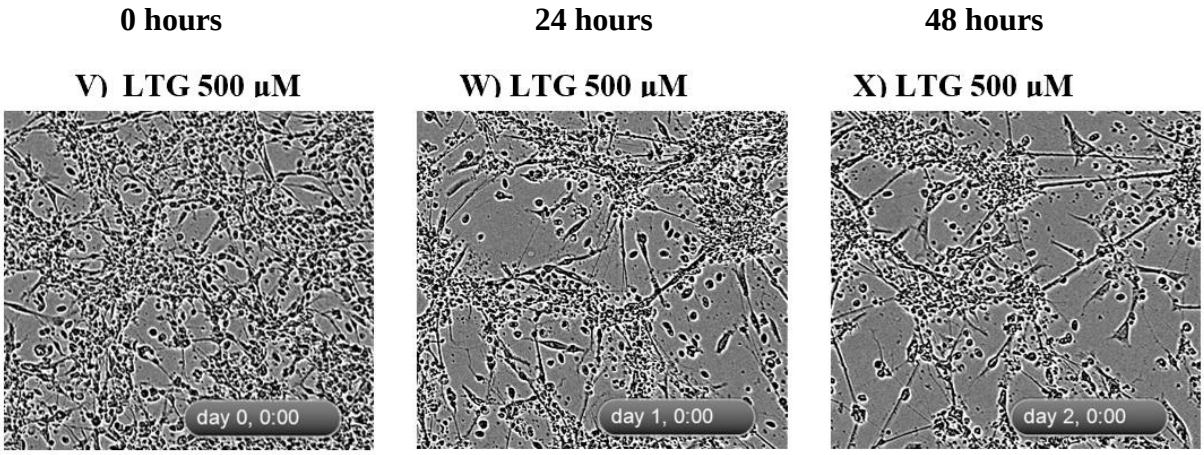

Figure 3.25 Neurite outgrowth of CGNs exposed to LTG. CGNs prepared from E17 chicken embryo cerbella were plated and exposed to LTG (1, 5, 10, 100, 500 µM), DMSO 0.2% or DMSO 1.2% combined with AraC 24 hours later. That very day, neurite outgrowth was assessed with IncuCyte™ over 51 hours. **A, D, G, J, M, P, S, V)** Neurite outgrowth at 0 hours. **B, E, H, K, N, Q, T, W)** Neurite outgrowth at 24 hours. **C, F, I, L, O, R, U, X)** Neurite outgrowth at 48 hours.

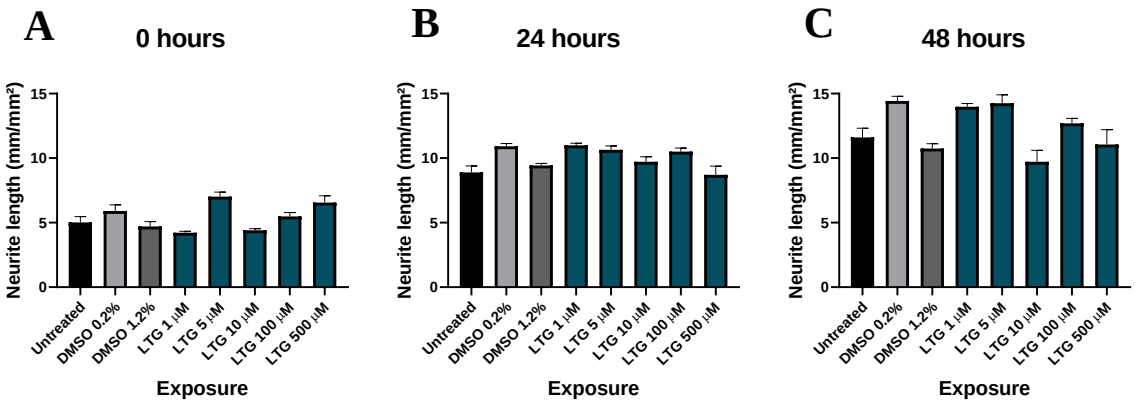

Figure 3.26 LTG does not affect neurite length. CGNs prepared from E17 chicken embryo cerbella were plated and exposed to LTG (1, 5, 10, 100, 500 µM), DMSO 0.2%, or DMSO 1.2% combined with AraC 24 hours later. That very day, neurite outgrowth was assessed with IncuCyte® over 51 hours. The figure shows the average ± SEM **A)** Neurite length of CGNs at 0 hours. **B)** Neurite length of CGNs at 24 hours. **C)** Neurite lengths of CGNs at 48 hours. N = 16 from two experiments for 10, 100, 500 µM, DMSO 0.2%, and DMSO 1.2%, whilst n = 8 for LTG 1 µM and LTG 5 µM. Statisical analysis with One Way ANOVA Kruskal-Wallis Dunn's *post hoc* test.

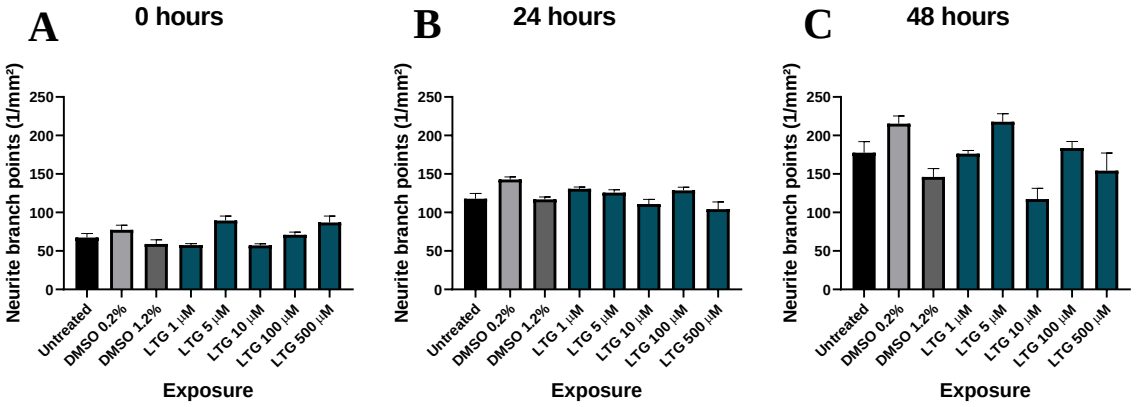

Figure 3.27 LTG does not affect branch points. CGN prepared from E17 chicken embryo cerbella were plated, and where exposed to LTG (1, 5, 10, 100, 500 μM), DMSO 0.2%, or DMSO 1.2% combined with AraC 24 hours later. That very day, neurite outgrowth was assessed with IncuCyte™ over 51 hours. The figure shows the average ± SEM **A)** Neurite length of CGNs at 0 hours. **B)** Neurite branch points of CGNs at 24 hours. **C)** Neurite branch points of CGNs at 48 hours. N = 16 from two experiments for 10, 100, 500 μM, DMSO 0.2%, and DMSO 1.2%, whilst n = 8 for LTG 1 μM and LTG 5 μM. Statisical analysis with One Way ANOVA Kruskal-Wallis Dunn's *post hoc* test.

4 Discussion

4.1 Choice of model systems

It is important to consider relevant model systems for safety pharmacology studies in order to gather information that is scientifically valid. The ICH 7A guideline specifies that animal models and *in vitro* preparations can be used as a test system, where the latter can be used to obtain a profile of the activity of a substance. It can also be used to investigate the effects that were observed *in vivo* [3]. In this thesis, the animal model employed was the chicken embryo model, which is not an established safety pharmacologic model, such as mouse, rat and monkey [106]. The guideline mentions that for general considerations on test model system, justification should be provided for the selection of the particular animal model or test system [3].

A minireview from 2015 discussed why the chicken embryo model should be considered as a suitable test model for safety pharmacology studies. Their reasons for utilising this model were that the chicken embryo can mimic natural tissue architecture and function, including how certain aspects in the developing CNS are similar in humans [72].

The chicken embryo is encapsulated by a membrane called chorioallantoic membrane (CAM). This membrane, as well as the chicken yolk sac, share some characteristic similarities with the mammalian placenta in terms of nutrition and gas exchange functions. It also develops in a comparable manner as the allantois in mammals [107]. Figure 4.1 illustrates a fertilised egg on E16.

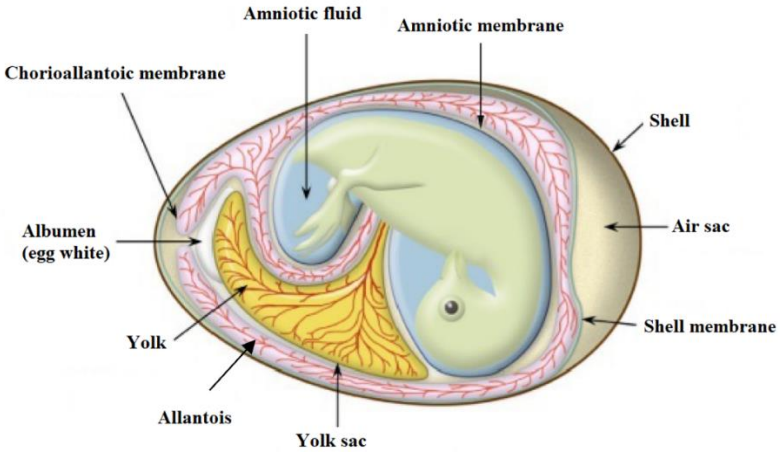

Figure 4.1 Schematic illustration of a fertilised egg on E16. The figure was obtained and modified from [108].

Humans also have a structure similar to the CAM, called the chorioallantoic placenta. It has two main parts; the foetal part and the maternal part. The foetal part bears resemblance to CAM in the chicken embryo model, whilst the maternal part originates from the uterine epithelium and sub-epithelial layers. They each have a separate circulation [109].

Through injection, the AED was administered onto the CAM. The drug transport followed the route illustrated in figure 4.2 for topical administration. With this form of drug delivery, the AEDs reach the systemic circulation via absorption through the membrane. This way of injecting was to emulate how a maternal exposure from blood traverses through the placental membrane and into foetal blood. A study comparing the placental villi with the avian yolk sac and CAM, found that the CAM could be extrapolated to the placenta in humans because they exhibit a similar morphology and functionality [107]. Yet others conclude that since there are many differences in placental structures and function, extrapolations from animals to humans are not sufficiently reliable, and should only be viewed as approximations [109]. There are also differences in drug metabolism and immune system with mammals [110].

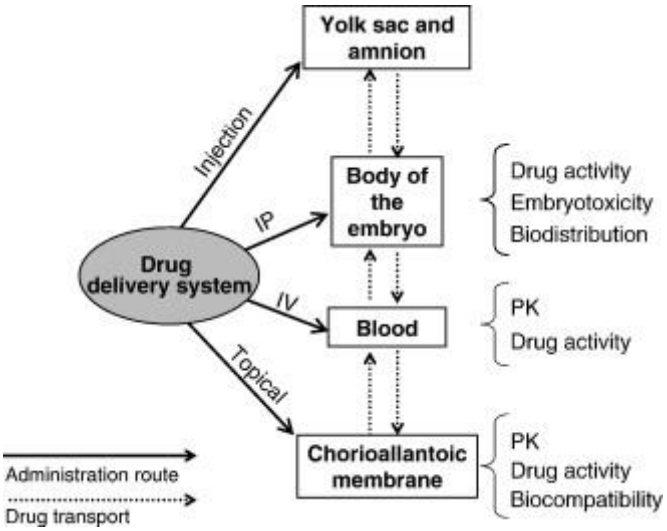

Figure 4.2 Different drug delivery methods for administrating a substance to chicken embryos and parameters that can be determined. The figure was obtained from [110].

The brain in chicken develops in a faster rate than in humans. The cerebellum on E16 is comparable to the cerebellum in humans at birth, whilst E13 is comparable to the last trimester [5]. The chicken embryos were exposed at E16 for all the experiments. Therefore, the alterations that might be detected equals to postnatal effects. The cerebellar cortex is highly conserved among species, yet there are differences from the human counterpart. Nevertheless,

the chicken embryo cerebellum resembles the human counterpart more closely than in other models, such as zebrafish [72].

The EMA guideline specifies what comprises CNS core battery studies. Motor activity, behavioural changes, coordination, sensory/motor reflex responses, and body temperature could not be tested with how the chicken embryo model was used in this thesis [3]. However, this could be examined after hatching [111]. Still, the information elucidated from this model system is important and provides supplementary data in a nonclinical safety assessment [5]

Cerebella from untreated chicken embryos were used to make primary cultures for *in vitro* studies. Over time *in vitro*, CGNs differentiate and acquire the characteristics of mature neurons, whilst retaining many of the properties in neurons *in situ* (specifically elaboration of axons and dendrites) [72, 112]. Exposure of these cultured neurons to a drug can determine whether the drug is toxic to these cells. A downfall is that these cultures are predominantly post-mitotic, therefore there is a need to continually prepare new cultures from animal tissue, increasing the potential for culture to culture variability [112].

PC12 cells were used for *in vitro* studies. These cells have neurites that cannot be distinguished as axons or dendrites. The phenotype of the cell line can change after multiple passages [112].

Different choices of *in vitro* models strengthen results, as it increases the possibility of the mechanisms being preserved between cell types and species, and the chance of a similar relevance in humans. *In vitro* models provide a well-controlled systems in which subtle changes in cell number, morphology and function can readily be detected compared to *in vivo* approaches [113].

4.2 Choice of exposures

VPA and LTG are widely used AEDs, where LTG is considered as a safer option to use during pregnancy. Therefore, it would be interesting to compare both of their possible toxic effects. The therapeutic window for VPA and LTG are 300-700 μM, and 10-50 μM, in serum respectively [114]. The EMA guideline specifies how safety pharmacological studies should include concentrations above the therapeutic range [3].

A way to monitor *in utero* exposure of a substance is by measuring the umbilical cord blood immediately after childbirth [115]. A study where the use of VPA caused both minor anomalies

and major malformations in infants, determined doses ranging from 4.9-70.5 μg/mL (equivalent to 34.0 – 488.9 μM) in the umbilical cord blood [116]. The concentrations used for this thesis covers this range (1-1000 μM) for *in vivo* and *in vitro* studies. A previous manuscript from the research group had used the same concentrations with significant result, hence the same were employed [5]. PC12 cells are more robust, therefore 2000 μM was used for MTT assay and Hoechst staining to examine viability after exposure to VPA.

Umbilical cord blood from foetuses exposed to LTG have been observed to range from 0.1-4.5 μg/mL (equivalent to 0.39-17.6 μM) [117]. The concentrations employed in thesis also covers this range, from 1-500 μM for *in vitro* studies, and 4.2-25 μM for *in vivo* studies. The aforementioned manuscript used some of these concentrations as well, and found significant results [5]. LTG was dissolved in DMSO which is a toxic solvent. A percentage concentration has been reported to affect cells, where higher concentrations can cause cell death, whilst lower can cause proliferation [118]. These effects are cell specific, therefore a higher concentration of DMSO (1.2%) was mostly used in PC12 cells on account of their robustness. It did affect PC12 cells, therefore the results were corrected to the solvent control that was included.

For pharmacokinetics, 5 μM and 4.2 μM were used to examine the difference between the water soluble LTG isethionate with the water insoluble LTG. Higher concentrations of LTG, 10 μM and 25 μM, were injected at T_{max} to see how much C_{max} would be affected. The determined concentration had an approximate linear relationship. The same could be said for VPA after exposing the chicken embryos to 500 μM and 1000 μM. The concentrations used for VPA and LTG are both below the therapeutic window, but they are in the concentration range found in umbilical cord blood.

The HDAC inhibitor, TSA, was used to examine if the effect VPA had on *Renilla* luciferase could be attributed to the aforementioned mechanism. There were no available data of TSA exposure in PC12 cells, hence a dose-response pilot was performed to select a concentration for the experiment. IC_{50} for TSA is ~1.8 nM [119]. The concentrations employed were 1 nM, 10 nM and 100 nM. Toxicity was not observed with 100 nM, which is why this concentration was used further.

4.3 Luciferase Dual Reporter Assay, RT-qPCR, and western blot

In this thesis, RT-qPCR, western blot and Luciferase Dual Reporter Assay were utilised. In the process of gene expression, DNA is transcribed to RNA and is translated into a protein. The assays employed in this thesis combined give information on all three levels. Western blotting semi-quantifies a specific protein, where the amount equates its level which was able to be transcribed, translated and was present from before. With RT-qPCR, one can quantitively measure cDNA through reverse transcription of RNA to estimate the abundance, and expression, of specific target genes. But it does not give information about transcriptional control [120]. With a luciferase assay, one can indirectly monitor the expression of the gene whose promoter has been cloned. The reporter gene is inserted downstream of a regulatory region (promoter) that is responsible for the controlled expression of a specific gene. These regulatory regions drive transcription, whereby DNA is converted to mRNA. This deciphers if an increase RT-qPCR result is due to a decreased removal or an increased transcription of that gene [121].

4.3.1 Luciferase Dual Reporter Assay

The luciferase system is extremely sensitive, and suitable for determining relative transfection performance between samples [122]. In addition, utilisation of the *Renilla* luciferase as a control increases accuracy. This allows the study of both weak and strong promoters, and the assay is simple and fast [96]. The *Renilla* luciferase is commonly used as an internal control to normalise the values of the experimental reporter gene for variations caused by transfection efficiency, and sample handling. It has been adopted for the use as an internal control for luciferase-based assay systems, since *Renilla* does not have any effect on firefly luciferase [96, 98].

The validity of using *Renilla* is based on the assumption that it is constitutively expressed in transfected cells, and that its expression is not modulated by experimental factors. Modulation of its expression could result in an up-regulation or down-regulation of the enzyme produced. There has been a number of reports identifying conditions where the basal constitutive expression of *Renilla* has been altered, such as exposure to dexamethasone [98].

In this thesis, *Renilla* luciferase was seen to be induced by VPA. In which case, the use of the internal control to normalise firefly luciferase would not be valid, since the experimental

conditions are affected. To be sure of this, total protein could be measured from the samples after measurement of *Renilla* luciferase. This will elucidate if the protein expression is altered, and be used to normalise the results. The HDAC inhibition experiment showed that the induction could be attributed to this mechanism. Others have experienced this as well, and could conclude the involvement of HDAC inhibition to be the cause [123].

Other types of *Renilla* luciferase plasmids, like pRL-CMV, could be co-transfected and exposed to VPA to see if it also would be induced.

After the first luciferase assay was conducted, the standard deviation obtained was used to perform a power analysis. A power analysis allows one to determine the sample size that is required to detect an effect of a given sample with a degree of confidence [124]. My standard deviation was small, hence the power of my results was high. Therefore, each parallel from the experiments could be compiled as individuals. http://biomath.info/power/ttest.htm was used to compute the power, and whether to pool the individual dishes from the luciferase assay.

4.3.2 RT-qPCR

Isolation of total RNA directly from a complex environmental sample is typically problematic, as RNA is a labile molecule. Due to the sensitivity of qPCR methods, it is particularly important that the RNA template is free from contaminating DNA that could contribute to the final amplification signal. The efficiency of the initial reverse transcription step is critical for sensitive and accurate quantification as the amount of cDNA produced must accurately reflect the starting RNA concentration [120].

RT-qPCR can be run using either a one-step, or two-step reaction. In this thesis, a two-step reaction was performed. An advantage of this is that the reverse transcription reaction can be optimised to increase cDNA yield, as can the subsequent qPCR amplification after measuring the purity degree and concentration. cDNA generated can be used as a template for a number of qPCR reactions, making a two-step reaction economically viable compared with the one-step model, where everything happens in a single tube. However, a one-step reaction will reduce contamination, but studies have reported a reduced sensitivity [120].

For RT-qPCR, *ACTB*, the reference gene, was significantly affected by the exposures for one group of eggs. A study has noted that the most used reference gene in chick embryo gene

expression experiments, *ACTB*, was the least stable, and concluded that it should not be used in these types of experiments in the brain, as well as *GAPDH* [125]. A study from 1-day old chicks experienced the same, where *ACTB* was the least stable. They recommended the use of *18S* ribosomal RNA [126]. With the kit employed in this thesis, it would be possible to use this reference gene. The use of multiple reference genes strengthens the results if one of them becomes affected. That is why *GAPDH* was also tried, even though the study recommended otherwise. The results with *GAPDH* were not identical with *ACTB*, but some of the results were qualitively similar.

There has been reports of how the reference gene has been affected not only in avian species, but in plants and insects. Multiple factors can be the cause, as the time at which a sample is obtained can lead to a variability in reference genes [127].

The same batch was run twice with *ACTB* to be certain, with a result of an identical manner. There was a qualitative similarity with running the samples once more, but a quantitative difference among the results.

4.3.3 Western blot

Western blot is a very sensitive technique, where it has the ability to detect as little as picogram levels of a protein in a sample [89, 128].

Western blot is very specific. Gel electrophoresis sorts the sample into proteins of different sizes, and as bands form, it gives clues to the size of the protein. Specific antibodies show affinity for specific proteins, and can thereby detect target protein even in a mixture of different proteins. In spite of its sensitivity and specificity, western blot can still produce inaccurate results. A false-positive result can occur when an antibody reacts with a non-intended protein (which is reduced by membrane blocking), whilst a false-negative can occur when larger proteins are not given sufficient time to transfer properly to the membrane. Western is an expensive technique, as well as being demanding, and time consuming [89, 128]. Training is needed to perform it well.

In this thesis, there were no significant results with western blot. The cerebella were isolated after 24 hours; therefore, the exposure period might not have been adequate enough. A longer exposure could be needed to see alterations in protein expression. And similarly to RT-qPCR,

β-actin was used to normalise the results. VPA seemed to significantly affect it at lower concentrations. This might be the reason for why PAX6 appeared to have a Gaussian shape, entailing a reduction in protein expression for the lowest and highest concentration, whilst an increase with the concentrations in the middle. Nevertheless, both RT-qPCR and western blot were conducted on cerebella from E17 chicken embryos and *ACTB* was mostly unaffected. It can therefore still be applicable as an internal standard.

4.4 Neurite outgrowth

The endpoints for neurite outgrowth in this thesis were neurite length, and branch points. It was assessed with IncuCyte®, which generates automated pictures after certain intervals. Neurite length and branch points are aspects which are important for neuronal development. During development, neurons extend numerous projections that differentiate into dendrites and axons. These processes are critical for communication between neurons. In primary cultures of neurons, distinct steps of neuronal differentiation can usually be observed [101]. The mechanism involved in establishing a branch point are poorly understood. It is likely that neurite branching requires the coordination of multiple events [129].

In this thesis, there were no significant difference in neurite outgrowth. Previous master students observed an increase in neurite length in PC12 cells after exposure to the AEDs [130, 131].

4.5 Discussion of biological findings

4.5.1 Distribution of VPA and LTG into the brain on E13 and E16 are different

GC/MS and LC-MS/MS are instruments used to detect substances or traces of them in human samples, namely urine and blood. Yet, they were able to determine concentrations of VPA and LTG in chicken embryo brains. The results from this thesis show how the absorption of the AEDs was rapid and detectable in the brain as early as 5 minutes after injection.

The results from the E13 exposure were comparatively different from E16 for both AEDs. The two different formulations of LTG had a reduction in C_{max} on E16 compared to E13, whilst

VPA experienced an increase. This difference could be a result of changes in protein expression in the span of three days. A study analysing proteins in chicken embryos observed a change in hepatic proteins in E14 and E19 chicken embryos and 1-day-old chickens. They concluded that there is a regulated coordination between certain proteins to satisfy the requirement for growth at different stages of development [132]. Interestingly, CYP1A2 was found to be significantly increased in 1-day- old chickens compared to E19 chicken embryos [132]. However, LTG and VPA are not metabolised nor affected by this enzyme [133, 134].

The movement of a compound across the blood-brain barrier not only depends on the lipophilicity and molecular size of the compound, but is also regulated by a specific carrier-mediated transport system that can export it from endothelial cells into the blood stream [135]. The CAM changes rapidly during embryonic development, and selective transport of macromolecules through the CAM microvascular endothelium varies [110].

There was a difference in LTG isethionate and LTG on E13, but the curves looked similar on E16 where both seemed to have a consistent concentration in the brain after 6 hours. This may have resulted from how the chicken embryo is a closed system. This means that there is no excretion of the drug, which causes a prolonged exposure after a single injection of a substance [72]. This could be a benefit for employing the chicken embryo model, reducing the need for repeat injections. For example, rats experience stress during handle [136]. K_{el} increased from E13 to E16 for VPA, whilst it decreased for LTG, though the latter data from LTG cannot be completely trusted.

4.5.2 The process of proliferation and differentiation

Early development is characterised by rapid proliferation of embryonic cells. They differentiate to produce specialised types of cells that make up tissue and organs [137]. PCNA is a protein important in DNA replication. In this thesis, *PCNA* expression was reduced in the cerebella from chicken embryos exposed to VPA, but not LTG. This could also be seen with the western blot results. VPA exhibited a dose-dependent tendency of reducing PCNA at higher concentrations that was not significant. More samples could readily establish a change in protein expression, since there were only 5 samples per group.

During embryonic development, a few types of differentiated cells, such as cardiomyocytes are produced. What is special with these cells are how they are only produced during this period

[137]. A reduction of *PCNA* could reduce the proliferation of cardiomyocytes and result in cardiac abnormalities, where a precise proliferation and differentiation of their progenitor cells is required for normal heart development [138].

In the developing brain, *PAX6* also modifies the proliferation of progenitor cells, as well as neural differentiation in CNS development [139]. PAX6 expression is also specific in the neural tube, therefore a correct regulation is important regarding major malformations [140]. In this thesis, LTG did not affect its expression, but VPA lead to a significant down-regulation. *GAPDH* corrected RT-qPCR results for VPA also showed a decrease in *PAX6* in a similar manner to *ACTB* corrected expression.

PAX6 was also reduced in western blot, mostly for the highest concentration. Nevertheless, the significant reduction of the *PAX6* gene and its expression could be a cause of the morphological malformation that is observed in infants resulting from *in utero* exposure. Its expression is considered as being involved in neurodevelopmental diseases [140].

4.5.3 The process of sensory-motor function and cognition

Voltage-gated ion channels are important mediators for physiological functions in the CNS. Their cyclic activation influence neurotransmitter release, neuron excitability, and plasticity. A growing body of data has implicated ion channels in the pathogenesis of psychiatric diseases [141].

The results from this thesis showed GluN2B to have a dose-dependent relation with VPA, where higher concentrations increased its levels. This was also seen with RT-qPCR, where there was an increase in *GRIN2B*. LTG also increased *GRIN2B*, but not to the same extent. An up-regulation of GluN2B would lead to more glutamate receptors. In neonatal brains, GluN2B is highly expressed, and over the course of development, they are substituted and replaced by GluN2A. An up-regulation of GluN2B would result in an increase in intracellular Ca^{2+} [142]. For adults, it is beneficial for cognition, but early postnatal elevated levels can lead to excitotoxicity, neuropathic pain and hyperexcitability. All these elements give rise to psychiatric disorders, as well as inducing cognitive impairments through an overabundance of intracellular Ca^{2+} signalling. At this stage it could have a long-lasting effect on neural structure and cognitive function, which was seen in the prefrontal cortex [143].

A study were chicken embryos were injected with VPA during the last week of embryogenesis, were impaired in social behaviours after hatching [111].

BDNF is important for developmental processes and influences the mechanisms of memory and cognition [144]. A reduction of this gene has been associated with psychiatric disorders, such as depression and schizophrenia [145]. The elevation of BDNF improves memory formation and the survival of neuronal development, and in animal models, it has ameliorated Huntington disease and Alzheimer disease [146]. The results from this thesis showed LTG to significantly induce, while VPA supressed *BDNF* expression in the chicken embryo cerebellum. One might think that an overexpression would not be detrimental to neurodevelopment, however, there are evidence to the contrary. A chronic overexpression of *BDNF* in the CNS causes learning deficits and short-term memory impairments, both in spatial and instrumental learning tasks [147]. Interestingly, mood stabilisers increase BDNF expression [148].

4.6 Future perspectives

Further pharmacokinetic experiments should be performed. Measuring the concentration after exposure in the yolk, allantois and amnion fluid would give more information about the distribution. Measuring the metabolites of the AEDs could also be of need.

In ovo exposure before *in vitro* experiments would be an interesting way to better see effects the AEDs might have, as well as being more comparable to the *in vivo* experiments. Interesting experiments would be to study GluN2B, BDNF and PAX6 mechanistically.

5 Conclusion

- The chicken embryo model is a good supplement for safety pharmacology where it displays similar development as humans, and can be used in conjunction with established models.

- VPA and LTG injected into the egg is distributed rapidly to the chicken embryo brain. The pharmacokinetics in the chicken embryo model is complex, and studies should be conducted to examine the compartments in the chicken embryo following exposure.

- Few of the genes studied were affected by VPA more than LTG. *PAX6* was down-regulated by VPA, and could contribute to the morphological aspects of its teratogenicity. LTG up-regulated *BDNF,* which could affect cognitive functions.

- Combining RT-qPCR, Luciferase Dual Reporter Assay and western blot gives a clearer picture of drug-induced alterations in gene expression.

List of references

1. Sheffield, J.S., et al., *Designing drug trials: considerations for pregnant women.* Clinical infectious diseases : an official publication of the Infectious Diseases Society of America, 2014. **59**(7): p. S437-S444.
2. Rice, D. and S. Barone, Jr., *Critical periods of vulnerability for the developing nervous system: evidence from humans and animal models.* Environmental health perspectives, 2000. **108**(3): p. 511-533.
3. EMA, *ICH Topic S 7 A Safety Pharmacology Studies for Human Pharmaceuticals* 2000.
4. Pugsley, M.K., S. Authier, and M.J. Curtis, *Principles of safety pharmacology.* British Journal of Pharmacology, 2008. **154**(7): p. 1382-1399.
5. Austdal, L.P.E., *New models for nonclinical safety assessment: targeting hallmark neurodevelopmental processes to examine if pharmaceuticals affect the immature brain*, in *Department of Pharmaceutical Biosciences*. 2018, University of Oslo.
6. Sills, G.J., *Mechanisms of action of antiepileptic drugs*, in *From channels to commissioning - a practical guide to epilepsy*.
7. Fisher, R.S., et al., *ILAE Official Report: A practical clinical definition of epilepsy.* Epilepsia, 2014. **55**(4): p. 475-482.
8. Scheffer, I.E., et al., *ILAE classification of the epilepsies: Position paper of the ILAE Commission for Classification and Terminology.* Epilepsia, 2017. **58**(4): p. 512-521.
9. Eriksson, A.-S. *Epilepsi 2009*. [cited 14.04.2019]; Available from: https://legeforeningen.no/fagmed/norsk-barnelegeforening/veiledere/generell-veileder-i-pediatri/kapittel-11-nevrologi/116-epilepsi-2009/.
10. Fisher, R.S. and A.M. Bonner, *The Revised Definition and Classification of Epilepsy for Neurodiagnostic Technologists.* The Neurodiagnostic Journal, 2018. **58**(1): p. 1-10.
11. Henning, O. and K.O. Nakken, *Ny klassifikasjon av epileptiske anfall.* Tidsskriftet for Den Norske Legeforening, [cited 13.02.2019]; Available from: https://tidsskriftet.no/2017/11/debatt/ny-klassifikasjon-av-epileptiske-anfall#ref1.
12. Lüders, H., et al., *Critique of the 2017 epileptic seizure and epilepsy classifications.* Epilepsia. **0**(0).
13. Pennell, P.B. and T. McElrath. *Risks associated with epilepsy during pregnancy and postpartum period*. (updated 04.12.2018) [cited 02.04.2019]; Available from: https://www.uptodate.com/contents/risks-associated-with-epilepsy-during-pregnancy-and-postpartum-period?sectionName=EFFECT%20OF%20AEDS%20ON%20THE%20FETUS%20AND%20NEONATE&search=antiepileptics%20in%20pregnancy&topicRef=17159&anchor=H4&source=see_link#H4.
14. Norsk legemiddelhåndbok. *T6.1.1 Epilepsi*. (updated 15.11.2017) [cited 25.04.2019]; Available from: https://www.legemiddelhandboka.no/T6.1.1/Nevrologiske_sykdommer#Tk-06-nevrol-74.
15. *Perinatal*, in *Oxford Concise Medical Dictionary*. Ordnett.
16. Schachter, S.C. *Antiseizure drugs: Mechanism of action, pharmacology, and adverse effects*. (updated 31.08.2018) [cited 20.09.2018]; Available from: https://www.uptodate.com/contents/antiseizure-drugs-mechanism-of-action-pharmacology-and-adverse-effects#H1.

17. Löscher, W., et al., *Synaptic Vesicle Glycoprotein 2A Ligands in the Treatment of Epilepsy and Beyond.* CNS Drugs, 2016. **30**(11): p. 1055-1077.
18. National Cancer Institute. *valproic acid*. [cited 28.10.2018]; Available from: https://www.cancer.gov/publications/dictionaries/cancer-drug/def/valproic-acid.
19. Pubchem Database. *Valproic acid*. [cited 31.03.2019]; Available from: https://pubchem.ncbi.nlm.nih.gov/compound/3121.
20. Menegola, E., et al., *Inhibition of histone deacetylase as a new mechanism of teratogenesis.* Birth Defects Research Part C: Embryo Today: Reviews, 2006. **78**(4): p. 345-353.
21. Krämer, O.H., et al., *The histone deacetylase inhibitor valproic acid selectively induces proteasomal degradation of HDAC2.* The EMBO journal, 2003. **22**(13): p. 3411-3420.
22. Gurvich, N., et al., *Association of valproate-induced teratogenesis with histone deacetylase inhibition in vivo.* The FASEB Journal, 2005. **19**(9): p. 1166-1168.
23. Whittle, N. and N. Singewald, *HDAC inhibitors as cognitive enhancers in fear, anxiety and trauma therapy: where do we stand?* Biochemical Society Transactions, 2014. **42**(2): p. 569-581.
24. Johannessen Landmark, C., et al., *Pharmacokinetic variability of valproate during pregnancy – Implications for the use of therapeutic drug monitoring.* Epilepsy Research, 2018. **141**: p. 31-37.
25. Tomson, T., *Commentary: Valproate in the treatment of epilepsy in women and girls: The need for recommendations.* Epilepsia, 2015. **56**(7): p. 1004-1005.
26. Alvestad, S., et al., *Valproat fortsatt viktig for kvinner med generalisert epilepsi.* Tidsskriftet for Den Norske Legeforening [cited 08.04.2019]; Available from: https://tidsskriftet.no/2019/01/debatt/valproat-er-kontraindisert-ved-graviditet.
27. EMA. *New measures to avoid valproate exposure in pregnancy endorsed* EMA/375438/2018. [cited 15.11.2018]; Available from: https://www.ema.europa.eu/documents/referral/valproate-article-31-referral-new-measures-avoid-valproate-exposure-pregnancy-endorsed_en-0.pdf.
28. Statens legemiddelverk, *Valproat til jenter og kvinner - risiko ved bruk under graviditet*. [cited 15.11.2018]; Available from: https://legemiddelverket.no/nyheter/valproat-til-jenter-og-kvinner-risiko-ved-bruk-under-graviditet?utm_source=Netlife%20Dialog&utm_medium=email&utm_campaign=Nytt%20om%20legemidler,%20Valproat%20og%20graviditet,%20nye%20MT%27er,%20legemiddelmangel
29. Desitin, *«Kjære helsepersonell» letter: Nye restriksjoner vedrørende bruk av ▼valproat; graviditetsforebyggende program skal introduseres.* Available from: https://legemiddelverket.no/Documents/Bivirkninger%20og%20sikkerhet/Kjære%20helsepersonell-brev/2018/Valproate_DHPC_NO_med%20logo.pdf.
30. Olsen, D.B. and A. Baftiu, *Valproat er kontraindisert ved graviditet.* Tidsskriftet for Den Norske Legeforening. [cited 28.04.2019]; Available from: https://tidsskriftet.no/2019/01/debatt/valproat-er-kontraindisert-ved-graviditet.
31. National Cancer Institute. *lamotrigine*. [cited 12.04.2019]; Available from: https://www.cancer.gov/publications/dictionaries/cancer-drug/def/lamotrigine.
32. Drugbank. *Lamotrigine*. [cited 24.10.2018]; Available from: https://www.drugbank.ca/drugs/DB00555.
33. Cummings, C., et al., *Neurodevelopment of children exposed in utero to lamotrigine, sodium valproate and carbamazepine.* Archives of Disease in Childhood, 2011. **96**(7): p. 643-647.

34. RELIS. *Antiepileptika og graviditet*. [cited 12.04.2019]; Available from: https://relis.no/sporsmal_og_svar/4-6749?source=relisdb.
35. Arslan, O.E., *Chapter 3 - Computational Basis of Neural Elements*, in *Artificial Neural Network for Drug Design, Delivery and Disposition*, M. Puri, et al., Editors. 2016, Academic Press: Boston. p. 29-82.
36. Purves, D., et al., *Principles of Cognitive Neuroscience*. 2 ed. 2013, Sunderland, MA USA: Sinauer Associates, Inc.
37. Hall, A.K., *Chapter 28 - Development of the Nervous System*, in *Basic Neurochemistry (Eighth Edition)*, S.T. Brady, et al., Editors. 2012, Academic Press: New York. p. 533-545.
38. Nasser, T.I.N. and G.E. Spencer, *Neurite Outgrowth*, in *Reference Module in Biomedical Sciences*. 2017, Elsevier.
39. Jansen, J. and J. Glover. *nervesystemet*. Store Medisinske Leksikon (updated 14.03.2019) [cited 20.04.2019]; Available from: https://sml.snl.no/nervesystemet.
40. Kalus, I., et al., *Sulf1 and Sulf2 Differentially Modulate Heparan Sulfate Proteoglycan Sulfation during Postnatal Cerebellum Development: Evidence for Neuroprotective and Neurite Outgrowth Promoting Functions*. PLOS ONE, 2015. **10**(10): p. e0139853.
41. Marzban, H., et al., *Cellular commitment in the developing cerebellum.* Frontiers in Cellular Neuroscience, 2015. **8**(450).
42. van Welie, I., I.T. Smith, and A.J. Watt, *The metamorphosis of the developing cerebellar microcircuit.* Current Opinion in Neurobiology, 2011. **21**(2): p. 245-253.
43. Lab, T.A.J. *Cerebellum development and regeneration*. [cited 08.04.2019]; Available from: https://www.mskcc.org/research/ski/labs/alexandra-joyner/cerebellum-development-and-regeneration.
44. Gene, N., *PCNA proliferating cell nuclear antigen [Homo sapiens (human)]*. 07.04.2019.
45. Strzalka, W. and A. Ziemienowicz, *Proliferating cell nuclear antigen (PCNA): a key factor in DNA replication and cell cycle regulation.* Annals of botany, 2011. **107**(7): p. 1127-1140.
46. Kelman, Z., *PCNA: structure, functions and interactions.* Oncogene, 1997. **14**(6): p. 629-640.
47. Wilson, R.H.C., et al., *PCNA dependent cellular activities tolerate dramatic perturbations in PCNA client interactions.* DNA repair, 2017. **50**: p. 22-35.
48. Celis, J.E., et al., *Cyclin: A nuclear protein whose level correlates directly with the proliferative state of normal as well as transformed cells.* Leukemia Research, 1984. **8**(2): p. 143-157.
49. NIH U.S. National Library of Medicine. *PAX6 gene (paired box 6)*. [cited 02.04.2019]; Available from: https://ghr.nlm.nih.gov/gene/PAX6.
50. Manuel, M.N., et al., *Regulation of cerebral cortical neurogenesis by the Pax6 transcription factor*. Frontiers in cellular neuroscience, 2015. **9**: p. 70-70.
51. Engelkamp, D., et al., *Role of Pax6 in development of the cerebellar system.* Development, 1999. **126**(16): p. 3585-3596.
52. Appleby, T.C., et al., *Biochemical characterization and structure determination of a potent, selective antibody inhibitor of human MMP9.* The Journal of biological chemistry, 2017. **292**(16): p. 6810-6820.
53. NCBI, *MMP9 matrix metallopeptidase 9 [Homo sapiens (human)]* 09.04.2019: NCBI Gene.
54. Shubayev, V.I. and R.R. Myers, *Matrix metalloproteinase-9 promotes nerve growth factor-induced neurite elongation but not new sprout formation in vitro.* Journal of Neuroscience Research, 2004. **77**(2): p. 229-239.

55. Curcio, M. and F. Bradke, *Axon Regeneration in the Central Nervous System: Facing the Challenges from the Inside.* Annual Review of Cell and Developmental Biology, 2018. **34**(1): p. 495-521.
56. Austdal, L.P.E., et al., *Glucocorticoid Effects on Cerebellar Development in a Chicken Embryo Model: Exploring Changes in PAX6 and Metalloproteinase-9 After Exposure to Dexamethasone.* Journal of Neuroendocrinology, 2016. **28**(12).
57. Shen, T., et al., *BDNF Polymorphism: A Review of Its Diagnostic and Clinical Relevance in Neurodegenerative Disorders.* Aging and disease, 2018. **9**(3): p. 523-536.
58. NIH U.S. National Library of Medicine. *BDNF gene (brain derived nuclear factor)*. [cited 02.04.2019]; Available from: https://ghr.nlm.nih.gov/gene/BDNF.
59. NIH U.S. National Library of Medicine. *GRIN2B gene (glutamate ionotropic receptor NMDA type subunit 2B)*. [cited 02.04.2019]; Available from: https://ghr.nlm.nih.gov/gene/GRIN2B.
60. NCBI. *GRIN2B glutamte ionotropic receptor NMDA type sunbunit 2B [Homo sapiens (human)]* [cited 14.04.2019]; Available from: https://www.ncbi.nlm.nih.gov/gene/2904.
61. NIH U.S. National Library of Medicine. *GABRR1 gene (gamma-aminobutyric acid type A receptor rho1 subunit)*. [cited 02.04.2019] Available from: https://ghr.nlm.nih.gov/gene/GABRR1.
62. Scimemi, A., *Structure, function, and plasticity of GABA transporters.* Frontiers in cellular neuroscience, 2014. **8**: p. 161-161.
63. Wu, C. and D. Sun, *GABA receptors in brain development, function, and injury.* Metabolic brain disease, 2015. **30**(2): p. 367-379.
64. Ben-Ari, Y., *Excitatory actions of gaba during development: the nature of the nurture.* Nature Reviews Neuroscience, 2002. **3**(9): p. 728-739.
65. Samardzic, J., *GABA and glutamate : new developments in neurotransmission research.* 2018.
66. Zhou, Y. and N.C. Danbolt, *GABA and Glutamate Transporters in Brain.* Frontiers in endocrinology, 2013. **4**: p. 165-165.
67. Takanaga, H., et al., *GAT2/BGT-1 as a System Responsible for the Transport of γ-Aminobutyric Acid at the Mouse Blood–Brain Barrier*. Journal of Cerebral Blood Flow & Metabolism, 2001. **21**(10): p. 1232-1239.
68. Braat, S. and R.F. Kooy, *The GABAA Receptor as a Therapeutic Target for Neurodevelopmental Disorders.* Neuron, 2015. **86**(5): p. 1119-1130.
69. Gadea, A. and A.M. López-Colomé, *Glial transporters for glutamate, glycine, and GABA: II. GABA transporters.* Journal of Neuroscience Research, 2001. **63**(6): p. 461-468.
70. Chamma, I., et al., *Role of the neuronal K-Cl co-transporter KCC2 in inhibitory and excitatory neurotransmission.* Frontiers in Cellular Neuroscience, 2012. **6**(5).
71. *Chicken as a Developmental Model*, in *eLS*.
72. Bjørnstad, S., et al., *Cracking the Egg: Potential of the Developing Chicken as a Model System for Nonclinical Safety Studies of Pharmaceuticals.* Journal of Pharmacology and Experimental Therapeutics, 2015. **355**(3): p. 386-396.
73. Sigma-Aldrich. *PC12 Cell line from rat*. [cited 23.10.2018] Available from: https://www.sigmaaldrich.com/catalog/product/sigma/cb_88022401?lang=en&region=NO.
74. Greene, L.A. and A.S. Tischler, *Establishment of a noradrenergic clonal line of rat adrenal pheochromocytoma cells which respond to nerve growth factor.* Proceedings

of the National Academy of Sciences of the United States of America, 1976. **73**(7): p. 2424-2428.
75. Martin, T.F.J. and R.N. Grishanin, *PC12 Cells as a Model for Studies of Regulated Secretion in Neuronal and Endocrine Cells*, in *Methods in Cell Biology*. 2003, Academic Press. p. 267-286.
76. Malagelada, C. and L.A. Greene, *Chapter 29 - PC12 Cells as a model for parkinson's disease research*, in *Parkinson's Disease*, R. Nass and S. Przedborski, Editors. 2008, Academic Press: San Diego. p. 375-387.
77. Mazia, D., G. Schatten, and W. Sale, *Adhesion of cells to surfaces coated with polylysine. Applications to electron microscopy.* The Journal of Cell Biology, 1975. **66**(1): p. 198-200.
78. Arigony, A.L., et al., *The Influence of Micronutrients in Cell Culture: A Reflection on Viability and Genomic Stability.* BioMed Research International, 2013. **2013**: p. 22.
79. Haney, S.A., *High Content Screening: Science, Techniques and Applications*. 2008: Wiley.
80. Sigma-Aldrich. *Pyrex® baffled trypsinizing flask, with beaded neck*. [cited 15.12.2018]; Available from: https://www.sigmaaldrich.com/catalog/product/aldrich/cls44602l?lang=en&region=NO.
81. Scientific, T.F. *DNase I*. [cited 13.03.2019]; Available from: https://www.thermofisher.com/order/catalog/product/18047019.
82. Technologies, S. *DNase I Treatment for Clumpy Cell Suspensions*. [cited 13.03.2019]; Available from: https://www.stemcell.com/dnase-i-treatment-for-clumpy-cell-suspensions.html.
83. Sigma-Aldrich. *Calcium in Cell Culture*. [cited 21.03.2019]; Available from: https://www.sigmaaldrich.com/life-science/cell-culture/learning-center/media-expert/calcium.html.
84. Le, J. *Overview of Pharmacokinetics*. [cited 24.03.2019]; Available from: https://www.msdmanuals.com/professional/clinical-pharmacology/pharmacokinetics/overview-of-pharmacokinetics.
85. Group, B.-G.R. *Pharmacokinetics Study*. [cited 24.03.2019]; Available from: https://www.braingut.com/pharmacokinetics.asp.
86. Scientific, T.F. *Gas Chromatography Mass Spectrometry (GC/MS) Information*. [cited 21.03.2019]; Available from: https://www.thermofisher.com/no/en/home/industrial/mass-spectrometry/mass-spectrometry-learning-center/gas-chromatography-mass-spectrometry-gc-ms-information.html.
87. Laboratories, E. *Liquid Chromatography - Tandem Mass Spectrometry (LC-MS-MS)*. [cited 23.04.2019]; Available from: https://www.eag.com/techniques/mass-spec/lc-ms-ms/.
88. The Human Protein Atlas. *Western blot*. [cited 17.12.2018]; Available from: https://www.proteinatlas.org/learn/method/western+blot.
89. Ghosh, R., J.E. Gilda, and A.V. Gomes, *The necessity of and strategies for improving confidence in the accuracy of western blots.* Expert review of proteomics, 2014. **11**(5): p. 549-560.
90. Thermo Fischer Scientific. *Basic Principles of RT-qPCR*. [cited 17.12.2018]; Available from: https://www.thermofisher.com/no/en/home/brands/thermo-scientific/molecular-biology/molecular-biology-learning-center/basic-principles-rt-qpcr.html.

91. QIAGEN. *RNeasy Plus Mini Kit*. [cited 19.04.2019]; Available from: https://www.qiagen.com/no/shop/sample-technologies/rna/total-rna/rneasy-plus-mini-kit/#productdetails.
92. QIAGEN, *RNeasy® Plus Mini Handbook: For purification of total RNA from animal cells and easy-to-lyse animal tissues using gDNA Eliminator columns* 2005.
93. Sigma-Aldrich. *Sample Purification and Quality Assessment*. [cited 25.04.2019]; Available from: https://www.sigmaaldrich.com/technical-documents/articles/biology/sample-purification-and-quality-assessment.html.
94. Khan, F. *The Luciferase Reporter Assay: How it works*. BiteSizeBio [cited 15.12.2018]; Available from: https://bitesizebio.com/10774/the-luciferase-reporter-assay-how-it-works/.
95. Herschman, H.R., *Noninvasive Imaging of Reporter Gene Expression in Living Subjects*, in *Advances in Cancer Research*. 2004, Academic Press. p. 29-80.
96. Arnone, M.I., I.J. Dmochowski, and C. Gache, *Using Reporter Genes to Study cis-Regulatory Elements*, in *Methods in Cell Biology*. 2004, Academic Press. p. 621-652.
97. Carter, M. and J. Shieh, *Chapter 15 - Biochemical Assays and Intracellular Signaling*, in *Guide to Research Techniques in Neuroscience (Second Edition)*, M. Carter and J. Shieh, Editors. 2015, Academic Press: San Diego. p. 311-343.
98. Shifera, A.S. and J.A. Hardin, *Factors modulating expression of Renilla luciferase from control plasmids used in luciferase reporter gene assays.* Analytical biochemistry, 2010. **396**(2): p. 167-172.
99. Scientific, T.F. *Introduction to Transfection*. [cited 26.03.2019]; Available from: https://www.thermofisher.com/no/en/home/references/gibco-cell-culture-basics/transfection-basics/introduction-to-transfection.html.
100. Biontex. *K2® Transfection System*. [cited 15.12.2018]; Available from: https://www.biontex.com/world/k2-transfection-system.html.
101. Kinney, H.C. and J.J. Volpe, *Chapter 7 - Organizational Events*, in *Volpe's Neurology of the Newborn (Sixth Edition)*, J.J. Volpe, et al., Editors. 2018, Elsevier. p. 145-175.e9.
102. BioScience, S.E. *About Essen BioScience: Enable real-time live-cell imaging and data analysis for life science researchers worldwide*. [cited 26.02.2019]; Available from: https://www.essenbioscience.com/hi/about/.
103. Riss, T.L., et al., *Cell Viability Assays*, in *Assay Guidance Manual*. 01.05.2013, Eli Lilly & Company and the National Center for Advancing Translational Sciences.
104. Bucevičius, J., G. Lukinavičius, and R. Gerasimaitė, *The Use of Hoechst Dyes for DNA Staining and Beyond.* Chemosensors, 2018. **6**(2): p. 18.
105. Crowley, L.C., B.J. Marfell, and N.J. Waterhouse, *Analyzing Cell Death by Nuclear Staining with Hoechst 33342.* Cold Spring Harb Protoc, 2016. **2016**(9).
106. Williams, M. and R.D. Porsolt, *CNS Safety Pharmacology*, in *xPharm: The Comprehensive Pharmacology Reference*, S.J. Enna and D.B. Bylund, Editors. 2007, Elsevier: New York. p. 1-13.
107. Ma, Z.-l., et al., *Investigating the effect of excess caffeine exposure on placental angiogenesis using chicken 'functional' placental blood vessel network.* Journal of Applied Toxicology, 2016. **36**(2): p. 285-295.
108. Dombre, C., et al., *Egg serpins: The chicken and/or the egg dilemma.* Seminars in Cell & Developmental Biology, 2017. **62**: p. 120-132.
109. Koren, G. and A. Ornoy, *The role of the placenta in drug transport and fetal drug exposure.* Expert Review of Clinical Pharmacology, 2018. **11**(4): p. 373-385.

110. Vargas, A., et al., *The chick embryo and its chorioallantoic membrane (CAM) for the in vivo evaluation of drug delivery systems.* Advanced Drug Delivery Reviews, 2007. **59**(11): p. 1162-1176.
111. Nishigori, H., et al., *Impaired social behavior in chicks exposed to sodium valproate during the last week of embryogenesis.* Psychopharmacology, 2013. **227**(3): p. 393-402.
112. Radio, N.M., et al., *Comparison of PC12 and cerebellar granule cell cultures for evaluating neurite outgrowth using high content analysis.* Neurotoxicology and Teratology, 2010. **32**(1): p. 25-35.
113. Mundy, W.R., et al., *Protein biomarkers associated with growth and synaptogenesis in a cell culture model of neuronal development.* Toxicology, 2008. **249**(2): p. 220-229.
114. Reimers, A., et al. *Felles referanseområder for antieileptika*. Tidsskrift for Den Norske Legeforening. [cited 13.05.2019]; Available from: https://tidsskriftet.no/2017/05/debatt/felles-referanseomrader-antiepileptika.
115. Gray, T. and M. Huestis, *Bioanalytical procedures for monitoring in utero drug exposure.* Analytical and bioanalytical chemistry, 2007. **388**(7): p. 1455-1465.
116. Jäger-Roman, E., et al., *Fetal growth, major malformations, and minor anomalies in infants born to women receiving valproic acid.* The Journal of Pediatrics, 1986. **108**(6): p. 997-1004.
117. Kacirova, I., M. Grundmann, and H. Brozmanova, *Serum levels of lamotrigine during delivery in mothers and their infants.* Epilepsy Research, 2010. **91**(2): p. 161-165.
118. Singh, M., K.M. Mckenzie, and X. Ma, *Effect of dimethyl sulfoxide on in vitro proliferation of skin fibroblast cells.* Journal of Biotech Research, 2017(8): p. 78-82.
119. Selleckchem. *Trichostatin A (TSA)*. [cited 12.03.2019] Available from: URL: https://www.selleckchem.com/products/Trichostatin-A.html.
120. Smith, C.J. and A.M. Osborn, *Advantages and limitations of quantitative PCR (Q-PCR)-based approaches in microbial ecology.* FEMS Microbiology Ecology, 2009. **67**(1): p. 6-20.
121. Expression, G., G. Sundaresan, and S.S. Gambhir, *29 - Radionuclide Imaging of Reporter Gene Expression*, in *Brain Mapping: The Methods (Second Edition)*, A.W. Toga and J.C. Mazziotta, Editors. 2002, Academic Press: San Diego. p. 799-818.
122. Homann, S., et al., *A novel rapid and reproducible flow cytometric method for optimization of transfection efficiency in cells.* PLOS ONE, 2017. **12**(9): p. e0182941.
123. Phiel, C.J., et al., *Histone deacetylase is a direct target of valproic acid, a potent anticonvulsant, mood stabilizer, and teratogen.* J Biol Chem, 2001. **276**(39): p. 36734-41.
124. DataCamp, Q.-R.b. *Power Analysis*. [cited 14.05.2019]; Available from: URL: https://www.statmethods.net/stats/power.html.
125. Lenart, J., K. Kogut, and E. Salinska, *Lateralization of housekeeping genes in the brain of one-day old chicks.* Gene Expression Patterns, 2017. **25-26**: p. 85-91.
126. Olias, P., et al., *Reference genes for quantitative gene expression studies in multiple avian species.* PloS one, 2014. **9**(6): p. e99678-e99678.
127. Kozera, B. and M. Rapacz, *Reference genes in real-time PCR.* Journal of Applied Genetics, 2013. **54**(4): p. 391-406.
128. Andrews, N. *Advantages and Disadvantages of Western Blot*. [cited 24.04.2017]; Available from: https://sciencing.com/advantages-disadvantages-western-blot-8670663.html.
129. Lalli, G. and A. Hall, *Ral GTPases regulate neurite branching through GAP-43 and the exocyst complex.* The Journal of Cell Biology, 2005. **171**(5): p. 857-869.

130. Evensen, S., *Sikkerhetsfarmakologiske studier av lamotrigin og valproat - mulige effekter på nevronkulturer*, in *Department of Pharmaceutical Biosciences*. 2013, Univerisity of Oslo: Oslo.
131. Daling, K.J., *Sikkerhetsfarmakologiske studier av lamotrigin og valproat - mekanismestudier i nevronkulturer*, in *Department of Pharmaceutical Biosciences*. 2014, University of Oslo: Oslo.
132. Peng, M., et al., *Proteomics reveals changes in hepatic proteins during chicken embryonic development: an alternative model to study human obesity.* BMC genomics, 2018. **19**(1): p. 29-29.
133. Ghodke-Puranik, Y., et al., *Valproic acid pathway: pharmacokinetics and pharmacodynamics.* Pharmacogenetics and genomics, 2013. **23**(4): p. 236-241.
134. Milosheska, D., et al., *Pharmacokinetics of lamotrigine and its metabolite N-2-glucuronide: Influence of polymorphism of UDP-glucuronosyltransferases and drug transporters.* British journal of clinical pharmacology, 2016. **82**(2): p. 399-411.
135. Daneman, R. and A. Prat, *The blood-brain barrier.* Cold Spring Harbor perspectives in biology. **7**(1): p. a020412-a020412.
136. *Stress response of rats to handling and experimental procedures.* Laboratory Animals, 1980. **14**(3): p. 267-274.
137. Cooper, G.M., *The Cell: A Molecular Approach*. 2 ed. 2000, Sunderland (MA): Sinauer Associates.
138. Hubert, F., S.M. Payan, and F. Rochais, *FGF10 Signaling in Heart Development, Homeostasis, Disease and Repair.* Frontiers in Genetics, 2018. **9**(599).
139. Enguix-Riego, M.V., et al., *Identification of different mechanisms leading to PAX6 down-regulation as potential events contributing to the onset of Hirschsprung disease.* Scientific Reports, 2016. **6**: p. 21160.
140. Osumi, N. and T. Kikkawa, *The Role of the Transcription Factor Pax6 in Brain Development and Evolution: Evidence and Hypothesis*, in *Cortical Development: Neural Diversity and Neocortical Organization*, R. Kageyama and T. Yamamori, Editors. 2013, Springer Japan: Tokyo. p. 43-61.
141. Imbrici, P., D.C. Camerino, and D. Tricarico, *Major channels involved in neuropsychiatric disorders and therapeutic perspectives.* Frontiers in genetics, 2013. **4**: p. 76-76.
142. Zhuo, M., *Plasticity of NMDA receptor NR2B subunit in memory and chronic pain.* Molecular Brain, 2009. **2**(1): p. 4.
143. Monaco, S.A., Y. Gulchina, and W.-J. Gao, *NR2B subunit in the prefrontal cortex: A double-edged sword for working memory function and psychiatric disorders.* Neuroscience & Biobehavioral Reviews, 2015. **56**: p. 127-138.
144. Kowiański, P., et al., *BDNF: A Key Factor with Multipotent Impact on Brain Signaling and Synaptic Plasticity.* Cellular and molecular neurobiology, 2018. **38**(3): p. 579-593.
145. Cattaneo, A., et al., *The human BDNF gene: peripheral gene expression and protein levels as biomarkers for psychiatric disorders.* Translational Psychiatry, 2016. **6**: p. 958.
146. Chen, K.-W. and L. Chen, *Epigenetic Regulation of BDNF Gene during Development and Diseases.* International journal of molecular sciences, 2017. **18**(3): p. 571.
147. Cunha, C., et al., *Brain-derived neurotrophic factor (BDNF) overexpression in the forebrain results in learning and memory impairments.* Neurobiology of Disease, 2009. **33**(3): p. 358-368.
148. Hashimoto, K., E. Shimizu, and M. Iyo, *Critical role of brain-derived neurotrophic factor in mood disorders.* Brain Research Reviews, 2004. **45**(2): p. 104-114.

Appendix I – GC-MS

Table a. Standard, internal standard, control

	Valproic acid (µM)
Standard 1	1
Standard 2	10
Standard 3	50
Standard 4	100
Standard 5	300
Control 1	60
Control 2	300
	Cyclohexanecarboxylic acid (µM)
Internal standard	800 1600

Table b. Instruments

GC/MS:	**Model**	**Producer**
Gas chromatograph	HP 6890	Agilent Technologies
Detector	HP 5973 MSD	Agilent Technologies
Autosampler	HP 7683A	Agilent Technologies
Lab-data system	HPCHEM version C.00.01.08	Agilent Technologies
Syringe/irrigator	10 µl (6 pk. 5181_3360 or 9301_0713)	Agilent Technologies
Septum	Thermogreen LB-2, 11 mm	Supelco
Liner	Cyclosplitter Liner (Cat # 20707), 4.0 mm id	Restec

Column	Factor Four VF-1MS (15 ± 1 m , 0.25 mm id, DF 0.4 µm)	Varian
Precolumn	5 m EZ-quard precolumn	
Vortexer	Multitube vortexer	VWR
Table centrifuge (≥ 4500 rpm)	Allerga X-15R/ Megafuge 1.0	Beckman Coulter/Heraeus

Table c. Instrument parameters

Method: 918.M

Oven	Maximum temp.	320 °C
	Equilibration time	0.50 min
	Initial temperature/time	50 °C/ 1.0 min
	Oven programme	50 °C in 1 min, 40 °C/min to 300 °C, hold 2 min
	Run time	9.25 min
Front Inlet	Mode	Split
	Initial temperature	250 °C
	Pressure	53.1 kPa
	Split ratio	10:1
	Split flow	15.0 ml/min
	Total flow	19.3 ml/min
	Gas saver	On
	Saver flow-time	20.0 ml/min-2.0 min
	Gas type	Helium
Column 1	Type	See table b.
	Mode	Constant flow
	Initial flow	1.5 ml/min
	Nominal init pressure	53.1 kPa
	Average velocity	55 cm/s

	Inlet	Front inlet
	Outlet	MSD
	Outlet pressure	Vacuum
Autosampler	Injection volume	1 (- 3) µl
	Sample Pumps	3
	PostInj Solvent A washes	3
	PostInj Solvent B washes	3
	Viscosity delay	1 s
MS	Tune File	atune.u
	Acquisition mode	SIM
	Solvent delay	2.0 min
	Group ID	1
	Resolution	Low
	Plot 1 ion	200.3
	Ions/Dwell In Group	200.3/30, internal standard;201.2/30, valproic acid
	MS Quad	150 °C (max 200 °C)
	MS Source	230 °C (max 250 °C)
	MS Off	9.0 min

Appendix II – LC-MS/MS

Table a. Standard, internal standard, control

	Lamotrigine (µM)
Standard 1	0.05
Standard 2	0.1
Standard 3	0.25
Standard 4	0.5
Standard 5	2.0
Standard 6	6.0
Control 1	0.15
Control 2	1.5
	Methaqualone (µM)
Internal standard	5 10

Table b. Conditions, instruments, compounds

Injector	Injection mode:	Partial loop with needle overfills	
	Injection volume:	5 µl	
	Loop-volume:	10 µl	
Solutions	Weak-wash:	600 µl 10 % MeOH in MQ-water	
	Strong wash:	200 µl 90 % MeOH in MQ-water	
	Wash solutions:	30 % MeOH in MQ-water	
	Mobile phase solution A:	5 mM Ammonium bicarbonate buffer (pH 7.9)	
	Mobile phase solution B:	Methanol	

UPLC conditions	Flow rate:	0.5 ml/min		
	Gradient:	Time (min)	% B	Curve
	1	0.00	2.5	
	2	1.00	5.0	6
	3	2.00	30.0	6
	4	3.60	50.0	6
	5	4.00	50.0	6
	6	4.30	80.0	6
	7	4.75	80.0	6
	8	4.80	98.0	6
	9	6.80	98.0	6
	10	6.90	2.5	6
	Column temperature:	65 °C		
	Run time:	7.90 min		
UPLC-Column	Brand:	Acquity UPLC® BEH phenyl		
	Length:	10 cm		
	Internal diameter:	2.1 mm		
	Particle size:	1.7 µm		
Precolumn	Brand:	Acquity UPLC® BEH phenyl VanGuard™ Pre-Column		
	Length:	5 mm		
	Internal diameter:	2.1 mm		
	Particle size:	1.7 µm		

Source	Capillary voltage	1 kV
	Cone	40 V
	Extractor voltage	3 V
	RF lens	0.0 V

	Source temperature	120 °C
	Desolvation temperature	450 °C
	Desolvation gas flow	900 L/hr
	Cone gas flow	60 L/hr
Analyzer	Low mass resolution 1	13
	High mass resolution 1	13
	Ion energy 1	1 V
	Entrance lens	2
	Collision gas flow	Instrument dependant
	Exit lens	2 V
	Low mass resolution 2	14
	High mass resolution 2	14
	Ion energy 2	1 V
Detector	Multiplier	Instrument dependant

MS method:							
	Solvent delay start 1:	0.0					
	Solvent delay end 1:	0.5					
	Solvent delay temperature 1:	0.0					
	Solvent delay start 2:	7.0					

	Solvent delay end 2:	8.0					
	Solvent delay temperature 2:	0.0					
Function 1: MRM of 6 mass pairs, ES+							
Inter channel delay (s):	0,005						
InterScan time (s):	0.02						
Span (da):	0.2						
Start time (min):	1.4						
End time (min):	2.4						
Compound		Prnt (Da)	Dau (Da)	Dwell (s)	Cone (V)	Coll (eV)	Delay (s)
Pregabalin		160.1	142.2/97.1	0.050	25	15	0.005
Levetiracetam		171.1	126.1/98.0	0.050	15	25	0.005
Gabapentin		172.1	137.1/154.3	0.050	25	15	0.005
Function 2: MRM of 2 mass pairs, ES-							
Inter channel delay (s):	0.005						
InterScan time (s):	0.02						
Span (da):	0.2						
Start time (min):	2.4						
End time (min):	3.0						

Compound		Prnt (Da)	Dau (Da)	Dwell (s)	Cone (V)	Coll (eV)	Delay (s)
Phenobarbital		231.1	188.1/84.8	0.100	20	10	0.005
Function 3: MRM of 15 mass pairs, ES+							
Inter channel delay (s):	0.005						
InterScan time (s):	0.02						
Span (da):	0.2						
Start time (min):	3.0						
End time (min):	5.0						
Compound		Prnt (Da)	Dau (Da)	Dwell (s)	Cone (V)	Coll (eV)	Delay (s)
Carbamazepine		236.8	179.0/165.0	0.005/0.010	44	32/28	0.005
Lacosamide		251.0	107.6/90.6	0.010	20	25	0.005
Methaqualone		251.0	132.0	0.010	40	30	0.005
Carbamazepine-10,11-epoxside		253.1	210.0/180.0	0.010	20	15/40	0.005
Phenytoin		253.1	225.1/182.0	0.010	30	10/25	0.005
Oxcarbazepine		253.1	236.1/210.1	0.010	40	15	0.005
10-OH-carbazepine		255.1	237.1/194.1	0.010	25	20/35	0.005
Lamotrigine		256.1	211.1/187.1	0.010	50	25	0.005
Topiramate		340.1	264.1/127.0	0.010	25	10/25	0.005

Appendix III – RT-qPCR data

Data from VPA (figure 3.6) *ACTB* (C_t)			
Untreated	**Saline**	**VPA 100 µM**	**VPA 1000 µM**
15.31	15.24	16.94	16.75
15.82	16.86	17.06	16.81
15.72	15.68	16.43	15.45
16.47	15.33	17.17	15.79
15.34	14.71	16.73	17.13
15.75	16.88		15.98
16.74	17.30		
17.62	16.78		
17.49	17.03		
17.49			

Data from VPA (figure 3.7) *GAPDH* (C_t)		
Untreated	**Saline**	**VPA 1000 µM**
17.48	17.89	18.30
19.41	18.14	18.91
17.56	17.47	17.42
20.16	18.45	18.25
18.28	18.25	19.17
20.39	17.89	19.39

Data from LTG (figure 3.11) *ACTB* (C_t)			
Untreated	**DMSO 0.1%**	**LTG 10 µM**	**LTG 25 µM**
15.10	15.20	15.69	15.55
15.23	15.72	14.87	15.66
15.19	15.14	14.81	14.95
15.09	15.27	15.22	15.23
14.96	15.14	14.89	17.28

Data from LTG (figure 3.12) *GAPDH* (C_t)			
Untreated	**DMSO 0.1%**	**LTG 10 µM**	**LTG 25 µM**
19.44	16.97	20.35	18.75
18.49	18.94	17.16	18.29
18.80	16.73	17.96	17.14
17.08	17.91	16.97	17.11
16.70	18.49	17.34	19.84

Data from RT-qPCR with an affected *ACTB* (C_t)			
Untreated	**Saline**	**VPA 100 µM**	**LTG 5 µM**
12.82	14.19	15.69	16.36
13.74	13.50	16.68	15.17
14.13	13.96	14.60	15.42
13.62	13.88	15.23	16.34
13.89	13.23	14.10	13.81
14.51	14.28	13.80	14.79
			15.63
			16.56

Appendix IV – Luciferase data

Data of firefly luciferase from PC12 cells			
Exposure	**Average**	**SEM**	**Number of experiments**
Untreated + PAX6	530 193	99 159	N = 18 from 6 experiments
Saline + PAX6	271 869	51 306	N = 12 from 4 experiments
VPA 1 μM + PAX6	355 890	87 208	N = 12 from 4 experiments
VPA 100 μM + PAX6	691 694	150 842	N = 15 from 5 experiments
VPA 500 μM + PAX6	628 672	162 930	N = 12 from 4 experiments
VPA 1000 μM + PAX6	1 153 497	259 672	N = 15 from 5 experiments
Untreated + MMP9	236	16	N = 9 from 3 experiments
Saline + MMP9	231	14	N = 9 from 3 experiments
VPA 1 μM + MMP9	164	29	N = 6 from 3 experiments
VPA 100 μM + MMP9	190	27	N = 9 from 3 experiments
VPA 500 μM + MMP9	223	30	N = 6 from 2 experiments
VPA 1000 μM + MMP9	224	44	N = 6 from 2 experiments
Untreated + PAX6	932 074	132 117	N = 9 from 3 experiments
DMSO 0.2% + PAX6	1 482 343	159 280	N = 6 from 2 experiments
DMSO 1.2% + PAX6	1 975 176	272 443	N = 9 from 3 experiments
LTG 10 μM + PAX6	1 747 025	112 236	N = 9 from 3 experiments
LTG 100 μM + PAX6	1 418 493	152 974	N = 9 from 3 experiments
LTG 500 μM + PAX6	1 478 777	112 203	N = 9 from 3 experiments
Untreated + MMP9	403	92	N = 9 from 3 experiments
DMSO 0.2% + MMP9	257	27	N = 6 from 2 experiments
DMSO 1.2% + MMP9	156	14	N = 6 from 2 experiments
LTG 10 μM + MMP9	299	47	N = 9 from 3 experiments
LTG 100 μM + MMP9	200	32	N = 9 from 3 experiments
LTG 500 μM + MMP9	50	8	N = 9 from 3 experiments
TSA 1 nM + PAX6	1 113 545	21 924	N = 3 from 1 experiment

TSA 10 nM + PAX6	846 867	92 892	N = 3 from 1 experiment
TSA 100 nM + PAX6	1 334 215	114 086	N = 6 from 2 experiment
Untreated + PAX6	1 021 405	95 127	N = 3 from 1 experiment
DMSO 0.1% + PAX6	1 218 387	86 221	N = 3 from 1 experiment
DMSO 0.1% + saline	1 126 356	112 657	N = 3 from 1 experiment
VPA 10 μM + PAX6	1 138 730	51 884	N = 3 from 1 experiment
VPA 10 μM + TSA + PAX6	1 826 634	115 638	N = 3 from 1 experiment
VPA 100 μM + PAX6	1 407 214	39 516	N = 3 from 1 experiment
VPA 100 μM + TSA + PAX6	2 141 067	205 196	N = 3 from 1 experiment
VPA 1000 μM + PAX6	2 745 885	83 958	N = 3 from 1 experiment
VPA 1000 μM + TSA + PAX6	3 201 445	144 240	N = 3 from 1 experiment

Data of *Renilla* luciferase from PC12 cells			
Exposure	**Average**	**SEM**	**Number of experiments**
Untreated + PAX6	169 061	38 513	N = 18 from 6 experiments
Saline + PAX6	94 904	7 276	N = 12 from 4 experiments
VPA 1 μM + PAX6	180 051	44 363	N = 12 from 4 experiments
VPA 100 μM + PAX6	123 845	18 677	N = 15 from 5 experiments
VPA 500 μM + PAX6	204 644	10 235	N = 12 from 4 experiments
VPA 1000 μM + PAX6	292 112	34 070	N = 15 from 5 experiments
Untreated + MMP9	156 227	33 827	N = 9 from 3 experiments
Saline + MMP9	184 063	49 602	N = 9 from 3 experiments
VPA 1 μM + MMP9	82 628	4 621	N = 6 from 3 experiments
VPA 100 μM + MMP9	241 607	54 597	N = 9 from 3 experiments
VPA 500 μM + MMP9	617 686	177 574	N = 6 from 2 experiments
VPA 1000 μM + MMP9	904 688	257 128	N = 6 from 2 experiments
TSA 1 nM + PAX6	455 349	33 622	N = 3 from 1 experiment
TSA 10 nM + PAX6	395 128	21 127	N = 3 from 1 experiment
TSA 100 nM + PAX6	259 583	105 871	N = 6 from 2 experiments

Untreated + PAX6	28 118	3 049	N = 3 from 1 experiment
DMSO 0.1% + PAX6	27 375	2 648	N = 3 from 1 experiment
DMSO 0.1% + saline	23 429	3 005	N = 3 from 1 experiment
VPA 10 μM + PAX6	24 911	677	N = 3 from 1 experiment
VPA 10 μM + TSA + PAX6	36 946	1 672	N = 3 from 1 experiment
VPA 100 μM + PAX6	32 440	1 239	N = 3 from 1 experiment
VPA 100 μM + TSA + PAX6	45 160	4 585	N = 3 from 1 experiment
VPA 1000 μM + PAX6	100 295	6 224	N = 3 from 1 experiment
VPA 1000 μM + TSA + PAX6	103 398	3 213	N = 3 from 1 experiment

Data of firefly luciferase from CGN			
Exposure	**Average**	**SEM**	**Number of experiments**
Untreated + PAX6	56 777	18 544	N = 12 from 4 experiments
Saline + PAX6	37 823	10 681	N = 11 from 4 experiments
VPA 1 μM + PAX6	103 507	9 931	N = 3 from 1 experiment
VPA 100 μM + PAX6	55 238	22 582	N = 6 from 2 experiments
VPA 500 μM + PAX6	98 831	15 874	N = 9 from 3 experiments
VPA 1000 μM + PAX6	168 518	53 407	N = 9 from 3 experiments
Untreated + MMP9	788	118	N = 6 from 2 experiments
Saline + MMP9	707	100	N = 6 from 2 experiments
VPA 500 μM + MMP9	1 493	360	N = 6 from 2 experiments
VPA 1000 μM + MMP9	2 421	1 145	N = 6 from 2 experiments
Untreated + PAX6	24 723	3 701	N = 9 from 3 experiments
DMSO 0.2% + PAX6	25 727	5 201	N = 9 from 3 experiments
LTG 1 μM + PAX6	28 248	353	N = 3 from 1 experiment
LTG 5 μM + PAX6	50 327	2 928	N = 3 from 1 experiment
LTG 10 μM + PAX6	27 596	4 272	N = 9 from 3 experiments
LTG 100 μM + PAX6	22 602	4 011	N = 9 from 3 experiments
Untreated + MMP9	2 067	767	N = 9 from 3 experiments

DMSO 0.2% + MMP9	2 068	712	N = 9 from 3 experiments
LTG 1 µM + MMP9	2 734	1 046	N = 6 from 2 experiments
LTG 5 µM + MMP9	2 238	655	N = 7 from 2 experiments
LTG 10 µM + MMP9	2 075	608	N = 9 from 3 experiments
LTG 100 µM + MMP9	2 670	816	N = 9 from 3 experiments

Data of *Renilla* luciferase from CGN			
Exposure	**Average**	**SEM**	**Number of experiments**
Untreated + PAX6	5 305	2 158	N = 12 from 4 experiments
Saline + PAX6	4 599	1 802	N = 11 from 4 experiments
VPA 1 µM + PAX6	16 330	2 638	N = 3 from 1 experiment
VPA 100 µM + PAX6	7 246	2 594	N = 6 from 2 experiments
VPA 500 µM + PAX6	24 470	10 617	N = 9 from 3 experiments
VPA 1000 µM + PAX6	60 294	28 269	N = 9 from 3 experiments
Untreated + MMP9	3 033	252	N = 6 from 2 experiments
Saline + MMP9	2 627	194	N = 6 from 2 experiments
VPA 500 µM + MMP9	15 633	1 992	N = 6 from 2 experiments
VPA 1000 µM + MMP9	25 020	4 064	N = 6 from 2 experiments
Untreated + PAX6	1 023	303	N = 9 from 3 experiments
DMSO 0.2% + PAX6	620	137	N = 9 from 3 experiments
LTG 1 µM + PAX6	1 613	45	N = 3 from 1 experiment
LTG 5 µM + PAX6	536	71	N = 3 from 1 experiment
LTG 10 µM + PAX6	690	199	N = 9 from 3 experiments
LTG 100 µM + PAX6	510	127	N = 9 from 3 experiments
Untreated + MMP9	2 200	449	N = 9 from 3 experiments
DMSO 0.2% + MMP9	1 498	257	N = 9 from 3 experiments
LTG 1 µM + MMP9	1 806	539	N = 6 from 2 experiments
LTG 5 µM + MMP9	1 545	325	N = 7 from 2 experiments

LTG 10 μM + MMP9	1 678	297	N = 9 from 3 experiments
LTG 100 μM + MMP9	1 890	355	N = 9 from 3 experiments

Appendix V – Neurite Outgrowth

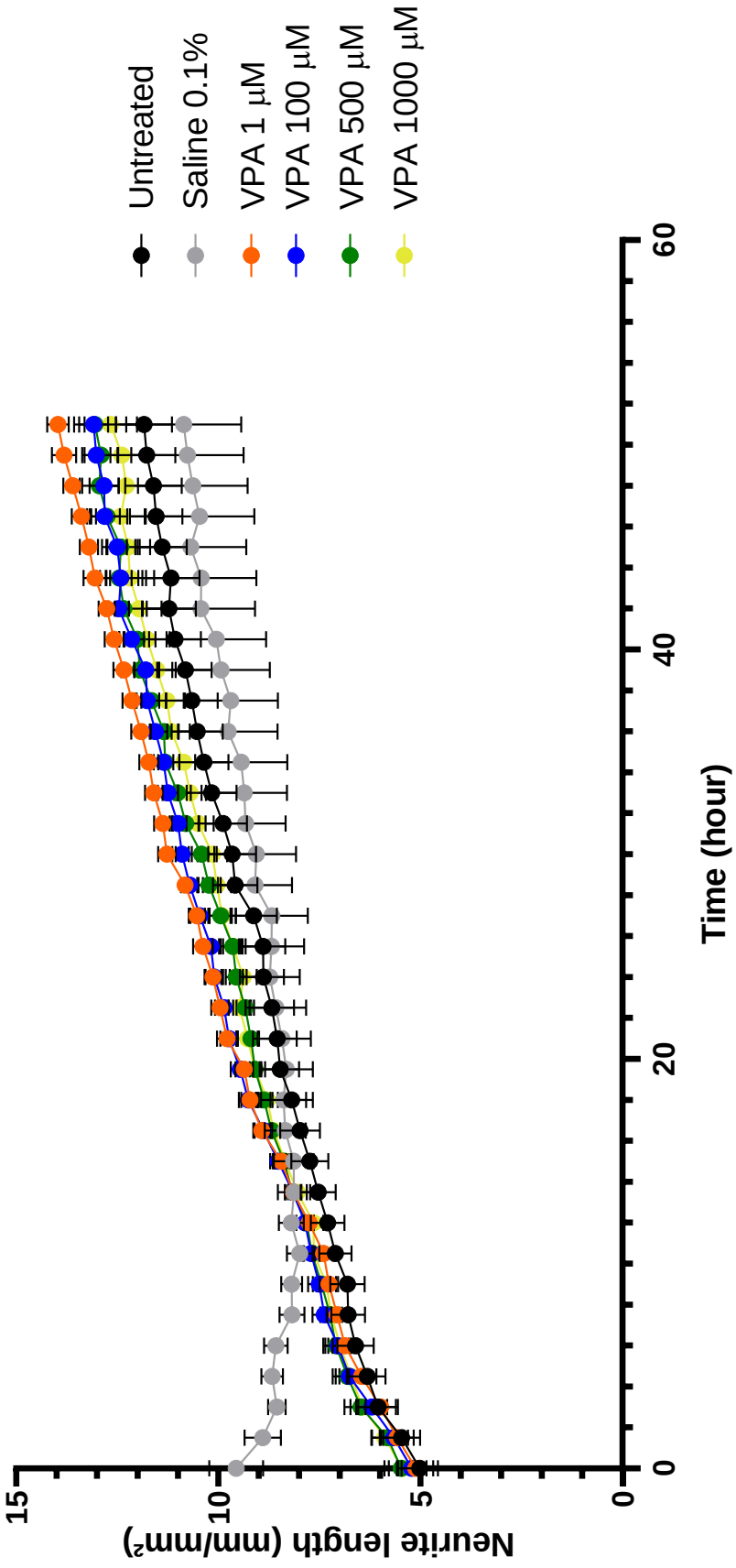
Untreated
Saline 0.1%
VPA 1 µM
VPA 100 µM
VPA 500 µM
VPA 1000 µM
Neurite length (mm/mm²)
0
5
10
15
Time (hour)
0
20
40
60

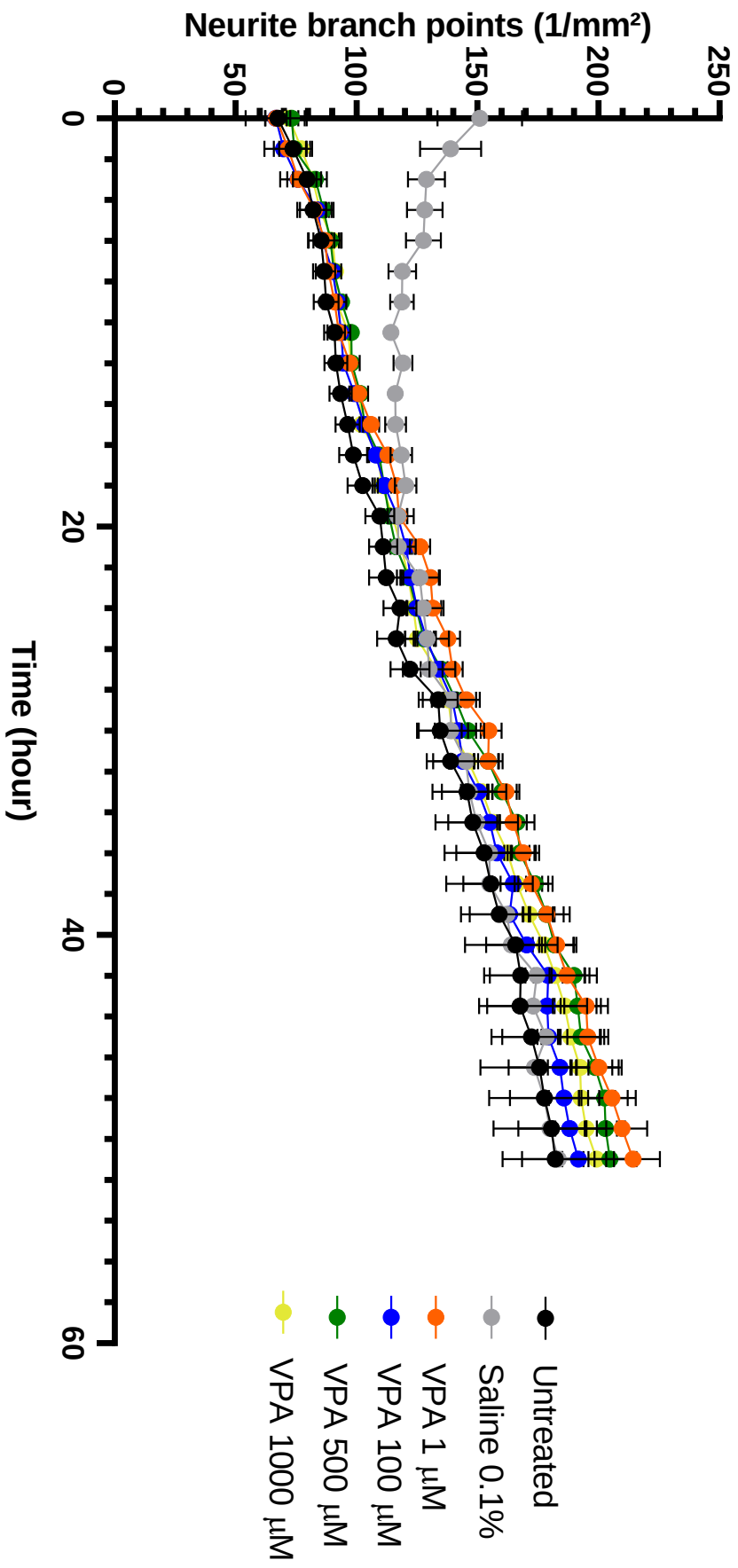
Neurite branch points (1/mm²)
0
50
100
150
200
250
Time (hour)
0
20
40
60
Untreated
Saline 0.1%
VPA 1 µM
VPA 100 µM
VPA 500 µM
VPA 1000 µM

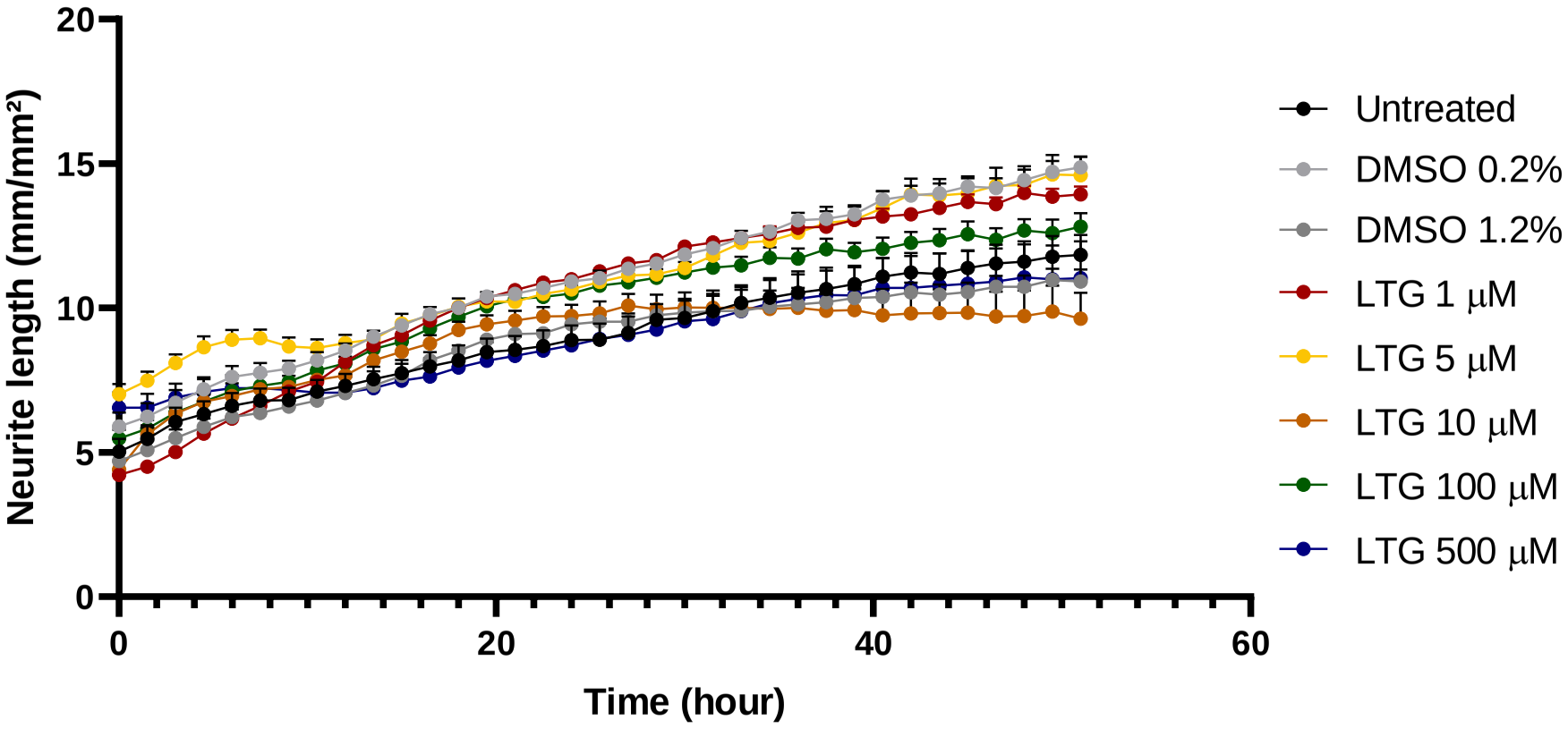
Neurite length (mm/mm²)
20
15
10
5
0
0
20
40
60
Time (hour)
Untreated
DMSO 0.2%
DMSO 1.2%
LTG 1 μM
LTG 5 μM
LTG 10 μM
LTG 100 μM
LTG 500 μM

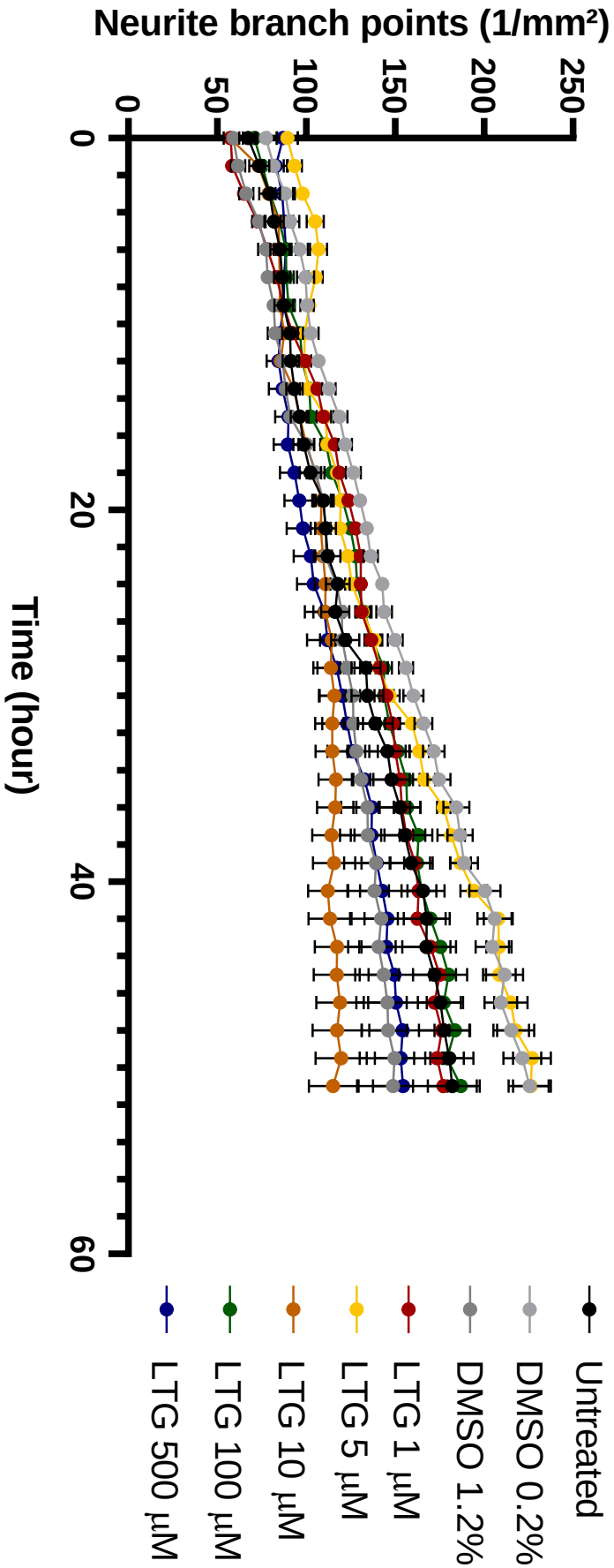
Neurite branch points (1/mm²)
0
50
100
150
200
250
Time (hour)
0
20
40
60
LTG 500 µM
LTG 100 µM
LTG 10 µM
LTG 5 µM
LTG 1 µM
DMSO 1.2%
DMSO 0.2%
Untreated